TIME DOMAIN, FREQUENCY DOMAIN AND INCOMPLETE MOMENT ANALYSIS FOR REACTIVE SOLUTE TRANSPORT

by

JUN LIN

Submitted in Partial Fulfillment of the Requirements for
the Degree of Master of Science in Hydrology

New Mexico Institute of Mining and Technology
Socorro, New Mexico

August 1995

ACKNOWLEDGMENTS

I would like to thank my committee for their support, encouragement, and suggestions throughout this study. The committee consisted of John Wilson, Allan L. Gutjahr, Robert Bowman, and Jan Hendrickx. I would especially like to thank John Wilson, my advisor, for providing insight and direction throughout the various phases of research.

This research involved several students who greatly contributed to the results presented in this paper. I would especially like to express my appreciation to Du Xiaohong, Jim(Jinz-hong) Liu, Tongying Shun and Wendy Ye for their discussion about the frequency domain analysis and incomplete moment analysis.

This study was funded by the Geophysics Research Center, New Mexico Tech, through contracts 11H-G-01060-502.

ABSTRACT

This research is concerned with reactive solute transport in an aquifer system under some external impacts, such as contamination and remediation. The concepts of time constant and storage capacity are employed to investigate the influence of heterogeneity of hydraulic conductivity and rate-limited sorption on reactive solute transport. In a particular geological formation, the time constant reflects kinetic processes and storage capacity represents equilibrium properties. Time domain analysis, using a lumped parameter model and a two-dimensional cross-sectional model, shows that the results of a remediation system on a contaminated aquifer depend on the geological formations with larger time constants and a significant amount of stored contaminants, as well as a few operational variables. Some improved remediation techniques, such as biodegradation and hydraulic fracturing, are also evaluated in this analysis. The frequency domain analysis illustrates the spectrum characteristic of reactive solute transport. The contaminated geological formation with a smaller time constant and storage capacity is more sensitive to external impacts, and thus, more easily remediated. A two-dimensional numerical model is also developed to evaluate the transfer function in a heterogeneous aquifer in this analysis. A new concept of incomplete moment is developed to gain more insight into the behavior of reactive solute transport. The corresponding incomplete moment-generating equations for a lumped parameter model and a two-dimensional model are also derived. Some examples show the characteristics of an incomplete moment with the variation of the time constants in the mobile zone and sorption sites. This study shows that the distribution of the time constant and the storage capacity in an aquifer system determine the results of a remediation, and the developed frequency domain analysis and incomplete moment analysis are useful tools in better understanding the behavior of reactive solute transport.

TABLE OF CONTENTS

LIST OF FIGURES

LIST OF SYMBOLS

Symbol	Description
C	aqueous phase concentration [M/L^3]
C_i	injection concentration in the first–type boundary[M/L^3]
$C_o(\omega)$	co–spectrum
C_q	injection concentration in the LPM model[M/L^3]
C_0	initial aqueous phase concentration[M/L^3]
D	dispersion coefficient [L^2/T]
D_p	pore diffusion coefficient in the grain [L^2/T]
D_a	apparent diffusion coefficient in the grain [L^2/T]
J_n	nth order incomplete moment for the solid phase concentration [T$^{(n+1)}$]
J_{nr}	nth order incomplete moment for the solid phase concentration in the grain scale [T$^{(n+1)}$]
K_d	distribution coefficient [L^3/M]
K_{dj}	distribution coefficient in the jth sorption site [L^3/M]
N_n	nth order incomplete moment for the aqueous phase concentration [T$^{(n+1)}$ M/L^3]
P	pumping rate in a unit volume [1/T]
Q	discharge rate in a unit volume [1/T]
$Q(\omega)$	quadrature spectrum
R	retardation factor
R_j	retardation factor in the jth sorption site
R_{im}	retardation factor in the immobile region
R_{in}	retardation factor in the grain
R_{xx}	autocorelation function
S	solid phase concentration
S_j	solid phase concentration in the jth sorption site
Sr	solid phase concentration as a function of the grain radius
T	input period [T]
T_p	intragranular tortuosity
V	average velocity [L/T]
$X(t)$	stationary input process
$Y(t)$	stationary output process

$dZ(\omega)$	complex Fourier amplitude
b	distance from the center to the edge of the sorption site [L]
f	fraction of the sorption site
g	geometry factor
l	characteristic vertical dimension of the lenses [L]
m	number of the sorption sites
p	parameter of the Laplace transformation
r	characteristic grain radius [L]
t	time [T]
α	mass transport coefficient [1/T]
α_j	mass transport coefficient in the *j*th sorption site [1/T]
α_L	longitudinal dispersivity coefficient [L^2]
α_T	transverse dispersivity coefficient [L^2]
ϱ_b	soil bulk density [M/L^3]
θ	porosity
θ_{sc}	phase spectrum of the processes, *S(t)* and *C(t)*.
λ	degradation rate [1/T]
τ	time constant [T]
τ_a	nonreactive aqueous phase time constant [T]
τ_b	biodegradation time constant [T]
τ_d	diffusion–type sorption time constant [T]
τ_{ra}	reactive aqueous phase time constant [T]
τ_s	sorption time constant in lenses and aquitards [T]
τ_j	sorption time constant in the *j*th sorption site[T]
ϕ	power spectral distribution
$\frac{\partial}{\partial t}, \frac{\partial}{\partial T}$	partial differentiation with respect to time
$\frac{\partial}{\partial x}; \frac{\partial}{\partial y}$	partial differentiation with respect to distance

1. INTRODUCTION

Pump–and–treat (PAT) remediation systems are one of the popular methods used to clean up contaminated aquifers. The contaminants in an aquifer are flushed out by clean water. However, it has been recognized that there is a long tail in the breakthrough curve at the pumping well during the remediation period, and thus, a very long period of cleanup is required to restore the aquifer to the drinking water level. When pumping is shut off, the contaminant concentration in an aquifer can gradually increase and may rise over the drinking water standard. This tailing and rebound behavior implies that the PAT system may be ineffective in some cases, meaning that water is treated without flushing the contaminants out.

Let us start with an example problem. Figure 1.1 is a cross–sectional diagram of an idealized fluvial aquifer. Four lower hydraulic conductivity lenses are imbedded in the sandy aquifer, and silt aquitards bound the top and bottom of the aquifer. Some parameters are shown in this figure. This aquifer system first experienced a 10–year history of industrial disposal contamination, followed by a 5–year contaminate redistribution period. After this contaminated aquifer was discovered, a 300–day PAT remediation was executed to restore it. A numerical model was used to simulate the solute transport during the contamination, redistribution, remediation, and rebound periods in order to evaluate the performance of the PAT system. Figure 1.2 shows the concentration change at the left boundary (during the remediation, this is the concentration in the pumping well). The 10 years of contamination and the 5–year redistribution essentially fully contaminate the aquifer. The 300–day remediation causes the concentration to drop off quickly and then tail out smoothly. The picture in the upper right corner of Figure 1.2 shows details of the concentration change during remediation. Observing the concentration change after remediation, we find that it gradually increases and reaches 40 percent of the maximum concentration before remediation. Thus, the PAT system does not achieve its cleanup goal, although the concentration in the pumping well may have dropped below the drinking water level during the remediation period. Why

does the breakthrough curve have a long tailing during remediation? Where does the contaminant come from during the rebound period? What processes cause the failure of the PAT system? And how do we evaluate the contributions of these related processes?

Many explanations about the ineffectiveness of the PAT system can be found in the literature: the slow release of trapped NAPLs, rate-limited adsorption/desorption, diffusion controlled contaminant transport in low hydraulic conductivity zones, and nonuniform flow caused by heterogeneous spatial hydraulic conductivity patterns (*Kelly* 1989; *Haley et al.* 1991; *Palmer and Fish* 1992; *Wilson*, 1992, 1995). These processes can cause much of the contaminants to remain in the aquifer at the end of remediation, although the concentration in the pumping well may be below the drinking water level, which often leads to an optimal estimate as to the effectiveness of the PAT system. Alternative schemes have been developed to amend the traditional PAT system, such as changing the configuration of a pumping/injection well pattern in the remediation period (*Keely* 1984; *Looney et al.,* 1992), injecting surfactant (e.g., *Vigon and Rubin*, 1989) or a co-solvent(e.g., *Palmer and Fish,* 1992) to speed up the desorption and degradation processes. However, these modified schemes are not always effective. For example, chemical enhancement is ineffective in reducing the lengthy tailing off of contamination concentration in the pumping well due to physical attributes of the system, including the diffusion-controlled mass transfer at the field scale and the grain scale. On the other hand, adjusting the pumping/injecting well distribution cannot be successful if the failure of the PAT system is caused by slow chemical reaction or diffusion-controlled rate-limited chemical desorption processes. Thus, a better understanding and evaluation of the different transport processes involved in subsurface is a major concern for remediation.

Quantitative tools have been applied to evaluate the influence of different processes on remediation. Many one-dimensional and two-dimensional analytical models have considered rate-limited sorption in a homogeneous aquifer with uniform flow (*Genuchten and Wierenga*, 1976, *Valocchi,* 1986; *Chen and Woodside*, 1988; *Goltz and Oxley*, 1991). More

complicated two-dimensional models that consider a heterogeneous pore medium, irregular boundary condition, and nonlinear and nonequilibrium sorption have also been developed (*Miller and Rabideau*, 1993; *Wilson*, 1995). Optimization methods have been explored to find out the best scheme in removing contaminants from the sorption sites (*Haggerty and Gorelick,* 1994). These models show that in the absence of NAPLS, heterogeneity and rate-limited desorption are the main reasons in hindering the removal of the contaminants, and they help us quantitatively analyze the influence of different processes. However, most of these models just do sensitivity analysis for some coefficients to identify the dominate process and neglect the relationship between the external impacts and properties of the aquifer system.

Any geological formation can be characterized by a time constant and storage capacity. The time constant represents the kinetic process and storage capacity reflects equilibrium properties. In this study, we use these two important parameters to identify the dominate processes that influence remediation results and determine the performance of a remediation system. Two new approaches, frequency domain analysis and incomplete moment analysis, are also developed to gain more insight into reactive solute transport.

Chapter 2 uses the concepts of a time constant and storage capacity to characterize a geological formation. Numerical example problems show the relationship between remediation results, time constants, and storage capacity. The influence of contamination history, hydraulic fracturing, and biodegradation on remediation are discussed in this chapter. Frequency domain analysis in Chapter 3 is applied to find how an aquifer system responds to external inputs. Analytical amplitude spectrums and phase spectrums are derived for a lumped parameter model and a one-dimensional advection-dispersion-sorption model. A two-dimensional numerical model is developed to calculate the distribution of transfer function in a heterogeneous aquifer. Chapter 4 introduces the new concept of the incomplete moment. The incomplete moment-generating equations for a lumped parameter model and a two-di-

mensional model are derived. Incomplete moment analysis can provide more information about the reactive solute transport from the breakthrough curve.

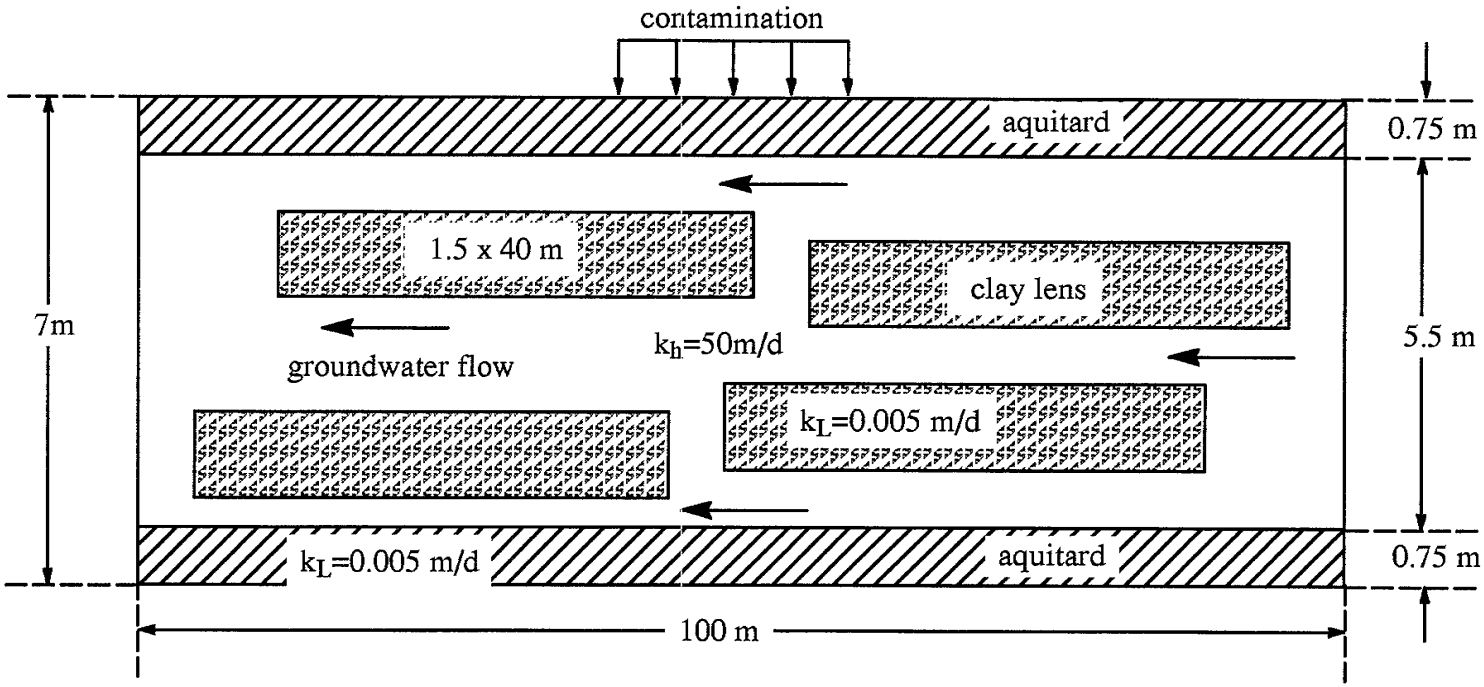

Figure 1.1 Cross-section of the idealized aquifer (From *Wilson*, 1995).

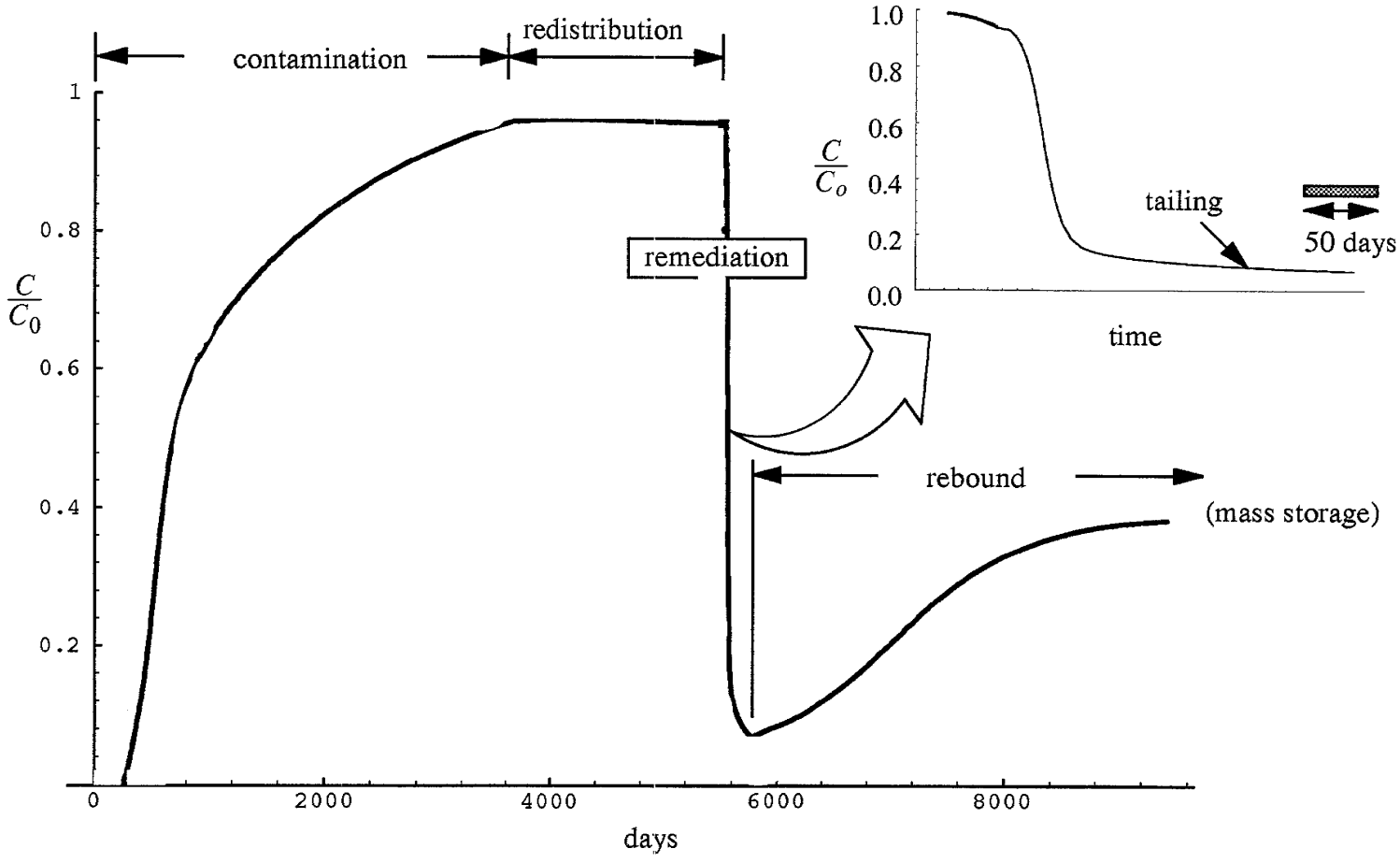

Figure 1.2 Aqueous phase concentrations at the the left boundary of the domain pictured in Figure 1.1 (From *Wilson*, 1995).

2 . TIME DOMAIN ANALYSIS FOR REACTIVE SOLUTE TRANSPORT

Solute transport in aquifer systems involves a large number of complicated chemical, physical, and microbiological processes. Depending on the characteristics of the aquifer, the influences of these processes on remediation and contamination are different. In this chapter, the concepts of a time constant and storage capacity will be used to characterize these different processes. A time constant in a particular geological formation represents how quickly a particular process can respond to an external impact; storage capacity provides the information about how much contaminant can store in this geological formation. These two important parameters reflect the responses of an aquifer system to impacts caused by nature and/or human activities, such as recharge and pumping.

Solute transport in a porous medium includes the processes of advection, dispersion, adsorption, and biodegradation. In the geological formation of an aquifer system, the dominant process depends on its properties, which are associated with the time constant and storage capacity. The effectiveness of a PAT system relies upon the distribution of time constants and mass storage capacity in the contaminated aquifer system. For example, a geological formation with a lower time constant and storage capacity is relatively easy to contaminate and/or remediate. These two parameters together control the results of a remediation system. If the time constant for a particular process is large, yet the storage capacity is small enough, the aquifer can be restored to the drinking water level, although a small amount of contaminant will remain in the aquifer. On the other hand, in a geological formation with a larger storage capacity and lower time constant, the contaminant may be quickly removed. The failure of the PAT system is associated with aquifers with larger time constants holding significant storage capacity.

In this chapter, a lumped parameter model will first be employed to show how the time constant and storage capacity can be applied to estimate the results of contamination and re-

mediation in an aquifer. The time constant for different processes such as advection, adsorption, and biodegradation are compared and analyzed in this model. After gaining insight into the time constant and storage capacity, a two-dimensional cross-section model is introduced to find the relationship between time constants in a heterogeneous porous medium with external impacts, including contamination, redistribution, and remediation. The comparison of the time constants and the period of remediation will help predict the result of a PAT system. The effect of contamination history and hydraulic fracturing are also evaluated.

2.1 Lumped Parameter Model (LPM) for Reactive Solute Transport

This lumped parameter model assumes the entire aquifer system is composed of one mobile zone and some immobile zones (sorption sites). The solute can exchange between mobile zone and sorption sites, but not between different sorption sites. Each sorption site can have their own properties. Figure 2.1.1 shows a population of sorption sites with different physical and chemical properties in contact with mobile water. Suppose that there are m aggregate classes, each of which consists of identical aggregates. The mass balance equations for this model are

$$\theta \frac{\partial C}{\partial t} + \varrho_b \sum_{j=1}^{m} f_j \frac{\partial S_j}{\partial t} = QC_q - PC - \lambda C \tag{2-1a}$$

$$\frac{\partial S_j}{\partial t} = \alpha_j (k_{dj} C - S_j) \tag{2-1b}$$

where θ is the porosity, ϱ_b is the bulk density, C is the resident concentration in the mobile liquid phase, S_j, α_j, f_j and k_{dj} are the solid phase concentration, the mass transfer coefficient, the fraction of sorbed volume, and the distribution coefficient in cell j ($j=1, m$), respectively; Q is the recharge rate, C_q is the recharge concentration, λ is the biodegradation rate, and P is the discharge rate.

Equation (2-1b) represents a system composed of a mobile zone and several parallel immobile zones (sorption sites). Solute exchange between the mobile and immobile regions

are regarded as a first–order dynamic process; that is, the mass transfer rate is proportional to the concentration between the regions. This model was first developed to describe the chemical nonequilibrium in sorption sites, but it has also employed to describe physical diffusion in aggregated soil and small stagnant zones (*Brusseau et al.*, 1989). We will use frequency domain analysis in Chapter 3 to compare this first–order mass transfer model with three other physical diffusion models, each having different aggregate geometry. Equation (2–1) also indicates that biodegradation processes occur only in the mobile zone because the compounds sorbed by aggregated soil are generally unavailable for biodegradation (*Fry and Istok*, 1994). The biodegradation coefficient for the first–order decay term can be determined from the Monod equation if the concentration of the substrate is small relative to the half velocity coefficient, meaning that the contaminant concentration in the mobile zone is the substance that is limiting the rate of decay (e. g., oxygen is not the limiting substance). The analytical solutions for one–site and two–site models (one fraction of rapidly equilibriating sorption sites; another fraction of slowly equilibrating sorption sites) have been fully developed by other authors (*Genuchten and Wierenga* 1976; *Toride et al.*, 1993). However, this multicelled nonequilibrium model has not been investigated thoroughly. A numerical method will be applied to solve this model.

2.1.1 Time Constant and Storage Capacity

In the lumped parameter model, we neglect the dispersion process in the mobile region, and neglect advection, dispersion, and biodegradation processes in the immobile region. Clearly, the advection and/or biodegradation processes can be the dominant processes in the mobile regions, and physical diffusion or chemical reaction processes may dominate in the immobile regions. The time constant can characterize these different processes. Based on this model, the nonreactive time constant for the advection process in the mobile region can be expressed by

$$\tau_a = \frac{\theta}{P} \quad . \qquad (2\text{–}2a)$$

It represents the time scale that the aqueous phase concentration drops from its original value to 1/e times that value, in the absence of any chemical reactions, immobile water, or first order decay. This expression can also be found in the study of the lumped parameter model for groundwater flow (*Gelhar and Wilson*, 1974). Increasing the pumping rate will decrease the time constant, meaning that the contaminant in the mobile region is more easily removed. This matches the general intuition about remediation of a contaminated aquifer. Sorption will increase the time constant in the advection process. Under the assumption of equilibrium sorption, the reactive time constant for advection can be

$$\tau_{ra} = \frac{R_{im}\theta}{P} = R_{im}\tau_a \qquad (2\text{–}2b)$$

where R_{im} is the retardation factor in the immobile regions. If sorption process is rate-limited, the reactive time constant in the mobile zone is also associated with the sorption time constant. We will illustrate how to estimate this reactive time constant in the examples. The time constant for the biodegradation process in the mobile zone can be expressed by

$$\tau_b = \frac{\theta}{\lambda} \qquad . \qquad (2\text{–}3)$$

It represents a time scale of biodegradation. This time constant may vary greatly because of the wider range of biodegradation coefficients (*Bouwer and McCarty*, 1985; *Alvarez et al.*, 1991). Other time constants represent the mass transfer rate in immobile zones. For example, in cell j, the time constant is

$$\tau_{sj} = \frac{1}{\alpha_j} \qquad . \qquad (2\text{–}4)$$

For chemical nonequilibrium, α_j is the chemical dynamic constant and it can be measured through chemical experiment. A slower chemical reaction leads to a larger time constant. For grain scale diffusion related physical nonequilibrium, α_j is the lumped parameter that represents how quickly the mass transfer occurs across a thin boundary layer to the grain surface, and/or within the intragranular porosity. More complicated models are available to describe

this kind of diffusion-controlled sorption. The time constant for some of these models, involving internal porosity, can written as

$$\alpha = \frac{R_{in} r^2}{g T_p D_p} \tag{2-5}$$

where r is the characteristic grain radius, g is the geometry factor, T_p is the intragranular tortuosity, D_p is the effective diffusion coefficient within the grain, and R_{in} is the internal retardation factor if the equilibrium sorption occurs in diffusion controlled immobile zones. Equation (2-5) represents the time scale of intraparticle diffusion and sorption. Because the characteristic length r is very small in grain scale, the contributions to a larger time constant can be the smaller tortuosity factor, a lower intraparticle diffusion coefficient, or the larger internal retardation factor R_{in}. Some experimental results have given us insight into long term sorption (*Brusseau et al.*, 1989; *Brusseau et al.*, 1991; *Ball and Roberts*, 1991; *Pedit and Miller*, 1994).

Storage capacity is another important parameter representing how much of the contaminant can be stored in a particular geological formation. In our lumped parameter model, the maximum volume that can be occupied by an aqueous phase contaminant is θ in the mobile zone, and $\varrho_b\, kd_j f_j$ for solid phase contaminant in cell j of the immobile zone; both are based on the total volume of the entire aquifer system. The retardation factor R ($R=1+\sum(\varrho_b\, kd_j f_j/\theta)$) can be used to compare these two volumes. The contaminant storage volume in sorption sites is greater than that in the mobile region if the retardation factor is greater than 2. In general, a great amount of sorption volume is associated with the existence of organic matter (*Brusseau et al.*, 1989).

2.1.2 Results and Discussion

Numerical simulations for a two-cell model (m=2 for equation (2-1a,b)) investigate the relationship among the remediation, time constants, and storage capacity. We assume that the groundwater flow is in steady state (P=Q). The sensitivity analysis for time constants

and storage capacity were performed over a range of coefficients. The major parameters for four examples are shown in the corresponding figures. The purpose of these simulations was to use the time constant analysis to quantitatively evaluate the relative importance of different processes on remediation of a contaminated aquifer. The results of remediation are predicted by comparing the system time constants and remediation period.

Example 1: Effect of Mobile Region Nonreactive Time Constant

The aqueous phase concentration, the total contaminant mass remaining in the aquifer system, and the contaminant mass remaining in different sorption sites are affected by the nonreactive time constant of the advection process in the mobile zone, as shown in figure 2.1.2. This example assumes that the aquifer system has been fully contaminated, the aqueous phase concentration was 1 mg/l initially, the time constant in sorption site 1 is 10 days and 60 days in sorption site 2, and retardation factor is 2. The 300-day remediation (clean water (C_q=0 mg/l) was injected and dirty water was pumped out) was executed to remove contaminants from this aquifer. For the case of the 10-day nonreactive time constant in the advection process (case 1), the occurrence of the sorption process makes the actual time scale larger, dropping the aqueous concentration from the initial concentration to its e fold value much later than 10 days. The reactive advection time constant should be 20 days if the sorption is equilibrium. However, the sorption processes are rate-limited in our example, meaning the reactive time constant in the mobile zone less than 20 days. Since the time constant for the sorption process in sorption site 1 is only 10 days, it can be approximately regarded as in equilibrium. However, the sorption process in site 2 with a 60-day time constant is obviously rate limited. Because sorption site 1 and sorption site 2 hold the same storage capacity, this makes the aqueous phase concentration drop to its e fold initial concentration between 15 to 20 days, as shown in figure 2.1.2a. This relatively faster cleanup in the mobile zone will be paid for by keeping more contaminant in sorption sites; thus, the drop of total contaminant mass lags the drop of aqueous phase concentration during remediation (figures 2.1.2a and 2.1.2b). Sorption site 2, with a rate limited desorption process, will

become the source of contamination after remediation, and the effectiveness of the PAT system also depends on its time constant and storage capacity. We will consider these influences in examples 2 and 3. In this case (case 1), the 15–20 day reactive advection time constant, a 10–day time constant of sorption site 1, and a 60–day time constant of sorption site 2 are much less than the 300–day remediation. 95 percent of the contaminants had been removed from the aquifer system after 240 days of remediation. In this sense, this contaminated aquifer can be restored by the PAT system.

A larger time constant for the advection process in the mobile zone can be attributed to the lower hydraulic conductivity in the aquifer system. Slower removal of contaminants from the mobile region also allows for a slower release of contaminants from the sorption sites because the gradient of concentrations is smaller between the sorption sites and mobile zone. Unfortunately, the lumped parameter model cannot represent spatial distribution of the hydraulic conductivity (we will consider the effect of heterogeneity in a two–dimensional cross–section model). Thus, we reduce the pumping rate to obtain a longer time constant for the advection process. In this first order lumped parameter model, the drop of the aqueous phase concentration has an exponential form, and three times the time constant will lead to 95 percent drop of the initial value. Thus remediation needs roughly three times the time constant to drop contamination in the mobile zone to 5 percent of its initial value. For the 240–day nonreactive time constant of the advection process in case 5, the sorption processes with the time constants of 10 days and 60 days can be regarded as equilibrium; thus, the reactive time constant for the advection process in this case is τ_{ra}=480 days. In order to get 95 percent removal of contamination in the mobile zone, the remediation needs to last 1440 days. This time scale is much more than actual remediation period of 300 days, leading to more contaminant mass reserved in the mobile zone and sorption sites. Failure of this remediation is unavoidable. It indicates that the larger the time constant for the advection process, the longer to clean the mobile zone and sorption sites.

We can conclude from this example that (1) for the rate-limited sorption process, the concentration in the mobile zone will, at first, drop faster than that for the equilibrium sorption process; however, more contaminants reserved in the rate-limited sorption sites will gradually release to the aquifer and, thus, increase the length of cleanup; (2) the slower advection process (larger time constant) caused by a lower hydraulic conductivity or smaller pumping rate not only leads to slow removal of the contaminant from the mobile zone, but also slow release of contaminants from sorption sites, leading to equilibrium sorption process; (3) the remediation period should be greater than three times the reactive advection time constant to clean up 95 percent of the aqueous phase contamination during the remediation period. The PAT system can reach this goal in many cases. However, this is not enough--a lot of contaminant is reserved at the sorption sites even at the end of remediation. The time constants and storage capacity in sorption sites play important roles in this phenomenon. We will consider these effects in following examples.

Example 2: Effect of Time Constant in Sorption Sites

The influence of the time constant in sorption sites on the effectiveness of a PAT system is shown in this example (figure 2.1.3). The nonreactive advection time constant is $\tau_a=\theta/P$=30 days, the time constant at sorption site 1 is 10 days, but is 10, 30, 60, 120, and 240 days for sorption site 2 in the different cases. The recharge rate is still equal to the discharge rate ($P=Q$), and the retardation factor is also 2 for this system. Considering the occurrence of sorption, the reactive time constant for the advection process in the mobile zone is between 45 and 60 days, at least four times the time constant in sorption site 1. Thus, the sorption process at site 1 can be regarded as equilibrium. On the other hand, the larger time constant at sorption site 2, implying slower mass transfer from this sorption site, makes the aqueous phase concentration drop more quickly (figure 2.1.3a) when the remediation takes 60 days or more (equating the time constant of the advection process with the assumption of equilibrium sorption); however, figure 2.1.3b shows that more contaminant remains in the aquifer system with the increasing time constant at sorption site 2. This behavior has been

examined in example 1. Figure 2.1.3d reveals that these remaining contaminants are located at sorption site 2, which has a rate-limited desorption process. Suppose the objective of remediation is to remove 95 percent of the contaminant out of the aquifer, we can use the time constant analysis to estimate the required time period. Let us look at case 3 (60-day time constant in sorption site 2). As shown in previous example, removing 95 percent of the contaminant in the mobile zone requires at least three times the reactive time constant of the advection process. Thus, in this example, we need at least 180 days. On the other hand, if the contamination in the mobile zone has been removed, three times the time constant of the sorption process is also needed for the remediation period to remove 95 percent of the contaminant from a sorption site because the rate-limited sorption is represented by the first order ordinary differential equation and the analytical solution is of the form of the exponential function; thus, we need 180 days for sorption site 2 and 30 days for sorption site1. Because of the parallel structure of the sorption sites, obviously we just need the additional 180 days for cleaning both sorption sites; thus, the total required remediation period is about 360 days. The 300-day actual remediation scheme is close to complete remediation. The required remediation periods for other cases can be estimated in the same manner. They are about 210, 270, 540, and 900 days for cases 1, 2, 4, and 5, respectively. The 300-day remediation system will be partially unsuccessful for a slow desorption process with time constants of 120 and 240 days in sorption site 2 (case 4 and case 5 in figure 2.1.3b).

From this analysis, it is also easy to derive that if an aquifer is difficult to remediate due to slow desorption, it is also difficult to contaminate (figure 2.1.4), assuming the same mass transfer rate in the adsorption and desorption process. Figure 2.1.4b shows that 300-days of contamination loading cannot fully contaminate the aquifer with the larger time constant sorption site even when the aqueous phase concentration has reached its maximum (figure 2.1.4a).

We can conclude that (1) a remediation system at least needs three times the sum of the reactive advection time constant and the largest sorption time constant (due to the parallel

structure of sorption sites) to remove 95 percent of the contaminants from the aquifer system; (2) a small nonreactive time constant of the advection process is not enough to ensure the success of a remediation system. If there is a larger time constant for a sorption process, slow desorption can be the controlling process that influences the effectiveness of a remediation system; and (3) the sorption site with a larger time constant is the most difficult to contaminate, as well as to remediate. Contamination present in an aquifer for many time constants will store far more contaminant in sorption sites that cannot be remediated quickly. We will highlight this point in the two-dimensional model.

Example 3: Effect of Storage Capacity in Sorption Sites

The larger reactive time constant for the advection process may be attributed to the larger storage capacity at the sorption sites. According to the conclusion in example 1, this larger time constant may lead to the failure of a remediation system. Assume that clean water (C_q=0 mg/l) is injected, the time constants in sorption site 1 and site 2 are 10 and 60 days, respectively. Figure 2.1.5 shows that the increase of storage capacity in sorption sites leads to more contaminant reserved in the mobile region and sorption sites. Let us use time constant analysis again. Because the retardation factors are 1,2,3,4, and 5 for different cases, the reactive time constants for the advection process are about 30, 60, 90, 120, and 150 days, respectively. This regards the desorption process (cases 2,3,4,and 5) as approximately in equilibrium (figure 2.1.5c,d). Case 1 represents no sorption in the immobile region, and its time constant goes to infinity and storage capacity is zero. In order to remove 95 percent of the contaminant from the aquifer system, the required remediation period needs at least three times the sum of the reactive time constant of the advection process and the largest time constant in the sorption sites. Thus, 90, 360, 450, 540, and 630 days, respectively, for different cases are needed to remediate this contaminated aquifer (figure 2.1.5b). Comparing with a 300-day real remediation period, the remediation is partially unsuccessful for cases with the occurrence of sorption. Because the storage capacity of sorption sites is different for different cases, the mass of the stored contaminants before remediation is different. For the case with larger storage

capacity, the remediation objective, restoring the aquifer to the an acceptable level, obviously leads to a need to remove more contamination and thus a need for a longer remediation period. We need more than 540 days and 630 days of remediation period for case 4 and case 5, respectively, to drop the aqueous phase concentration to this acceptable level. This example shows the compound effect of a larger storage capacity in the sorption site during remediation. It increases the effective time constant of an advection process, causing slower removal of contaminants from the mobile zone and sorption sites. On the other hand, it leads to a higher aqueous phase concentration and a longer remediation period to drop the concentration to an acceptable level.

Example 4: Effect of Biodegradation Time Constant

Biodegradation is usually used to speed up the remediation process and/or reduce the cost of a PAT system. The effectiveness of this improved remediation depends on whether the nutrients and/or electron acceptors can be delivered to contaminated zones and how fast the contaminant can be degraded. Assuming that the contaminants can be degraded in the mobile zone but not in sorption sites, our model will investigate the effect of the biodegradation process under different desorption rates (figure 2.1.6 and figure 2.1.7), without limitation due to nutrient or electron acceptors availability. The nonreactive time constant in the mobile zone is $\tau_a=P/\theta=30$ days, the time constant for sorption site 1 is 10 days, and 60 days for sorption site 2 (figure 2.1.6), and the retardation factor is 3. The time constants for biodegradation processes are $\tau_b=\theta/\lambda=5$, 20, 40, 60, and ∞ days (no degradation) for different cases. The dominant processes in the mobile zone are advection and biodegradation; thus, the nonreactive time constant in this zone can be calculated by

$$\tau_m = \frac{\theta}{P + \lambda}$$

Under the occurrence of approximately equilibrium sorption, the reactive time constants in the mobile zone are about 13, 36, 51, and 59 days, respectively for first four cases; all are less than the 90–day reactive time constant in the mobile zone without the biodegradation

process (case 5). Time constant analysis indicates that removing 95 percent of the contaminants from the entire aquifer system requires about 220, 300, 330, and 360 days (figure 2.1.6b), respectively, for first four cases. Comparing with the 450-day requirement for 95 percent remediation without biodegradation (case 5), this improved remediation is more effective (figure 2.1.6a, 2.1.6b). However, a slower sorption process may weaken this positive effect. Figure 2.1.7 reveals that when the time constant in sorption site 2 is 240 days, a larger amount of contaminant still remains in the aquifer system (figure 2.1.7b,d) even under quick degradation of the contaminants in the mobile zone (case 1). The biodegradation is not very effective in speeding up the removal of the contaminants from a slow desorption site (figure 2.1.7d). From this example, we conclude that biodegradation always plays a positive role in improving the effectiveness of a remediation system. It can significantly reduce the time constant in the mobile zone and, thus, speed up the contaminant removal. However, slower desorption process with a larger time constant in the sorption site may still make a remediation system partially unsuccessful, even under quick degradation, since the contaminants in the sorption site cannot biodegrade. The required cleanup time still depends on the time constant at the sorption site.

2.1.3 Summary

The lumped parameter model was employed to provide insight into time constant and storage capacity. The influences of the advection, sorption, and biodegradation processes on remediation are evaluated by using time constant analysis. The examples show

(1) Time constant analysis is a useful tool in estimating a required remediation period, identifying the major process that influences the results of remediation and evaluating an improved remediation system.

(2) The smaller time constants in the mobile zone and sorption sites are necessary for an effective PAT remediation system. To remove 95 percent of the contaminant out of the

aquifer, remediation at least needs three times the sum of the reactive time constant of the advection processes and the time constant of the slowest desorption process.

(3) A larger storage capacity in sorption sites not only increases the storage of the contaminants, but also increases the time constant in the mobile zone, leading to slower removal of contaminants from the mobile zone. Rate-limited desorption will reduce this effect at first, but the sorption site can become a long-term contamination source even after remediation.

(4) Biodegradation occurring in the mobile zone can make the aqueous phase concentration drop quickly and speed up the removal of the contaminants from sorption sites. However, it still cannot greatly improve the remediation from slower desorption sites.

2.2 Two-Dimensional Reactive Solute Transport Model

Although the lumped parameter model above is enough to show the usefulness of time constant analysis, it cannot characterize a more complicated real aquifer system. In fact, the spatial average of an entire aquifer system always neglects some important local processes, such as diffusion processes in lower hydraulic conductivity zones and sorption sites, whose storage capacity and time constants determine the effectiveness of a remediation system. Thus, in practice, a distributed parameter model is more useful in studying a real aquifer system.

Some one-dimensional analytical models based on Laplace transform methods have been used for the case of a single, fully penetrating pumping well in a confined aquifer, incorporating linear nonequilibrium sorption (*Goltz and Oxley*, 1991). Assuming a homogeneous aquifer and a sorption site, these models do not consider the effects of heterogeneity of hydraulic conductivity, and multicell sorption. One-dimensional numerical models used to simulate multicell sorption processes at the laboratory scale have been developed to provide insight into the processes (*Brusseau et al.*, 1989) and their influence on field-scale remediation (e.g., *Crittenden et al.*, 1986). However, one-dimensional models are still inappropri-

ate to represent the field flow and transport behavior because they cannot represent complicated flow fields and realistic geological formations. Numerical solutions of the models incorporating both heterogeneity and sorption nonequilibrium also have been developed (*Rabideau and Miller*, 1993; *Burr et al.*, 1994; *Wilson*, 1995). Some of the solutions only applied to a natural gradient system or radial flow, and most of them required a large amount of computer storage and computational time to calculate sorption effect. More effective methods still need to be developed. In this section, we will follow *Wilson*, 1995 and use a two-dimensional cross-sectional advection-dispersion-sorption transport model to discuss the relationship between time constants in low-k zones and sorption sites and periods of contamination and remediation. This is an anthropogenic impact against a natural system. The Laplace Transform Galerkin (LTG) code (*Sudicky*, 1989) was modified to simulate contaminant transport under nonequilibrium sorption.

2.2.1 Mathematical Model

In two-dimensional space, the governing advection-dispersion equations (ADEs) for a single adsorbing solute are

$$\frac{\partial C}{\partial t} + \frac{\varrho_b}{\theta}\frac{\partial S}{\partial t} = \frac{\partial}{\partial x}(D_{xx}\frac{\partial C}{\partial x} + D_{xz}\frac{\partial C}{\partial z}) + \frac{\partial}{\partial z}(D_{zz}\frac{\partial C}{\partial z} + D_{zx}\frac{\partial C}{\partial x}) - V_x\frac{\partial C}{\partial x} - V_z\frac{\partial C}{\partial z} = L(C) \tag{2-6a}$$

$$\frac{\partial S}{\partial t} = \alpha(k_d C - S) \tag{2-6b}$$

where θ is porosity, ϱ_b is dry bulk density of the medium, C is the concentration, S is the adsorbed concentration, x and z are spatial coordinates, t is the time, V_x and V_y are the pore velocity in x and z direction, respectively, α is rate constant, and k_d is the distribution coefficient. These governing equations show that the porous medium can be subdivided into a mobile zone and an immobile zone (or sorption site) in a representative element volume (REV). Equation (2-6b) assumes that the linear sorption isotherm, $S=k_dC$, governs under local equilibrium conditions, and it also can be written as

$$\frac{\partial S}{\partial t} = k_f C - k_r S \tag{2-7}$$

where k_f and k_r are the forward and reverse rate coefficients, respectively. Equations (2-6b) and (2-7) are commonly used in first-order mass transfer models, and they are equivalent if we adjust their parameter groups, such as $k_f/k_r=k_d$ and $k_f=\alpha$. Any other first order mass transfer models, developed for different chemical and physical sorption mechanisms, can be easily interchanged with these models. A first-order model, in fact, is a lumped parameter model representing a mass transfer process.

Another kind of mass transfer model is the diffusion model, whereby diffusion into and out of an immobile zone can be modeled using Fick's law. Assuming that the chemical sorption in an internal pore of an immobile zone is in equilibrium, this model can be written as

$$R_{in}\frac{\partial S_r}{\partial t} = \frac{D_p}{r^{k-1}}\frac{\partial}{\partial r}\left(r^{k-1}\frac{\partial S_r}{\partial r}\right) \tag{2-8}$$

where S_r is the concentration in mobile zone, varying with distance r from the center of the mobile zone, D_p is the effective pore diffusion coefficient, R_{in} is the retardation factor in the immobile zone; and k is the marker of the style of immobile zone. $k=1$ is for the immobile zone composed of layers; $k=2$ is for the immobile zone composed of cylinders; and $k=3$ is for the immobile zone composed of spheres. The boundary conditions for (2-8) are

$$\frac{\partial S_r}{\partial r} = 0 \qquad at\ r = 0 \tag{2-9}$$

$$S_r = k_d C \qquad at\ r = b \tag{2-10}$$

where b is the distance from the center to the edge of the immobile zone. The solid phase concentration S shown in equation (2-6) can be represented by the average of the concentration in the immobile zone. It can be expressed as

$$S = \frac{k}{b^k}\int_0^b r^{k-1} S_r dr \quad . \tag{2-11}$$

Equation (2-6) coupled with the proper mass transfer model and boundary conditions can

be used to simulate solute transport in a physically and chemically heterogeneous aquifer system and, thus, evaluate the effectiveness of a remediation scheme.

2.2.2 Numerical Scheme

The Laplace Transform Galerkin method has been demonstrated to effectively solve the advection–dispersion equation describing solute transport in porous and fractured medium (*Sudicky* 1989; *Sudicky et al.*,1991). The Laplace transformation was first used to eliminate temporal derivative term to obtain the p–space steady solute transport equation. Then, the Galerkin finite element method was applied to get the p–space concentration at any spatial node. After that, an effective inversion algorithm was employed to obtain the real concentration at any particular time of interest. The LTG method is effective in solving the linear differential equation system and, thus, is very appropriate for handling our model, which assumes linear mass transfer in a steady flow field. Application of the Laplace transformation to the governing equation (2–6) leads to

$$p\overline{C} + p\frac{\varrho_b}{\theta}\overline{S} = L(\overline{C}) + C_0 + \frac{\varrho_b}{\theta}S_0 \qquad (2\text{–}12)$$

where $\overline{C}$ is the p–space aqueous phase concentration, $\overline{S}$ is the p–space solid phase concentration, p is the Laplace parameter, L is the operator representing the right side of the equation (2–6a), and C_0 and S_0 are initial concentration in aqueous phase and solid phase, respectively. The temporal derivative of mass transfer models can also be eliminated by Laplace transformation. The results can be written as

$$\overline{S} = \frac{S_0}{p} + (k_d\overline{C} - \frac{S_0}{p})\, A_i \qquad i = 0,1,2,3 \tag{2-13}$$

where

$$A_0 = \frac{\alpha}{p+\alpha} \qquad \textit{for first order sorption model} \tag{2-14}$$

$$A_1 = \frac{1}{\beta}\frac{\sinh(\beta)}{\cosh(\beta)} \qquad \textit{for layer diffusion model } (k = 1) \tag{2-15}$$

$$A_2 = \frac{2}{\beta}\frac{I_1(\beta)}{I_0(\beta)} \qquad \textit{for cylinderical diffusion model } (k = 2) \tag{2-16}$$

$$A_3 = \frac{3}{\beta}\frac{i_1(\beta)}{i_0(\beta)} \qquad \textit{for spherical diffusion model } (k = 3) \tag{2-17}$$

$$\beta = b\sqrt{\frac{p}{D_a}} \qquad D_a = \frac{D_p}{R_{im}}$$

where I_n is the modified Bessel function of the first kind, and i_n is the modified spherical Bessel function. By substituting equation (2–13) into equation (2–12), we can obtain

$$p(1 + k_d\frac{\varrho_b}{\theta}\, A_i)\overline{C} = L(\overline{C}) + C_0 + \frac{\varrho_b}{\theta}A_i S_0 \qquad . \tag{2-18}$$

Equations (2–13) through (2–18) are the transformed system of time–dependent differential equations (2–6), (2–8), and (2–11). We first solve equation (2–18) by the Galerkin finite element method to obtain the p–space aqueous phase concentration $\overline{C}$ at any spatial nodal, and then using equation (2–13) to get the solid phase concentration $\overline{S}$. After that, the accurate and robust Crump algorithm is performed to inverse the p–space concentrations, $\overline{C}$ and $\overline{S}$, into the time–domain concentrations, C and S. This numerical method is suited well for our model. It uses much less computer time than other numerical schemes, such as the split–operator approach (*Miller and Rabideau*, 1993), and it need not build computational grids in the grain scale to calculate the average sorption concentration. Thus, this algorithm saves more computational storage and uses less CPU time. The p–space resident mass in an aquifer system can also be calculated to obtain the time–domain mass distribution to evaluate the effectiveness of a remediation system. Some new subroutines had been developed for the original

code (*Sudicky* 1989) to consider the effect of the rate-limited mass transfer process, represented by different sorption models, and to calculate the mass distribution in an aquifer system.

2.2.3 Results and Discussion

In a real aquifer system, each geological formation can be characterized by a time constant and storage capacity. In this section, following Wilson (1995), we employed an idealized aquifer imbedded with some lenses and aquitards to account for the influence of time constants and storage capacity in these geological formations on the contamination and remediation. Figure 2.2.1 shows the profile of this idealized aquifer; major basic parameters are listed in this figure, and we change sorption time constant, retardation factor and hydraulic conductivity of lenses and aquitards in following examples. Figure 2.2.2 shows the basic simulation scenario. After 10 years of contamination and 5 years of redistribution, the aquifer experienced one-year of remediation. When the remediation was shut off, we continued to simulate solute transport in the aquifer system for 10 years to investigate the effectiveness of this remediation system. The head difference between left and right boundaries is 0.01m during contamination, redistribution and rebound periods, but 1m during remediation. In the following examples, sorption process only occurs in the low-k zone, and $\tau_s=1/\alpha$ and $R=1+\varrho_b k_d/\theta$ represent sorption time constant and retardation factor, respectively. The time constant analysis is still used to estimate the results of this remediation scheme.

Example 1: Effect of Heterogeneity on Hydraulic Conductivity

The pore velocity is slower in lower permeability zones, and this makes the contaminant in lenses and aquitards difficult to move in and out. Thus, the mass transfer rate and storage capacity in the low-k zones will influence contamination and/or remediation for this aquifer system. Figure 2.2.3 and figure 2.2.4 show the resident mass in the aquifer (high-k zones) and in lenses and aquitards (low-k zones), respectively, for four stages. Five cases correspond to different k values in lenses and aquitards (case 1 is homogeneous, but still has sorption). The sorption occurred only in the lenses and aquitards with the retardation factor is

2. The storage capacity in the aquifer (high–k zone) is about 110kg (assume that the source concentration is 1mg/l), but is about 280kg in low–k zones, which includes the sorption capacity. Obviously, we are concerned with the mass change in the low–k zones, which have a smaller mass transfer rate.

Let us look at the contamination period first. For case 1 (homogeneous case), the aquifer is slower, at first, to become contaminated because more contaminants can move easily into the lenses. For case 5 (k=0.005m/day for lenses and aquitards), the mass in the aquifer increases quickly at first, but it does not mean that the aquifer system can be fully contaminated. Figure 2.2.4 indicates that even at the end of the contamination period, low–k zones are still able to store more contaminants. This implies that the aquifer system with far lower–k zones is more difficult to locally contaminate because more contaminant passes through the aquifer system without moving into them (figure 2.2.5). Of course, contamination not stored must have migrated elsewhere, in this case, off to the left. In the redistribution period, not much happens: a small amount of contamination moves into the low–k zones from the aquifer and leads to a slight increase of mass in lenses and aquitards.

One year's remediation almost cleans the aquifer for all cases: the contaminant mass in the aquifer goes almost to zero (Figure 2.2.3); thus, this remediation scheme seems to be successful. But, figure 2.2.3 reveals that a large amount of contaminant still remains in low–k zones for case 3, 4 and 5; the lower the permeability in lenses and aquitards, the more contaminant remains. This indicates that the failure of a remediation scheme to restore a contaminated aquifer system can be attributed to the slower release of contaminant from low–k zones. After the remediation system is stopped, we find that the aquifer becomes recontaminated for the cases with the hydraulic conductivity smaller than 5m/day in aquitards and lenses (figure 2.2.3), and contaminants again occupy about 40 percent of the storage capacity of the aquifer after 10 years of postremediation for case 5 (k_L=0.005m/d). Clearly, contaminant in low–k zones is the source for the recontamination in the aquifer.

Figure 2.2.6 shows contour plots of the aqueous phase concentration and solid phase concentration for case 5. It clearly reveals the storage location of contaminants in the remediation period and how they move into the aquifer after it had been remediated.

Why are low–k zones difficult to contaminate, or remediate if they have been contaminated? Slow diffusion rate is an important reason. With the decrease of hydraulic conductivity in lenses and aquitards, the diffusion process dominates over the advection process, and the contaminant mass is mainly transferred by diffusion in these zones. The Peclet number can be applied to compare these two processes.

$$\mathcal{P} = \frac{V\alpha_T}{D_a}$$

Where V is the local pore velocity, α_T is the transverse dispersivity, and D_a is the effective diffusion coefficient. The Peclet number in low–k zones is two orders smaller than 1 when hydraulic conductivity value is 0.005m/day, and the mass transfer is a completely diffusion–controlled process. We will use time constant analysis to evaluate the mass transfer rate. For case 5, the nonreactive time constant for diffusion controlled process in low–k zones can be estimated by (*Wilson*,1995)

$$\tau_l = \frac{l^2}{gD_a} \qquad (2\text{–}19)$$

where l is the characteristic vertical dimension of the lenses, g is the geometry factor and D_a is the effective pore diffusion coefficient. The calculated nonreactive time constant is about three years for lenses and aquitards in case 5. Compared to this, the rate–limited sorption, with just a 40–day time constant, can be regarded approximately as an equilibrium process. Thus, the reactive time constant in low–k zones under the sorption and diffusion processes is about six years due to the retardation factor of 2 at sorption sites. 18 years (three times the reactive time constant) of contamination are necessary to move the contaminants to fill 95 percent of the storage capacity of aquifer system; thus, ten years of real contamination cannot fully contaminate the aquifer system. However, there is no reason to conclude that less con-

taminant remaining in low–k zones will lead to better remediation results in the remediation period. The six years' time constant is still much more than just one year of remediation.

Figure 2.2.4 indicates that there is more contaminant still reserved in the lower–k zones although they hold less contaminant before remediation. We conclude from this simulation that (1) an aquifer system with a greater volume of diffusion controlled low–k zones is harder to contaminate, or remediate if it has been contaminated; (2) a diffusion–controlled process can be a major reason to obtain a larger time constant in the lower–k zone, and sorption may increase the time constant in this zone, and (3) time constant analysis can be used to predict the response of an aquifer system to external impacts, such as contamination and remediation.

Example 2: Effect of Rate Limited Sorption

Rate–limited sorption/desorption can be caused by a slow chemical reaction or physical diffusion at the grain scale. The mass transfer between the mobile zone and sorption site cannot be spead up directly by a traditional PAT system because a sorption site cannot be touched by the advection flow. Thus, the mass transfer rate and storage capacity at sorption sites greatly influences the degree of contamination or remediation of an aquifer. Figures 2.2.7, 2.2.8, and 2.2.9 show the contaminant mass change in the aquifer, lenses and aquitards, and total aquifer system, respectively for different time constants at the sorption site. The sorption only occurs in the lenses and aquitards which have a hydraulic conductivity of 10m/day. The previous example has proved that advection dominates in these zones; thus, the rate–limited sorption process is more important than heterogeneity in this aquifer system, and we are mainly concerned with the sorption site, not the entire low–k zones. The storage capacity of the sorption sites is about 140kg, just half of the storage capacity in the diffusion–controlled low–k zone in example 1 (figure 2.2.5).

The sorption site with a time constant of zero (equilibrium sorption case) is more easily contaminated and remediated than in other cases (figure 2.2.9) because mass transfer is faster in this process. 10 years of real contamination is much more than three times the time

constant of 40 days, 180 days, or 1 year in the sorption site, thus, an aquifer system is fully contaminated. But considering the effect of heterogeneity, the sorption site with a three year time constant is not completely contaminated, and it has unfilled potential to store about 30kg more contaminant at the end of the contamination period (figure 2.2.8). A year of remediation is sufficient to remove contaminants from the sorption sites with a time constant of zero or 40 days, but not sufficient for the sorption sites with a time constant of 180 days, 1 year, or 3 years (Figure 2.2.8 and 2.2.9). Figure 2.2.10 is the contour plot of the aqueous phase and solid phase concentration for a time constant of three years in sorption process (case 5). The figure reveals that one year of remediation has cleaned the mobile zones in lenses and aquitards, but the remaining contaminant in sorption sites recontaminate the aquifer in the postremediation period. Ten years postremediation will be enough to release most contaminants from the sorption sites to the aquifer for all cases, but slower advection in the aquifer during this period still keeps a large amount of contaminant in the aquifer.

The slow mass transfer in the low–k zone results from the rate–limited sorption process in this example, although advection is the dominate process in this zone. Comparing with the case 5 in the previous example, in which diffusion is the dominated process in the low–k zones, with only 40 days' sorption time constant but 6 years' diffusion time constant, the contaminated low–k zones with 3 years' desorption time constant (cases 5 in this example) are relatively easy to remediate. This indicates that the sorption in the diffusion controlled low–k zone will increase the time constant in this zone, even when the sorption is an equilibrium process.

We can conclude from this example that (1) the time constant and storage capacity in a sorption site influences the effectiveness of a remediation system: the larger the time constant, the more time is required for a remediation; (2) sorption occurring in the diffusion–controlled low–k zones not only increases contaminant storage potential, but also causes the increase of the time constant in the mobile zone and makes the contaminant more difficult to move out.

Example 3: Effect of Storage Capacity in Sorption Sites

As we saw in the lumped parameter model, more storage capacity at a sorption site not only increases the potential to store more contaminants, but it also increases the time constant in the mobile zone, leading to a slower mass transfer. This example assumes that the hydraulic conductivity in lenses and aquitards is 1 m/day, thus experiencing some diffusion control, with a sorption time constant of 40 days. The net effect is that within the lenses and aquitards, sorption is for all practical purposes, at equilibrium. According to example 1, the diffusion process dominates in lenses and aquitards. We change the retardation factor at the sorption sites from 1 to 4 for different cases; thus, in low-k zones, the storage capacity is about 140kg (no sorption), 280kg, 420kg, and 560kg, respectively. Ten years of contamination does not fully contaminate the low-k zones for cases 2,3, and 4 (figure 2.2.12), because of the larger reactive time constant in those zones. And the more storage capacity there is at sorption sites, the more unfilled potential there is to store additional contaminants at the end of contamination. During the redistribution period, more contaminant can move into low-k zones (figure 2.2.11) with their larger storage capacity. One year of remediation is obviously not enough to restore an aquifer with a larger storage capacity at the sorption sites (figure 2.2.13), because the time constant in low-k zones is far more than three years. The rebound happens after remediation (figure 2.2.11). Although the rebound mass is almost the same for cases 2, 3, and 4 for ten years, figure 2.2.13 shows that more contaminants can remain in the larger storage capacity aquifer system; thus, if observed time is long enough, we will find that more contaminants can release into aquifer. It is difficult to identify the exact nonreactive time constant for the low-k zone in this example, because the advection process cannot be completely neglected; but lets say that it is probably around 2 years. However, it is clear that the larger storage capacity at the sorption sites can increase the time constant in the pore space of the diffusion controlled lenses and aquitards, and thus reduce the effective mass transfer rate. For an equilibrium sorption process, the reactive time constant in low-k zones is the multiplication of a nonreactive time constant with a retardation factor. The rate-limited sorp-

tion process will reduce this effect at first, but can sustain a long–term influence, which leads to the behavior of the tailing and rebound in the breakthrough curve of the aqueous phase concentration in the pumping well.

Example 4: Effect of Contamination History

The success of remediation also depends on the initial distribution of contamination in an aquifer system. The geological formation with a lower time constant, such as a high–k aquifer, is relatively easy to remediate. However, the diffusion–controlled low–k zones and sorption sites with larger time constants and a significant storage of contaminants are difficult to clean up. Thus, the effectiveness of a remediation system also depends upon the contamination history, which has a great influence in the distribution of the contaminants. Interaction between time constants of an aquifer system and contamination history leads to a different distribution pattern of the contaminants. In this example, we assume that the hydraulic conductivity is 0.005m/day in lenses and aquitards, time constant of the sorption process is 40 days, and retardation factor is 2. Example 2 had indicated that the reactive time constant for lenses and aquitards was about six years, and sorption can be approximately regarded as an equilibrium process. Four different contamination source cases, with different injection periods (10, 5, 3, and 1 year, respectively), have different influences on the aquifer system. All four cases have the same total amount of mass injected; that is, they involve the same amount of waste with the same concentration (1mg/l), but injected at different injection rates. The shorter contamination period leads to a larger contaminant mass in the aquifer, but more attenuation in the redistribution period (figure 2.2.14) because the contaminants in the aquifer can move into the aquitards and lenses (figure 2.2.15). The storage of the contaminants in low–k zones is less for a shorter contamination period because a larger amount of contaminant can pass through the high–k aquifer due to a higher hydraulic gradient. Although remediation removes the same percent of contaminant storage from low–k zones due to the same time constant for all cases, the different storage of the contaminants before remediation leads to the different reserve of contaminants after remediation. The shorter con-

tamination period reserves less contaminant after remediation, and thus a lower rebound (figures 2.2.14 and 2.2.15). We conclude from this example that contamination present in the aquifer for only a short time, relative to the aquifer time constant, can be relatively easy to clean up because it does not have a chance to move into the slow responding zones. Contamination residing in the aquifer for many time constants can store a significant amount of contaminant and cannot be remediated quickly.

Example 5: Effect of Hydraulic Fracturing

Hydraulic fracturing techniques have been developed to improve remediation. This method can speed up the mass transfer from the low–k zone to high–k zone, and thus, it primarily deals with contamination stored at a field scale such as low–k lenses and aquitards, but not at the grain scale such as aggregated soil. In fact, hydraulic fracturing can break the low–k zones into several smaller blocks, and thus, the time constants in each subblock may be smaller, leading to faster mass transfer. Assuming that the aquifer system had been fully contaminated, and that the adsorption/desorption occurs only in lenses and aquitards with a time constant of 40 days, our example investigates the influence of the hydraulic fracturing technique on a remediation system. The modified LTG code (*Sudicky*, 1989) can be employed again to evaluate this improved remediation scheme. The hydraulic fractures are horizontal, located in the center of the lenses. The aquitards are not fractured. Two different cases with different lengths of hydraulic fractures have different impacts on remediation. Fractures go through the entire lenses (40m) in case 1, but just cut through the middle part of lenses (20m) in case 2. The aperture is 0.1cm, and equivalent cubic law hydraulic conductivity is about 70m/day, a little more than the hydraulic conductivity of 50m/day in the aquifer. In case 1, the original four lenses have been broken into eight equivalent sublenses. The reactive time constant for each smaller lense is 1/4th of the original reactive time constant according to equation (2–19); that is, the reactive time constant is about 1.5 years for each sublense. Comparing the original reactive time constant of 6 years, hydraulic fracturing should greatly improve the mass transfer rate from low–k zones. However, in case 2, non–

cut–through fractures may not greatly increase the mass transfer rate because the contaminants accumulated in the internal hydraulic fracture cannot be removed immediately. Figures 2.2.17 – 2.2.20 show that more contaminant can move out of the low–k zones with cut–through hydraulic fractures during remediation, resulting in less rebound in the aquifer after remediation. This example shows that the connection of a hydraulic fracture to the high–k zone is an important factor influencing a improved PAT system. However, the effectiveness of the hydraulic fracturing technique also depends on the direction and aperture of the fractures. More work should be done to evaluate the effect of these factors.

2.2.4 Summary

The Laplace Transform Galerkin method has been used to solve ADEs coupled with a rate–limited sorption process. Several examples provided in this section show the influences of the heterogeneity, rate–limited sorption, and contamination history on a remediation system. An improved remediation scheme, the hydraulic fracturing technique, is also evaluated in this section. Time constant analysis is used to evaluate effectiveness of a remediation system. The main conclusions include

(1) The diffusion controlled process in a low–k zone can be characterized by a time constant. It represents the mass transfer rate in that zone. A geological formation with a larger time constant and a significant storage of contaminants is difficult to clean up.

(2) Sorption occurring in a diffusion–controlled low–k zone not only can increase the storage capacity, but also can increase the effective time constant. Rate–limited sorption will reduce this effect at first, but will have a long–term influence on remediation and contamination.

(3) Interaction between time constants of an aquifer system and a contamination history leads to a different distribution of contaminants and, thus, influences the results of a remediation system. The faster the original contamination in a aquifer system makes the contami-

nant pass quickly through the high–k zones, and there is less opportunity to move into the diffusion–controlled low–k zone. This kind of contamination is relatively easy to remediate.

(4) The effectiveness of a hydraulic fracturing technique depends upon the location of the fractures. The cut–through fracture is helpful in increasing the mass transfer rate in low–k zones. Time constant analysis can be used to evaluate this improved scheme. More work should be done to explore the effect of other influencing factors, such as the fracture direction and aperture.

2.3 Conclusions

In general, in the absence of NAPLs, the failure of traditional nonchemically enhanced PAT systems can be attributed to the presence of heterogeneity and rate–limited sorption. This study stresses that diffusion–controlled processes associated with sorption and low–k zones can be an important mechanisms in explaining slow contaminant removal from these zones, which leads to lengthy tailing and rebound at the breakthrough curve of the aqueous phase concentration in a observed well. Time constants and capacity are used to characterize this process in low–k zones and at sorption sites of the aquifer system. They represent the dynamic and equilibrium properties of these geological formations. The larger the time constant, the slower the mass transfer from these diffusion–controlled zones. Time constant analysis can identify the dominate processes that influence remediation and can also evaluate the effectiveness of a remediation system.

Several examples in this chapter show that a smaller time constant in an advection process is a prerequisite to quick cleanup in an aquifer. Most of a remediation system can reach this goal in high–k zones, but it is not enough. In low–k zones, the diffusion may be a dominated process, and clean water cannot flush out the contaminants from this zones. The larger time constant of this process and a significant amount of contaminants reserved in this zone results in a longer cleanup time. This explains why the presence of heterogeneity leads to the failure of a remediation system. The rate–limited sorption in grain scale may be diffu-

sion–controlled again. Advection cannot touch the micropore in an aggregated soil, and the removal of contaminants from a sorption site completely depends on the diffusion rate, which can be characterized by a time constant. Basically, three times the time constant is need to diffuse 95 percent of contamination out of the sorption site. A larger time constant with a larger storage capacity at a sorption site leads to the failure of a PAT system due to rate–limited sorption. Sorption occurring in diffusion–controlled low–k zone not only can increase the storage in this zone, but also can increase the time constant, even when the sorption process is in equilibrium. Rate–limited sorption will reduce this effect at first, but can retain more contaminant in the sorption site at the end of remediation and then slowly release to the aquifer in postremediation period.

Time constant analysis can also be employed to estimate the results of several improved PAT techniques. Biodegradation that occurs in a mobile zone can degrade a contaminant in a mobile zone quickly and, thus, increase the gradient of concentration between the mobile zone and sorption sites. However, it cannot greatly improve remediation in the diffusion–controlled low–k zones and sorption sites because the nutrients and electron acceptors are not easily delivered to these zones, and thus biodegradation is difficult. The hydraulic fractuing technique may decrease the time constant of diffusion–controlled low–k zones, but it cannot speed up the removal of the contaminant stored in the sorption sites. The cut–through fractures in low–k zones are more useful in improving the effectiveness of a remediation system than the non–cut–through fractures. More work should be done to evaluate this improved technique.

The influences of the contamination history on remediation are also investigated. Contamination present in the aquifer for only short time, relative to the aquifer time constant, can be remediated relatively easy. Contamination residing in the aquifer for many time constants can store a significant amount of contaminant and cannot be remediated quickly.

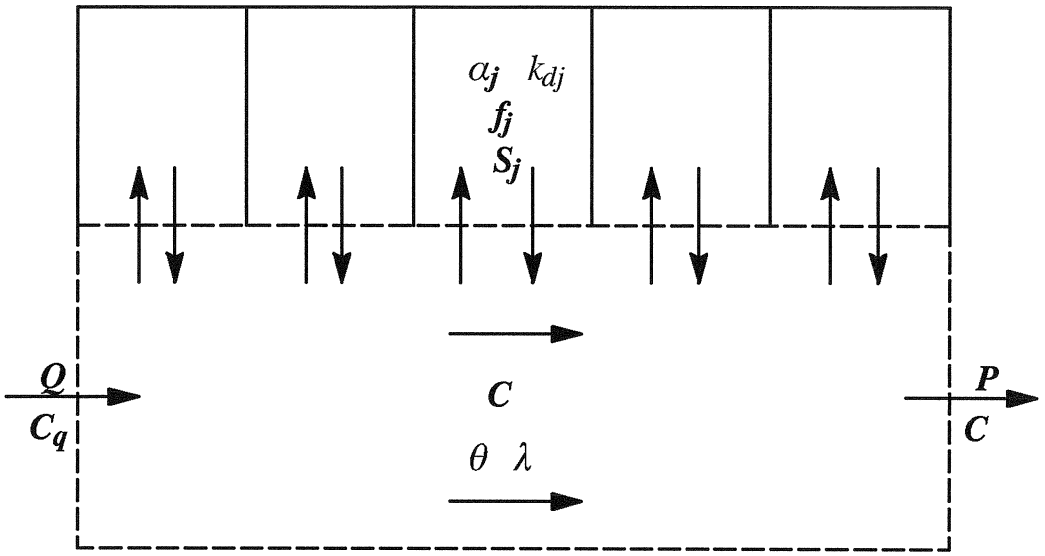

Figure 2.1.1 Schematic of the lumped parameter model

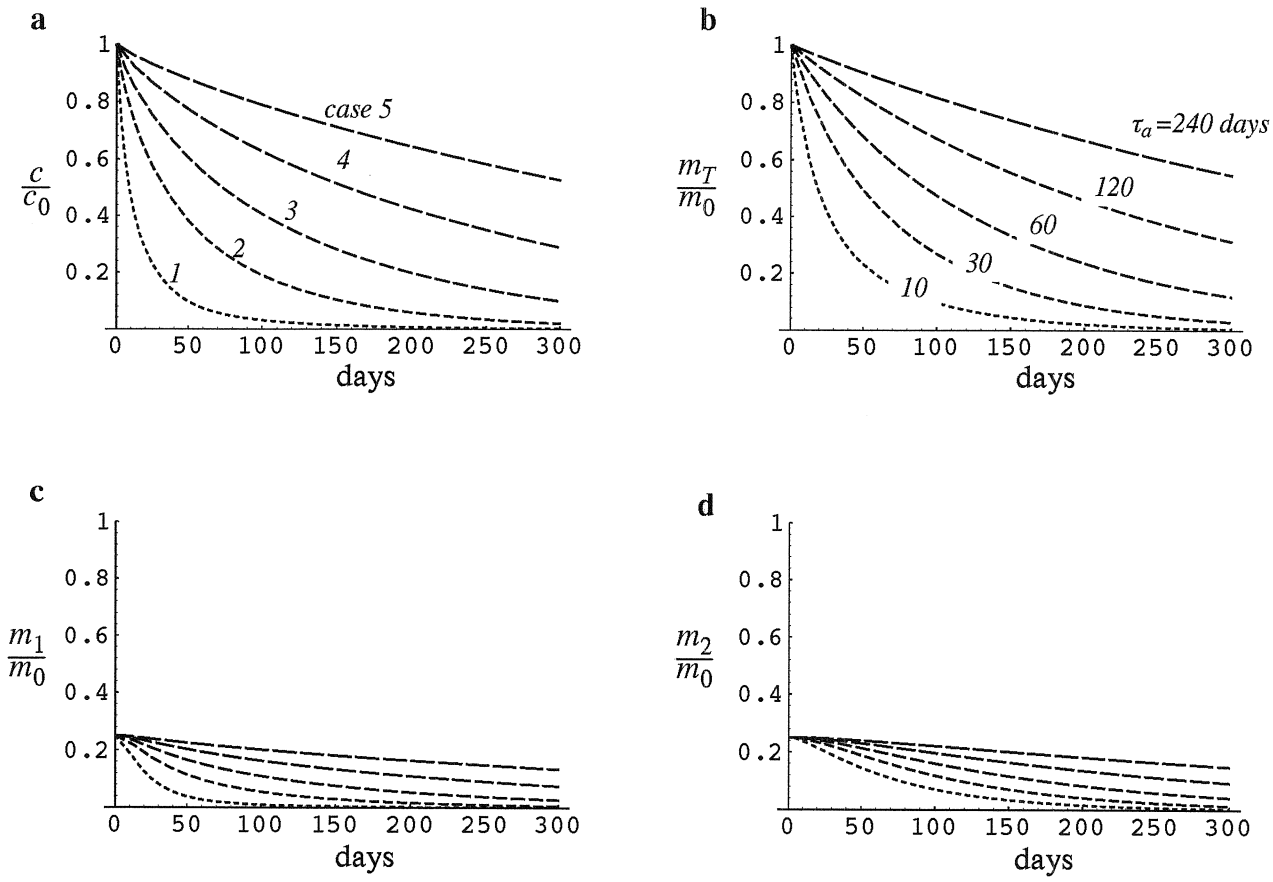

Figure 2.1.2 Effects of different non–reactive aqueous phase time constants assuming θ =0.356, f_1=0.5, f_2=0.5, R=2, τ_{s1}=10 days, τ_{s2}=60 days, C_0=1mg/l, C_q=0mg/l and λ=0. (*a*) is for the aqueues phase concentration, (*b*) is for the total residual contaminant mass, (*c*) is for the residual contaminant mass in sorption site 1, and (*d*) is for the residual contaminant mass in sorption site 2.

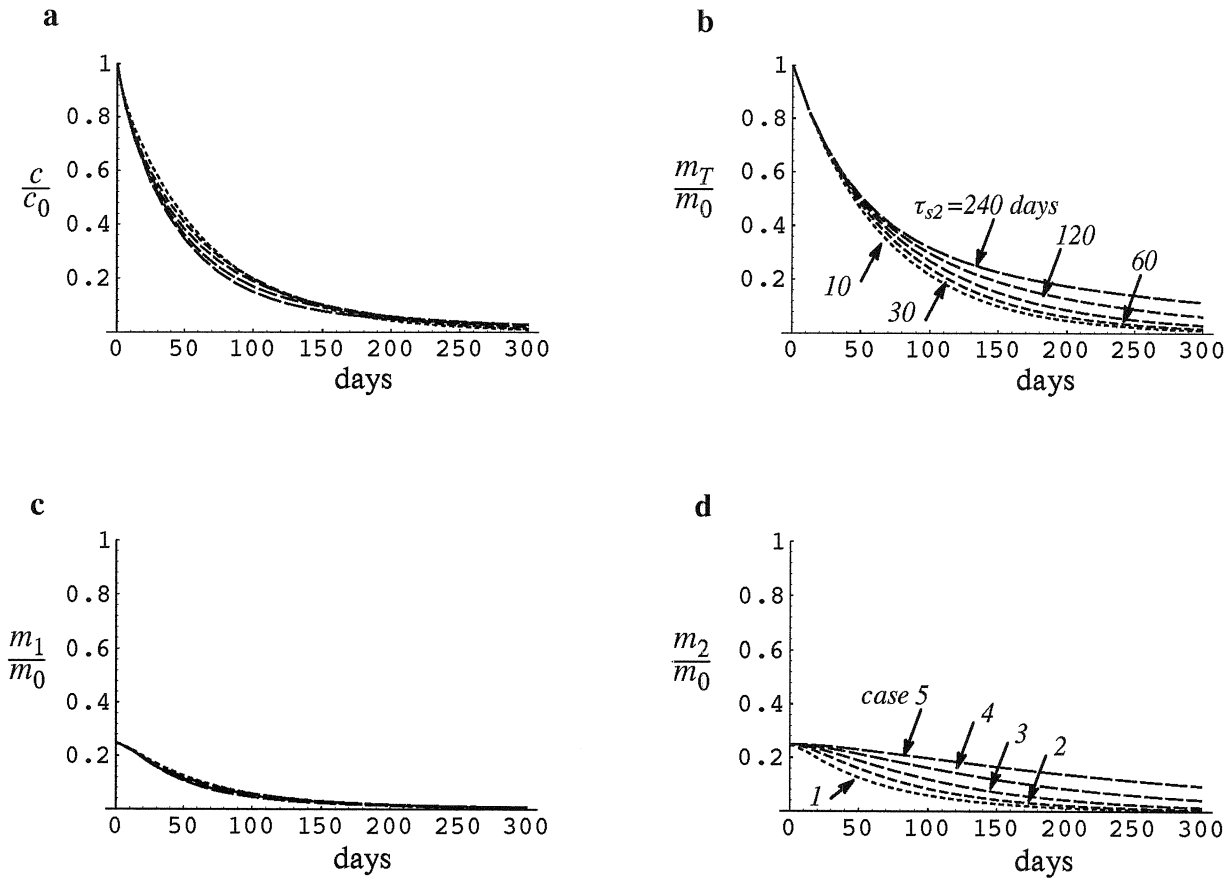

Figure 2.1.3 Effects of different sorption time constants of sorption site 2 during remediation assuming $\theta = 0.356, f_1 = 0.5, f_2 = 0.5, R = 2, \tau_a = 30$ *days*, $\tau_{s1} = 10$ *days*, $C_0 = 1 mg/l$ $C_q = 0 mg/l$ and $\lambda = 0$. *(a)* is for the aqueous phase concentration, (*b*) is for the total residual contaminant mass, (*c*) is for the residual contaminant mass in sorption site 1, and (*d*) is for the residual contaminant mass in sorption site 2.

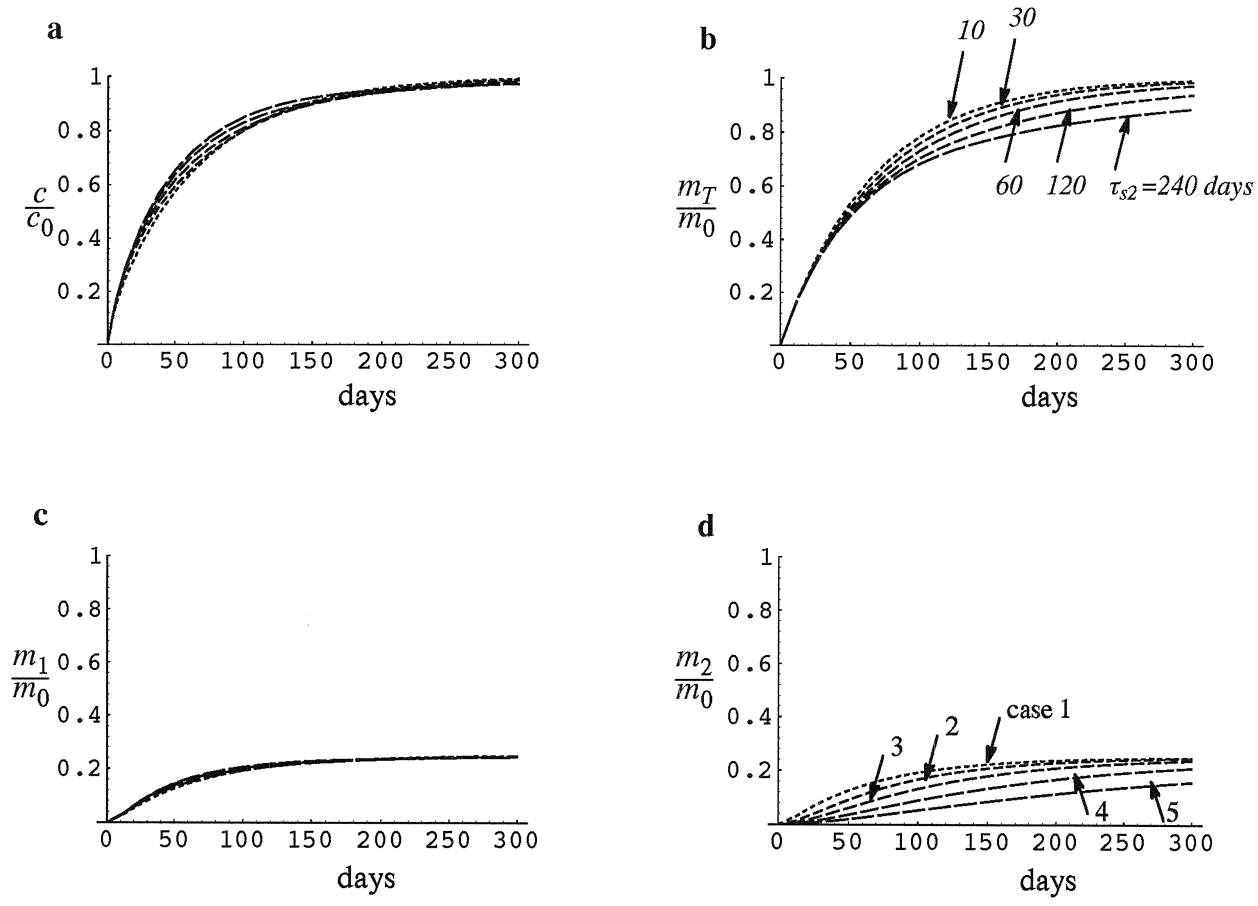

Figure 2.1.4 Effects of different sorption time constants of sorption site 2 during contamination assuming θ =0.356, f_1=0.5, f_2=0.5, R=2, τ_a=30 days, τ_{s1}=10 days, C_0=0mg/l, C_q=0mg/l and λ=0. (*a*) is for the aqueous phase concentration, (*b*) is for the total residual contaminant mass, (*c*) is for the residual contaminant mass in sorption site 1, and (*d*) is for the residual contaminant mass in sorption site 2.

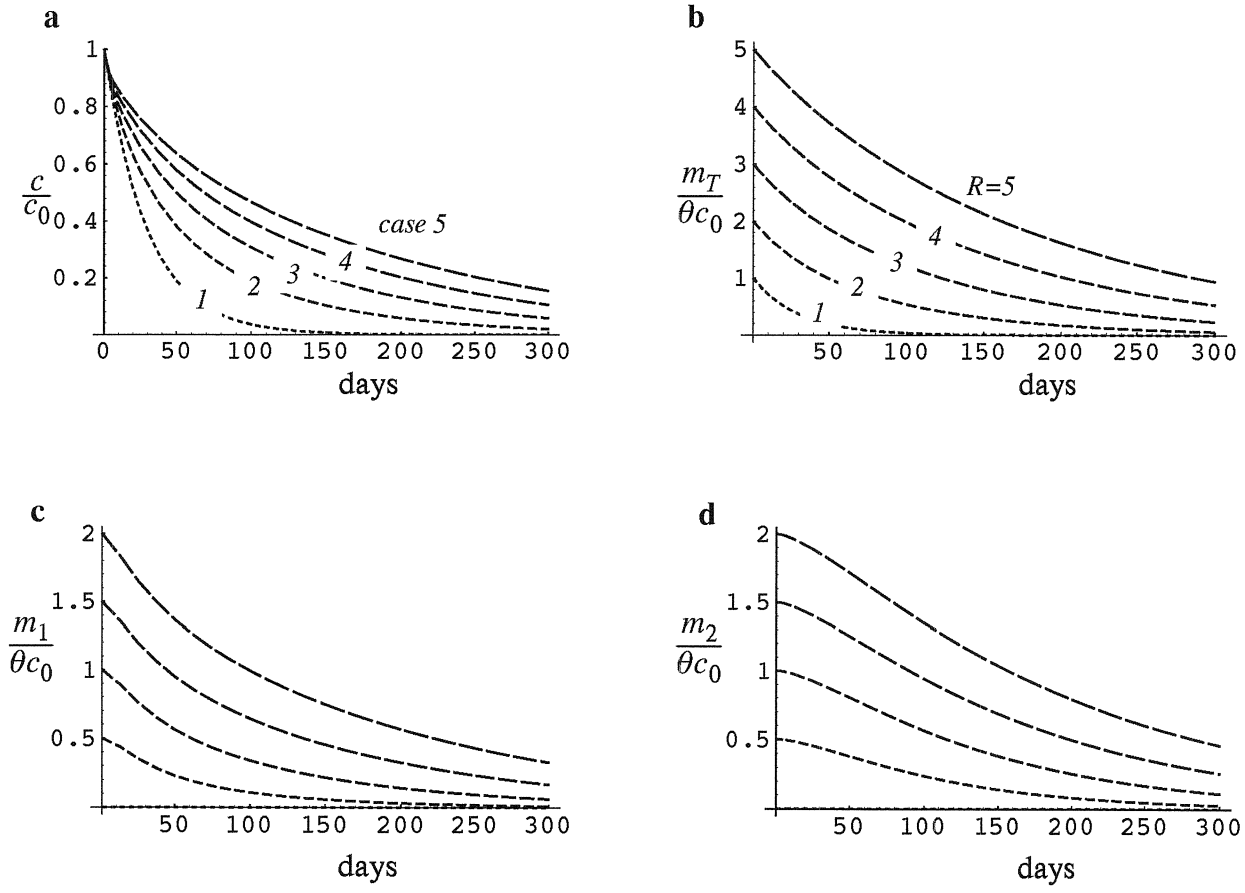

Figure 2.1.5 Effects of different storage capacity in sorption sites assuming $\theta=0.356$, $f_1=0.5$, $f_2=0.5$, $\tau_a=30$ days, $\tau_{s1}=10$ days, $\tau_{s2}=60$ days, $C_0=1mg/l$, $C_q=0mg/l$ and $\lambda=0$. *(a)* is for the aqueous phase concentration, (*b*) is for the total residual contaminant mass, (*c*) is for the residual contaminant mass in sorption site 1, and (*d*) is for the residual contaminant mass in sorption site 2.

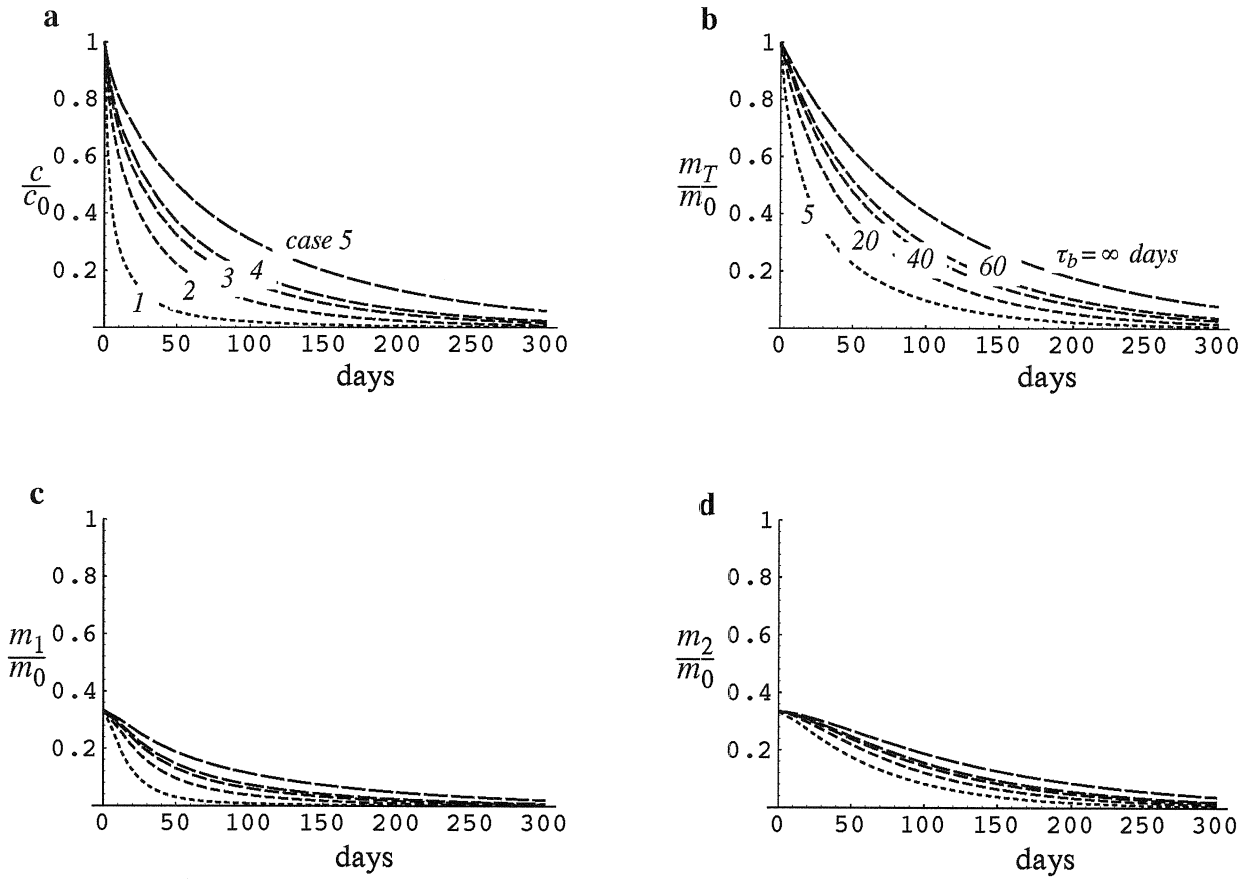

Figure 2.1.6 Effects of different biodegradation time constants under smaller sorption time constant in sorption site 2 assuming $\theta = 0.356, f_1 = 0.5, f_2 = 0.5, R = 3, \tau_a = 30$ *days*, $\tau_{s1} = 10$ *days*, $\tau_{s2} = 60$ *days*, $C_q = 0 mg/l$ and $C_0 = 1 mg/l$. *(a)* is for the aqueous phase concentration, (*b*) is for the total residual contaminant mass, (*c*) is for the residual contaminant mass in sorption site 1, and (*d*) is for the residual contaminant mass in sorption site 2.

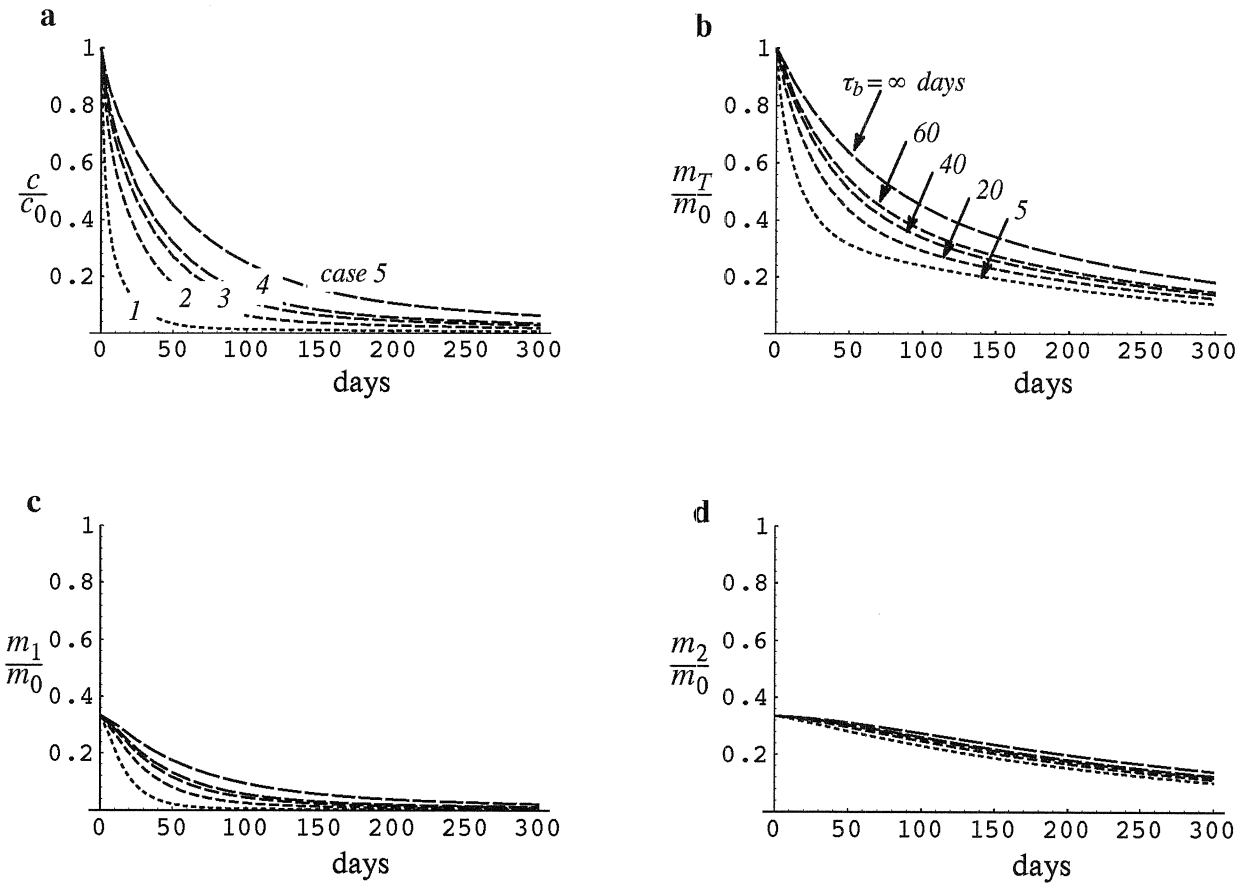

Figure 2.1.7 Effects of different biodegredation time constants under larger sorption time constant in sorption site 2 assuming $\theta = 0.356$, $f_1 = 0.5$, $f_2 = 0.5$, $R = 3$, $\tau_a = 30$ days, $\tau_{s1} = 10$ days, $\tau_{s2} = 240$ days, $C_q = 0 mg/l$ and $C_0 = 1 mg/l$. *(a)* is for the aqueous phase concentration, (*b*) is for the total residual contaminant mass, (*c*) is for the residual contaminant mass in sorption site 1, and (*d*) is for the residual contaminant mass in sorption site 2.

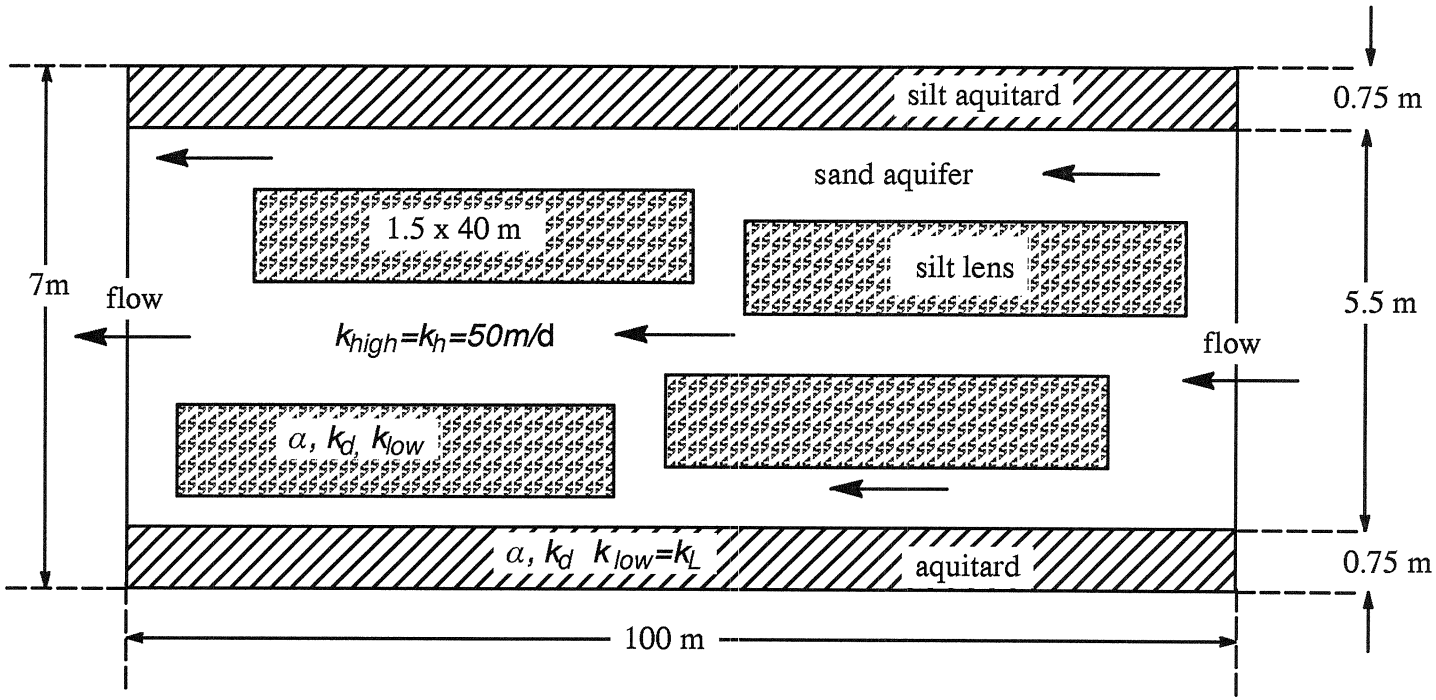

Figure 2.2.1 The cross section of the idealized aquifer system assuming sorption only occurs in the silt lenses and aquitards

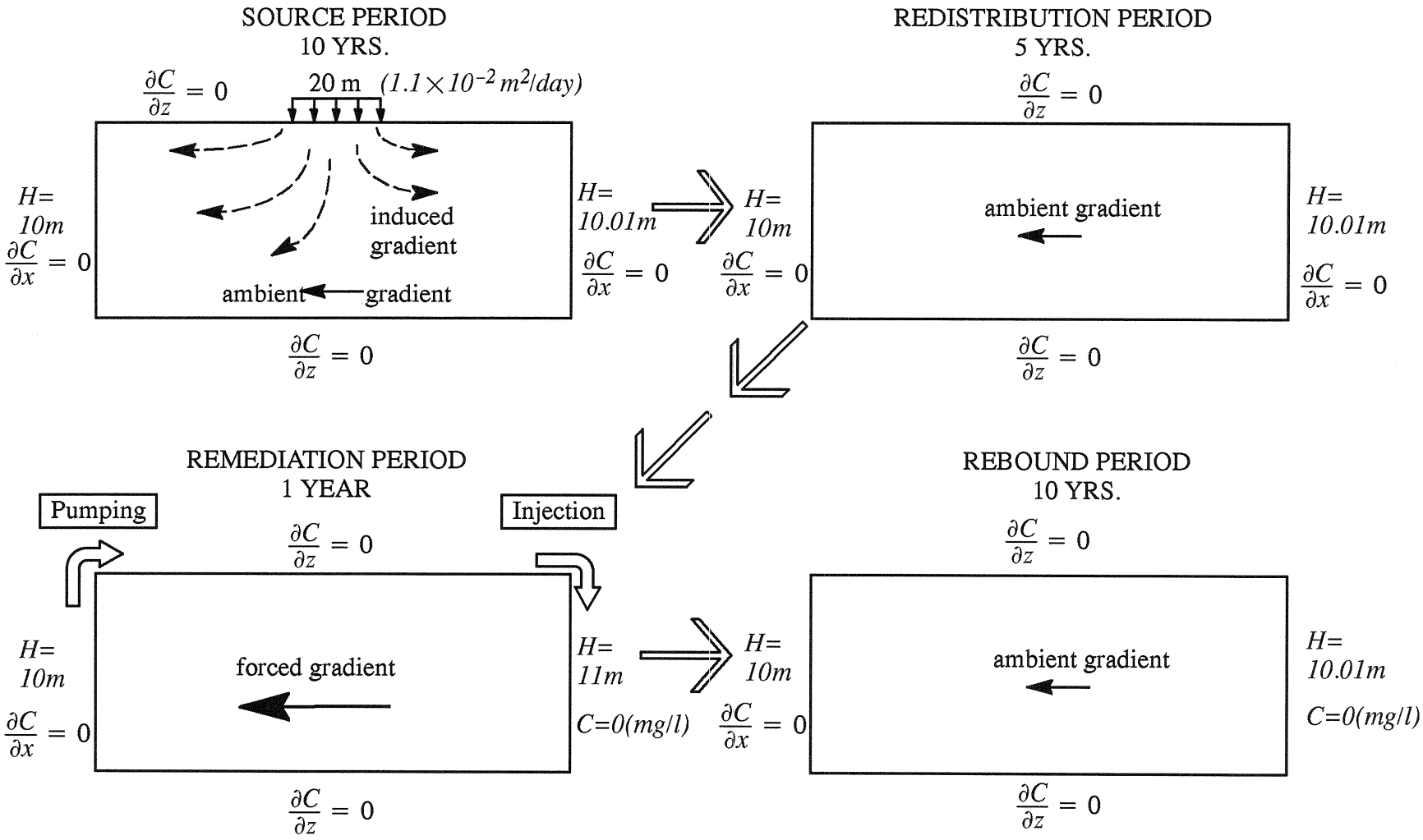

Figure 2.2.2 The scenario of the solute transport in the aquifer system

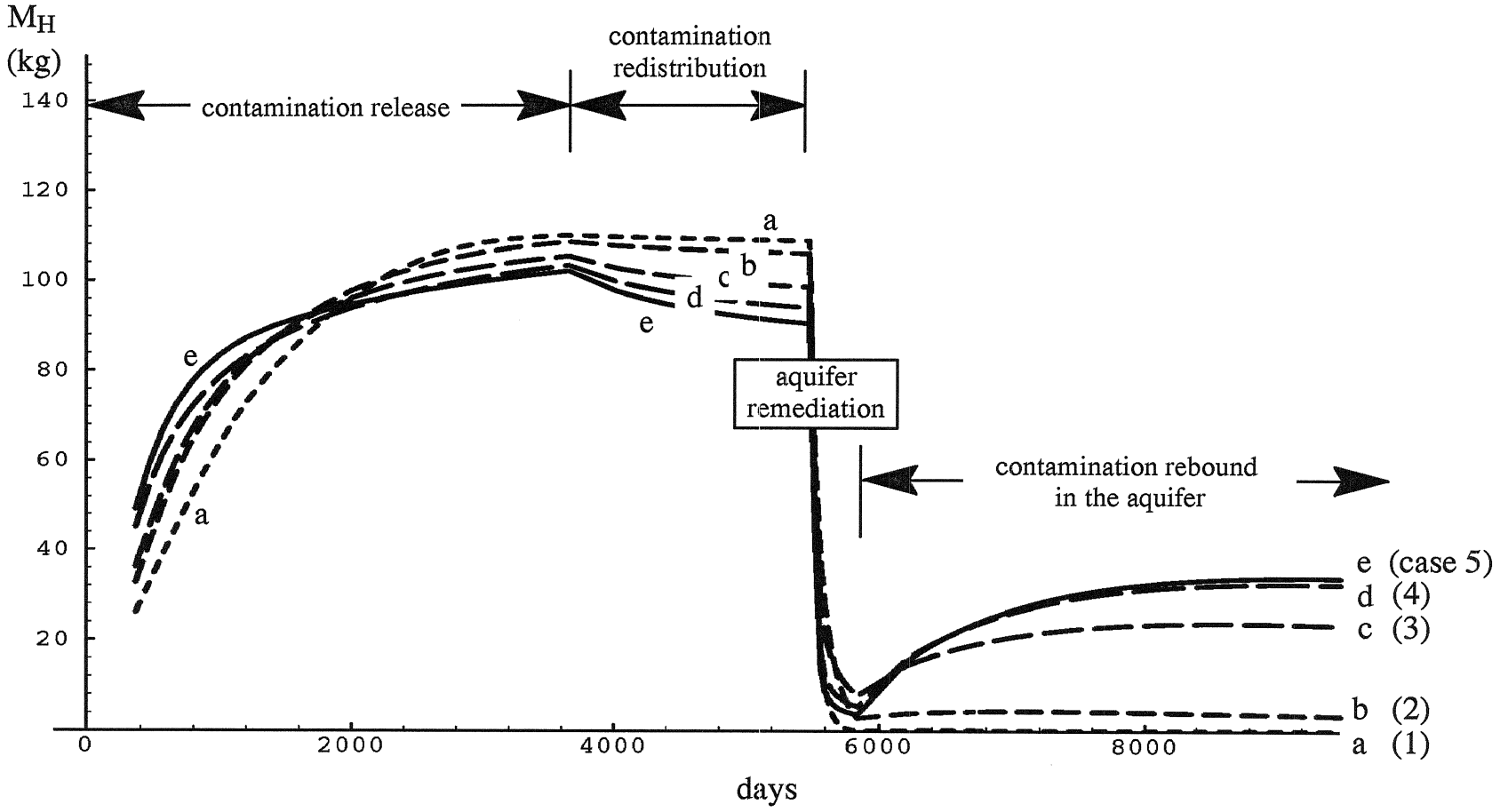

Figure 2.2.3 Comparison of the contaminant mass in the high–k aquifer showing the effects of different hydraulic conductivity in lenses and aquitards (k_h=50m/d, τ_s=40 days, R=2, and (a) k_L=50m/d; (b) k_L=10m/d; (c) k_L=1m/d; (d) k_L=0.05m/d; (e) k_L=0.005m/d)

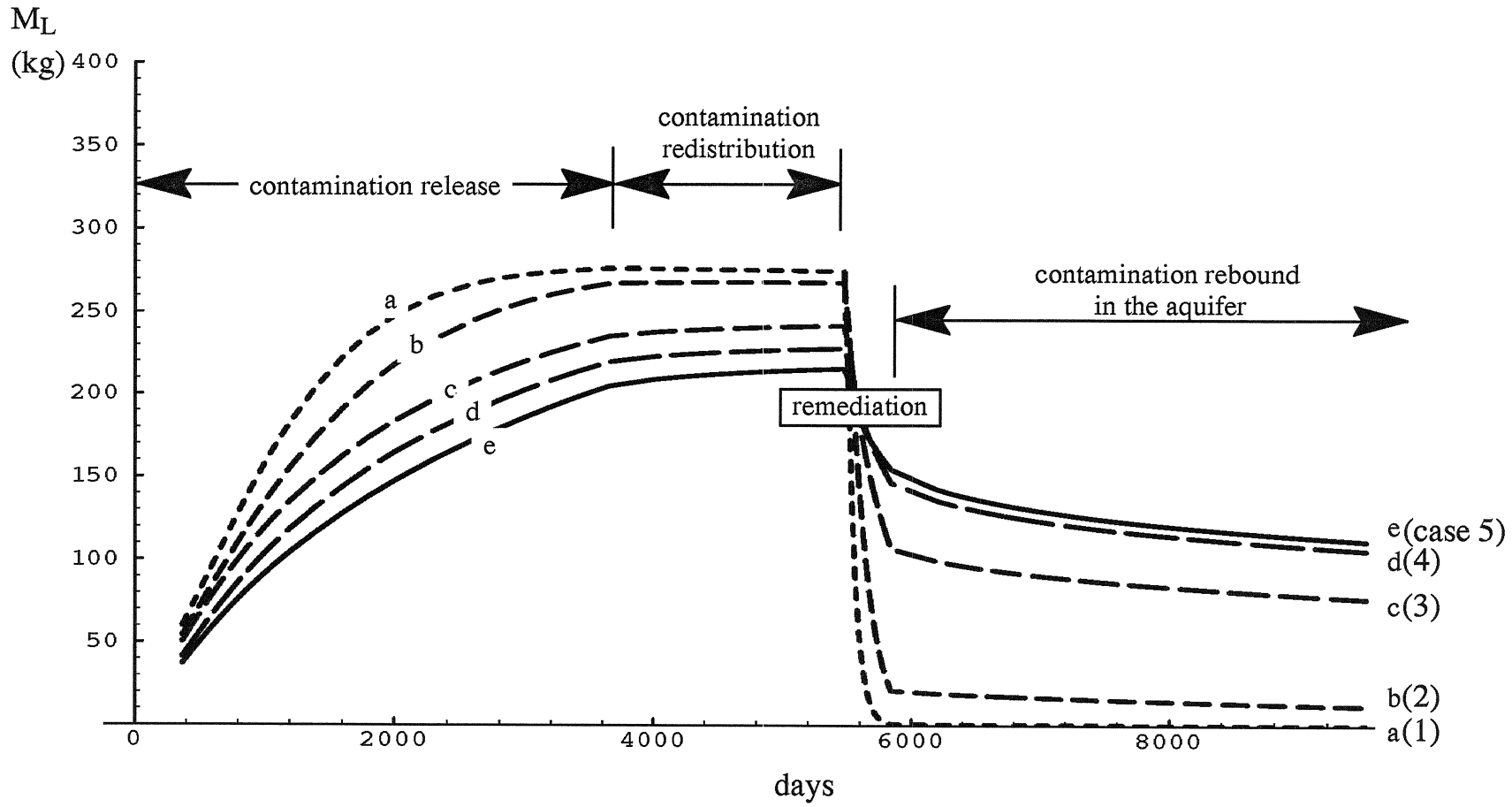

Figure 2.2.4 Comparison of the contaminant mass in the low-k lenses and aquitards showing the effects of different hydraulic conductivity in lenses and aquitards (k_h=50m/d, τ_s=40 days, R=2, and (a) k_L=50m/d; (b) k_L=10m/d; (c) k_L=1m/d; (d) k_L=0.05m/d; (e) k_L=0.005m/d)

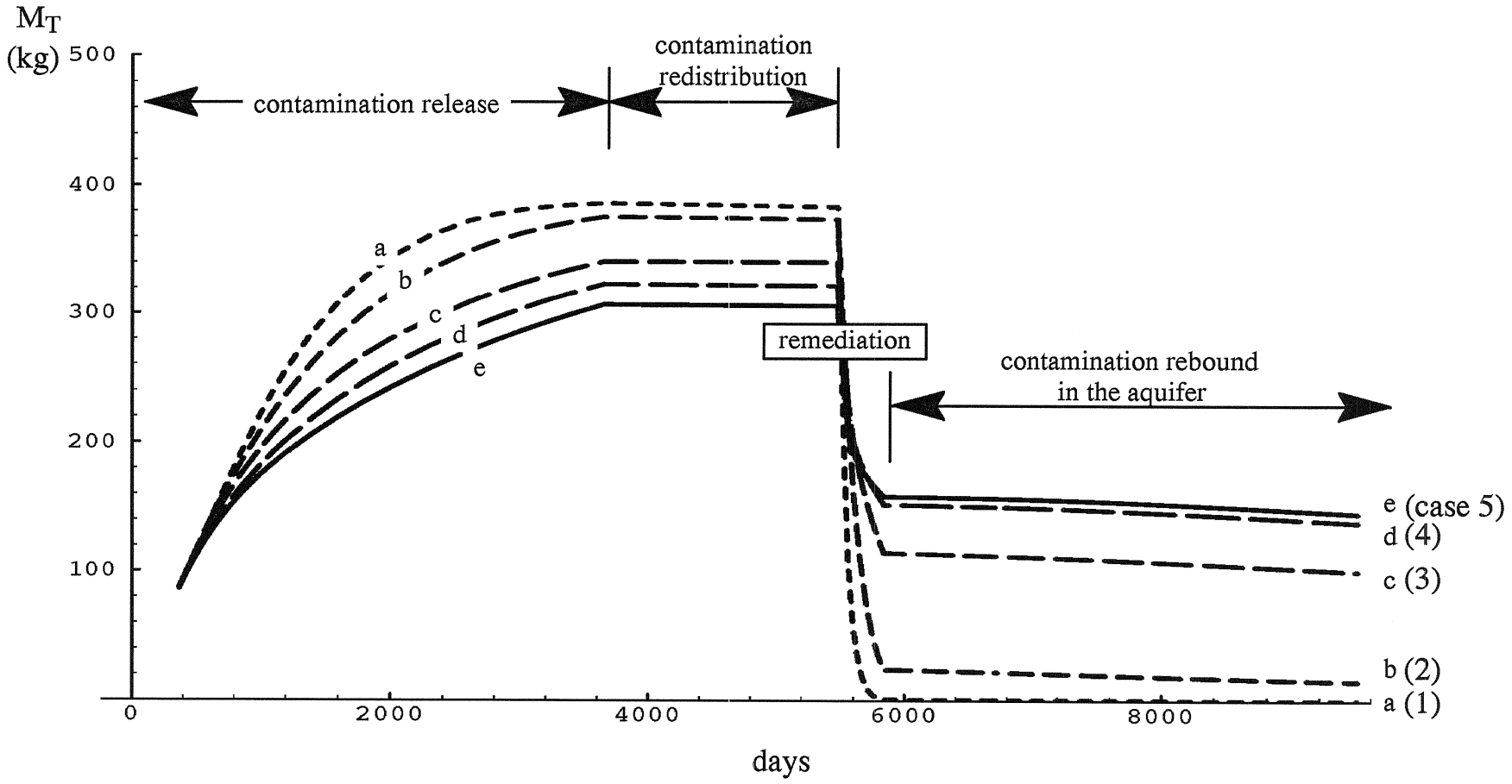

Figure 2.2.5 Comparison of the contaminant mass in the entire aquifer system showing the effects of different hydraulic conductivity in lenses and aquitards (k_h=50m/d, τ_s=40 days, R=2, and (a) k_L=50m/d; (b) k_L=10m/d; (c) k_L=1m/d; (d) k_L=0.05m/d; (e)k_L=0.005m/d)

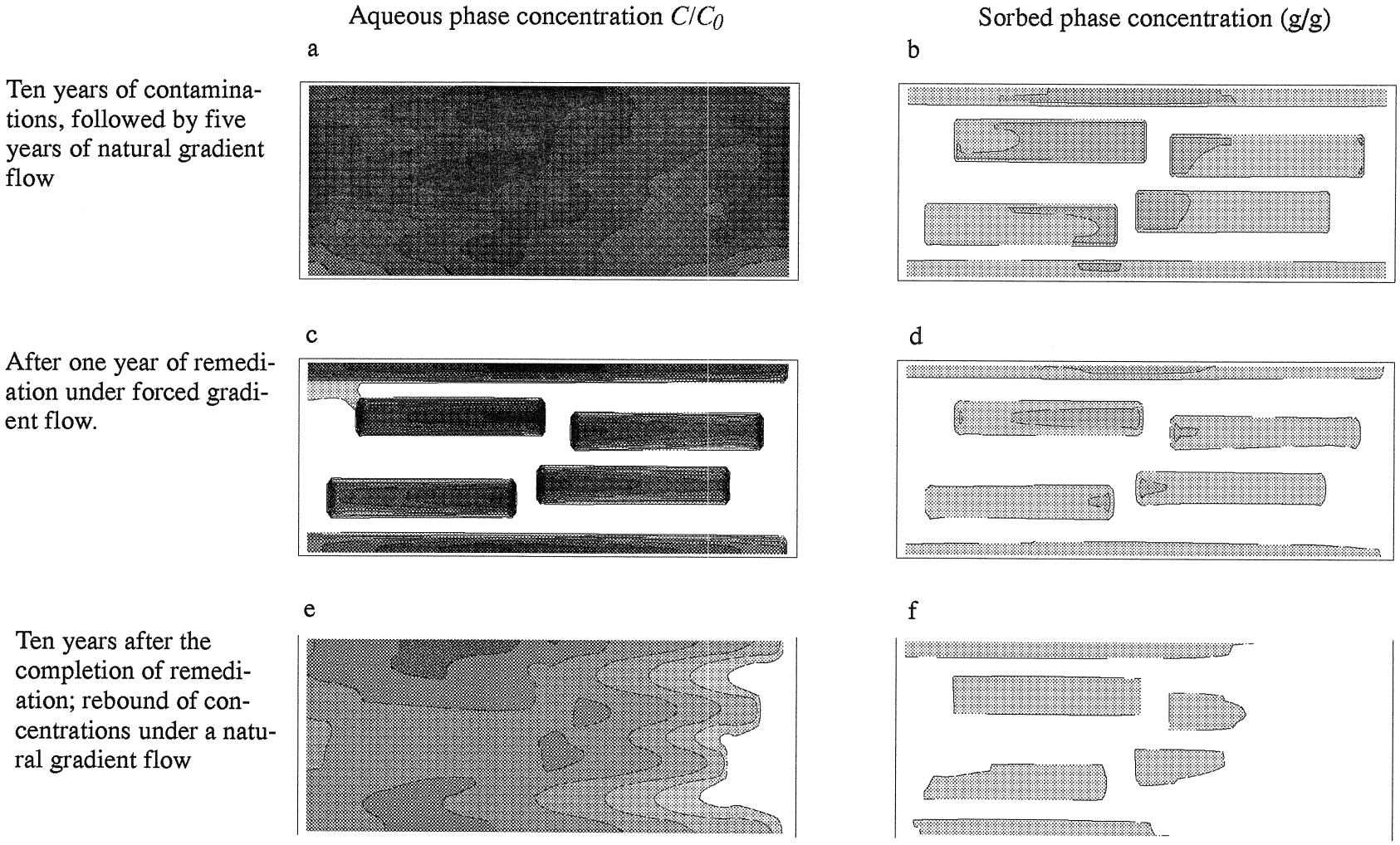

Figure 2.2.6 Contamination and remediation of a heterogeneous aquifer system experiencing rate–limited sorption in lenses and aquitards. Contour lines are shaded from black (>0.9) to white (<0.1) (k_h=50m/d, k_L=0.005m/d, τ_s=40 days and R=2).

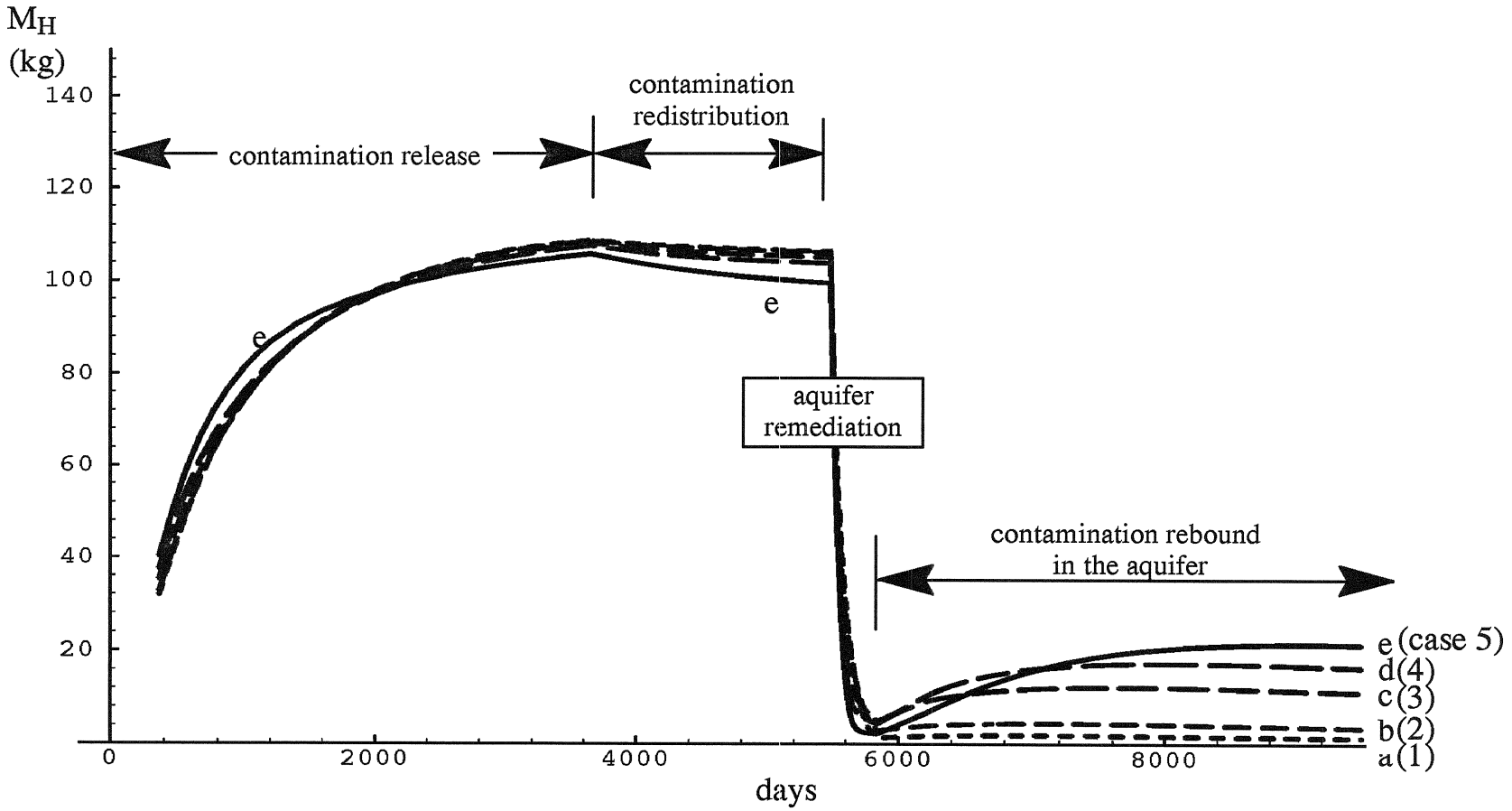

Figure 2.2.7 Comparison of the contaminant mass in the high–k aquifer showing the effects of sorption time constants (k_h=50m/d, k_L=10m/d, R=2, and (a) τ_s=0 days; (b) τ_s=40 days; (c) τ_s=180 days; (d) τ_s=1 year; (e) τ_s=3 years)

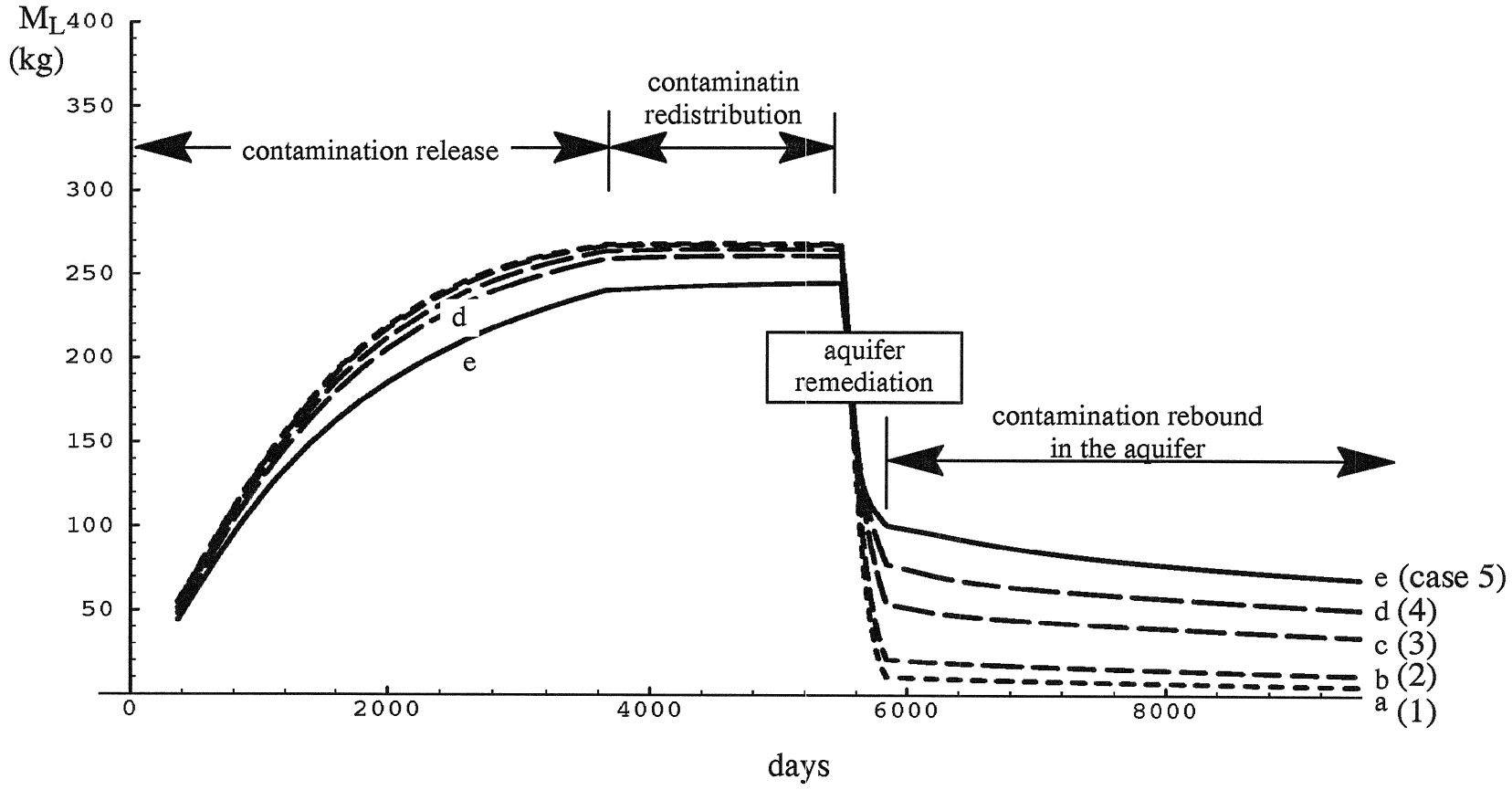

Figure 2.2.8 Comparison of the contaminant mass in the lenses and aquitards showing the effects of sorption time constants (k_h=50m/d, k_L=10m/d, R=2, and (a) τ_s=0 day; (b) τ_s=40 days; (c) τ_s=180 days; (d) τ_s=1 year; (e) τ_s=3 years)

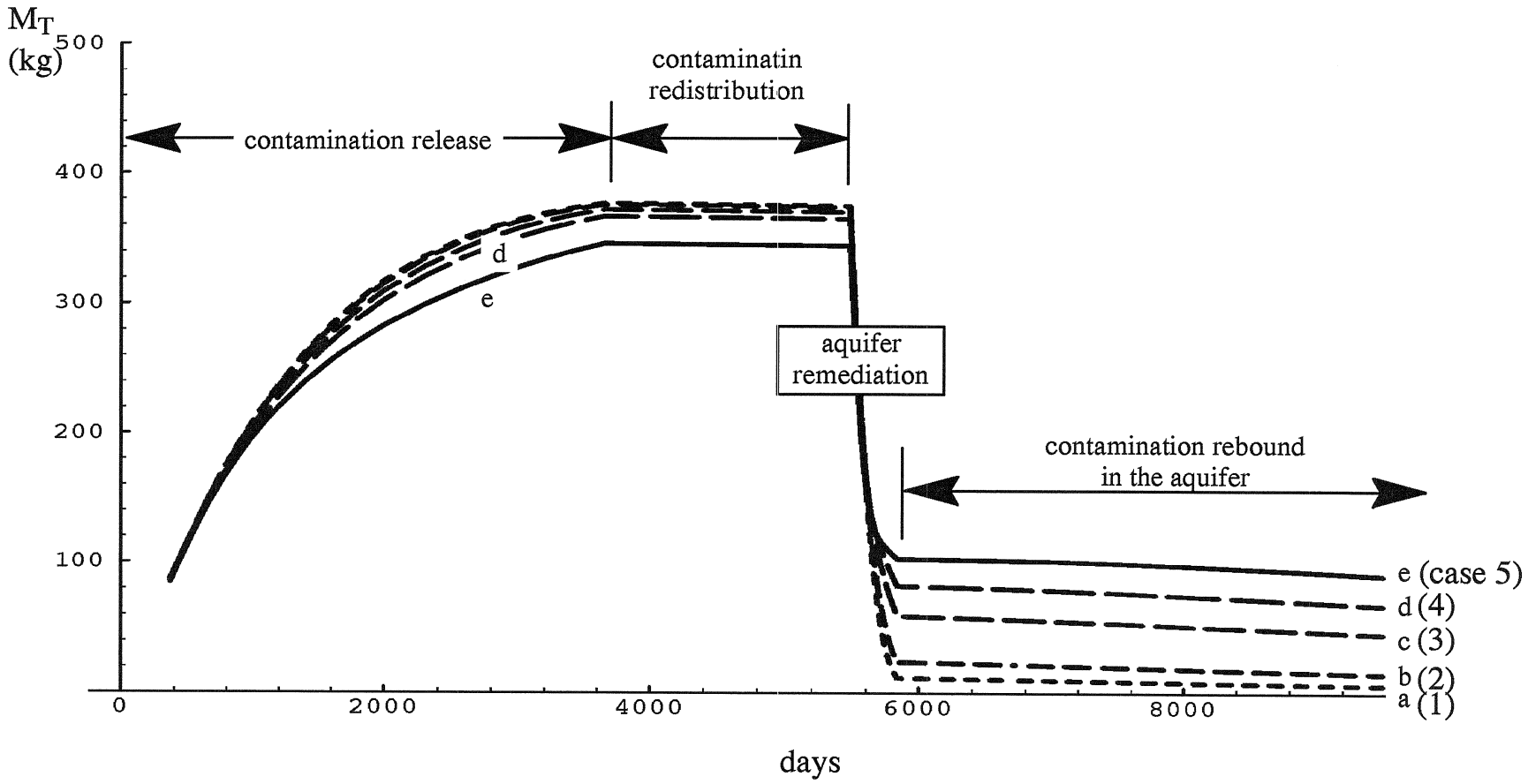

Figure 2.2.9 Comparison of the contaminant mass in the entire aquifer system showing the effects of sorption time constants (k_h=50m/d, k_L=10m/d, R=2, and (a) τ_s=0 day; (b) τ_s=40 days; (c) τ_s=180 days; (d) τ_s=1 year; (e) τ_s=3 years)

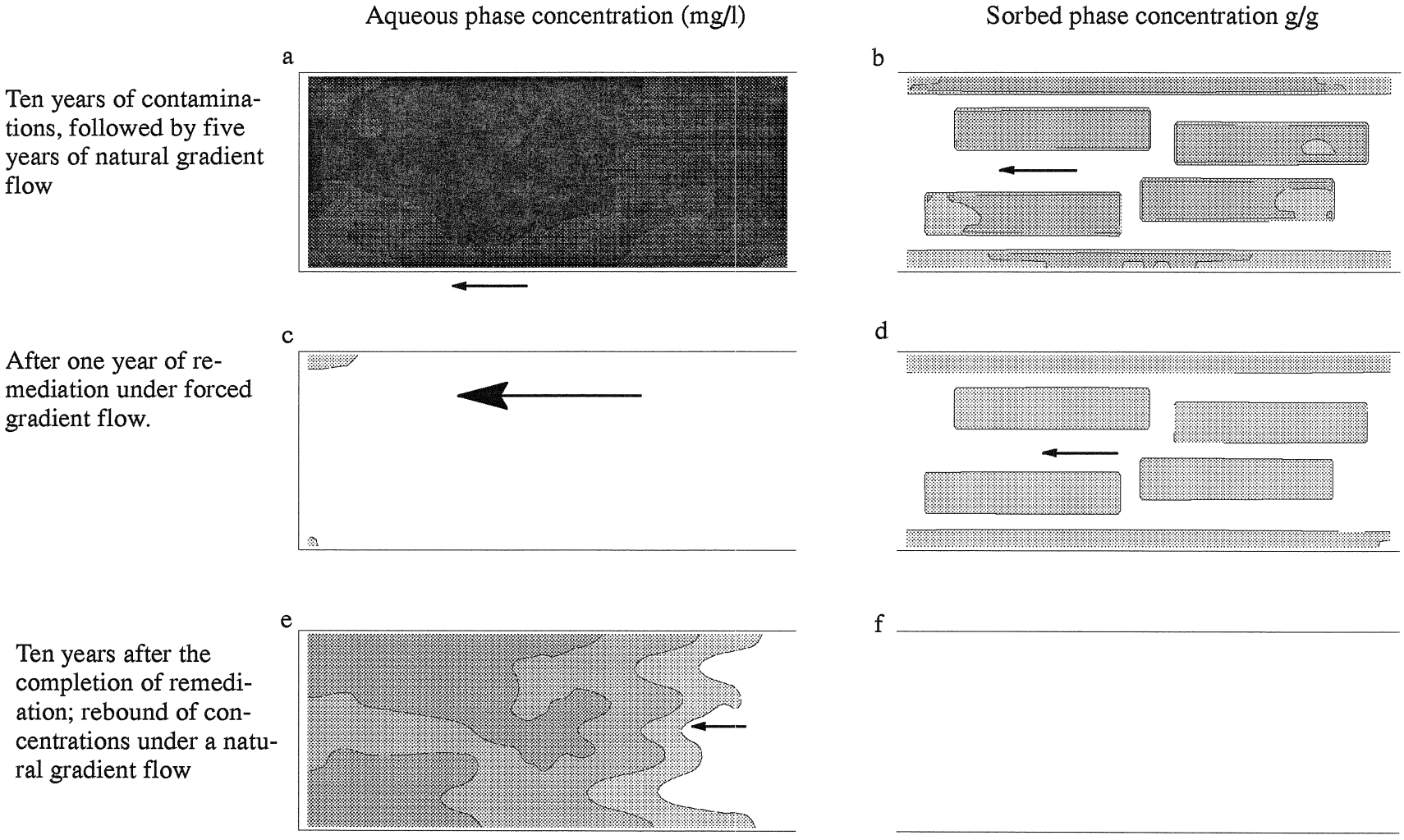

Figure 2.2.10 Contamination and remediation of a heterogeneous aquifer system experiencing rate-limited sorption in lenses and aquitards. Contour lines are shaded from black (>0.9) to white (<0.1). (k_h=50m/d, k_L=10m/d, τ_s=3 years and R=2)

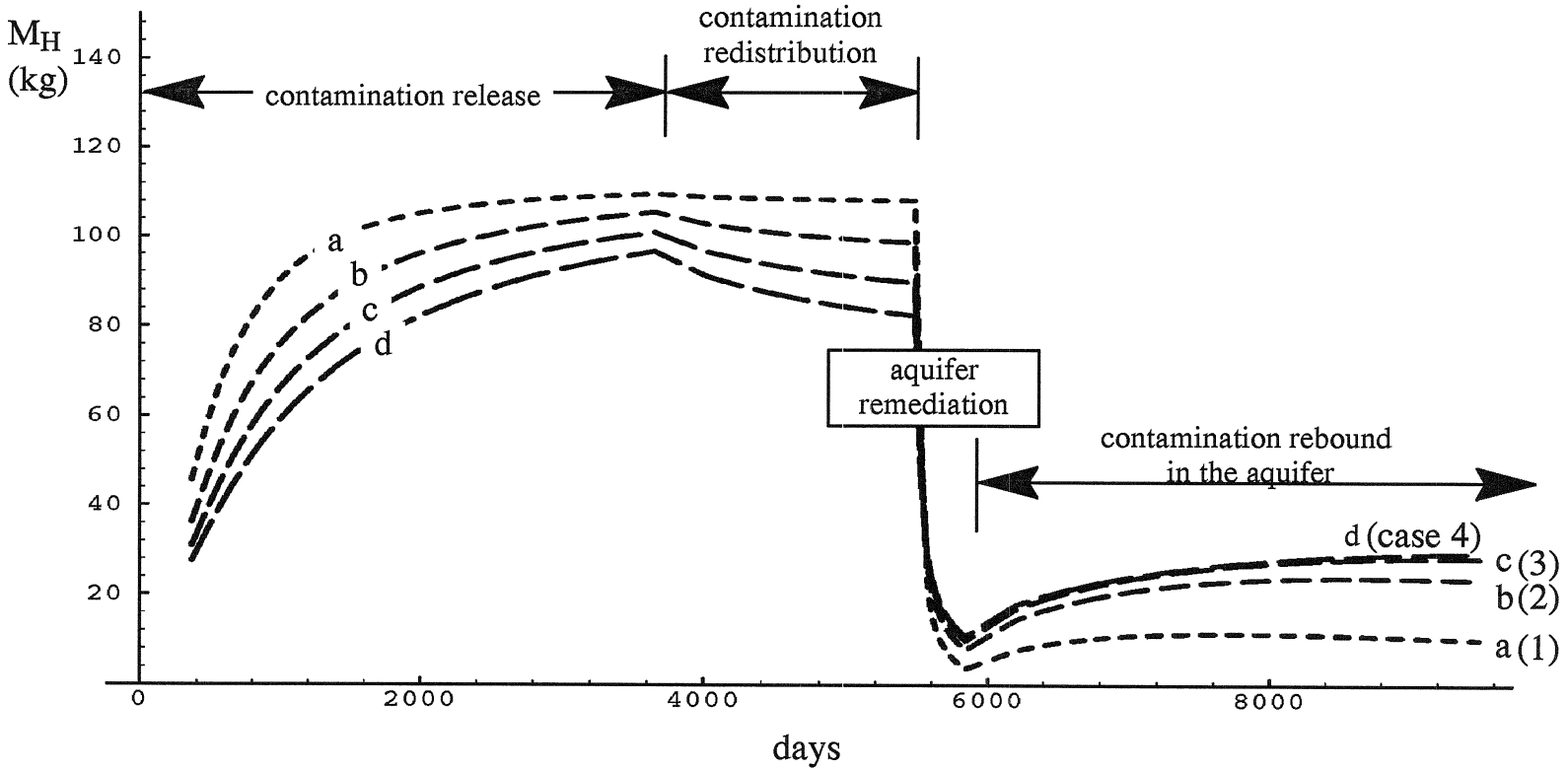

Figure 2.2.11 Comparison of the contaminant mass in the high–k aquifer showing the effects of storage capacity in the sorption site (k_h=50m/d, k_L=1m/d, τ_s= 40days, and (a) R=1; (b) R=2; (c) R=3; (d) R=4.)

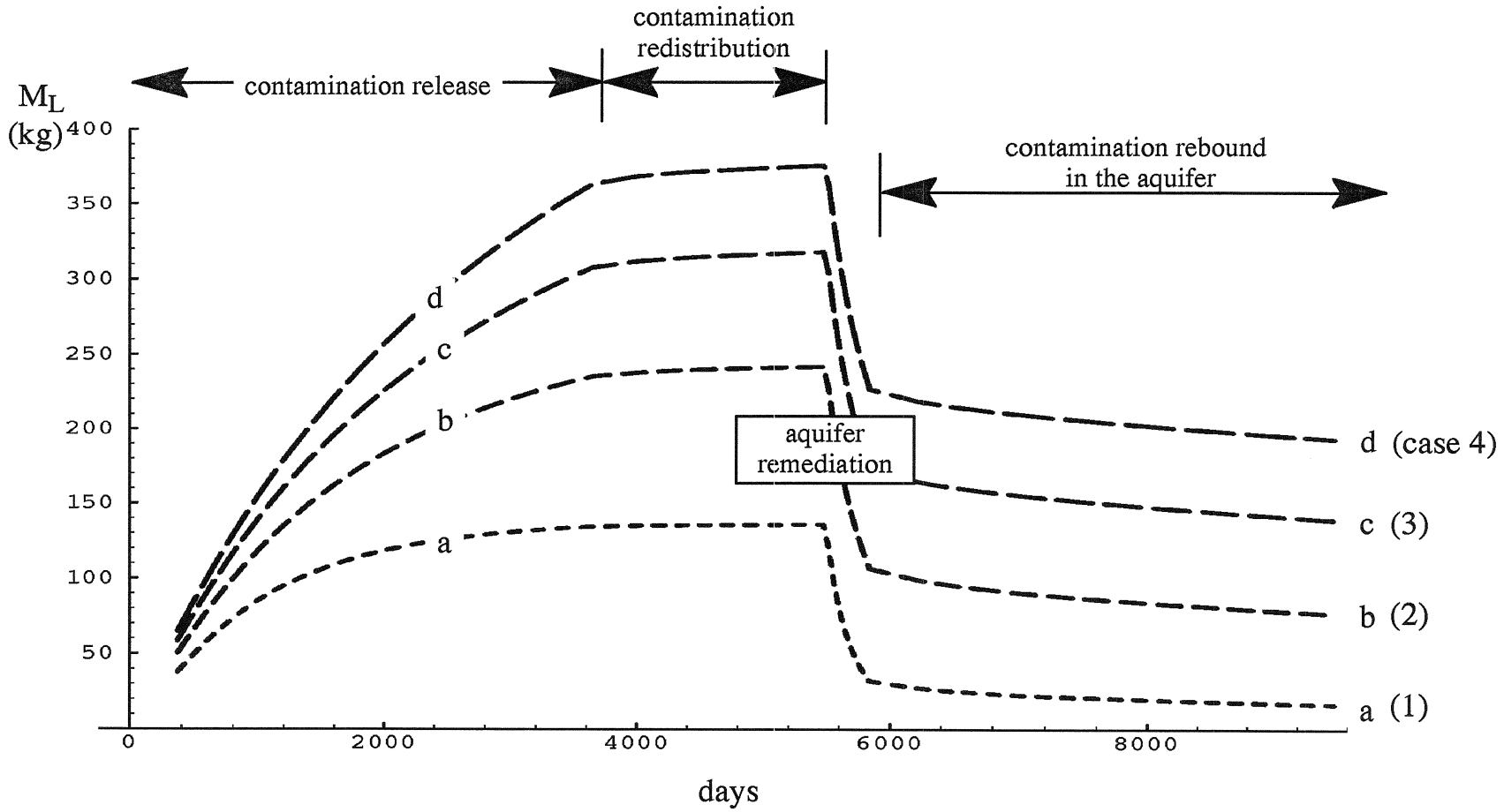

Figure 2.2.12 Comparison of the contaminant mass in lenses and aquitards showing the effects of storage capacity in the sorption site (k_h=50m/d, k_L=1m/d, τ_s=40 days, and (a) R=1; (b) R=2; (c) R=3; (d) R=4.)

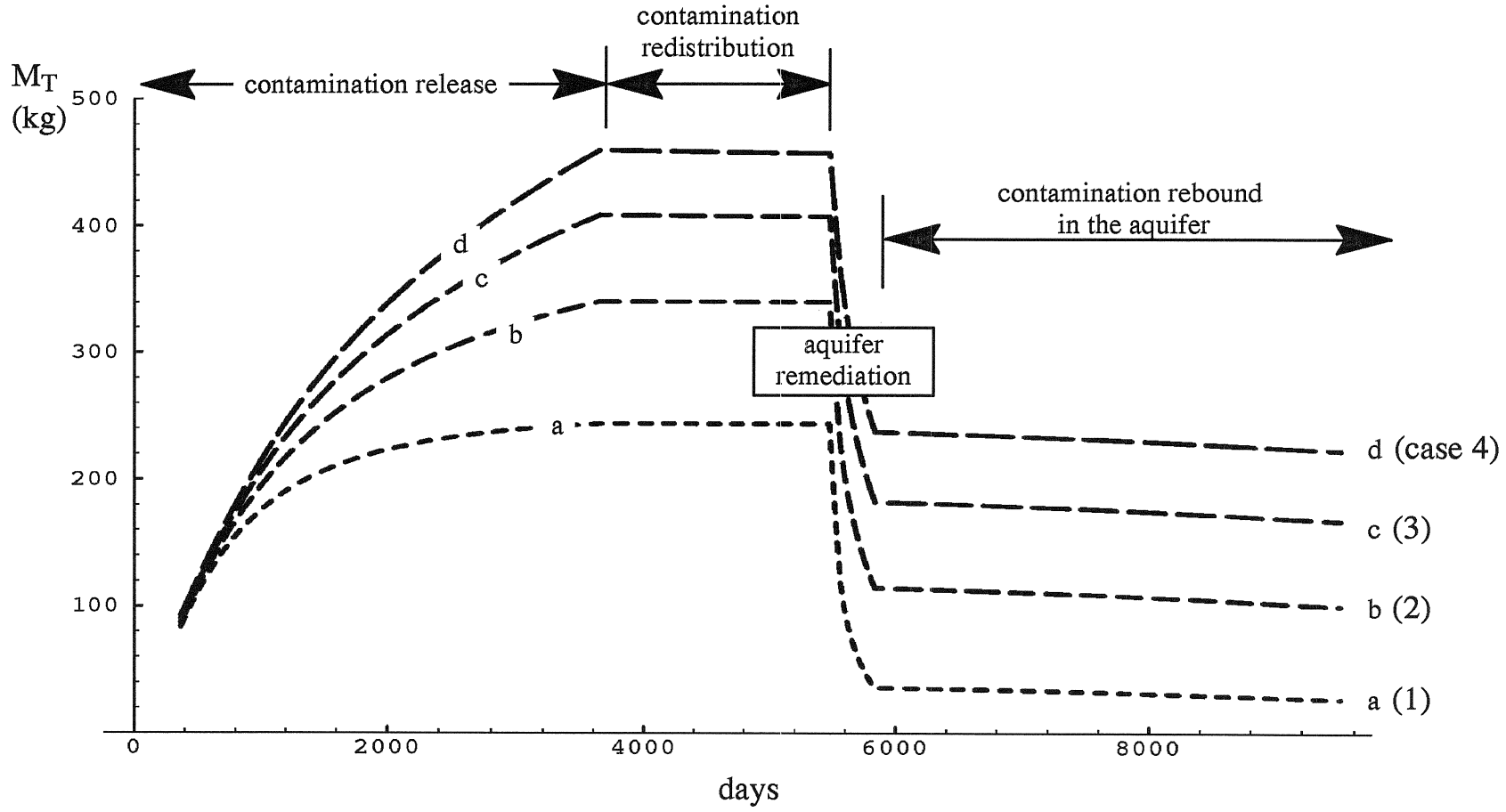

Figure 2.2.13 Comparison of the contaminant mass in the entire aquifer system showing the effects of storage capacity in the sorption site (k_h=50m/d, k_L=1m/d, τ_s=40 days, and (a) R=1; (b) R=2; (c) R=3; (d) R=4.)

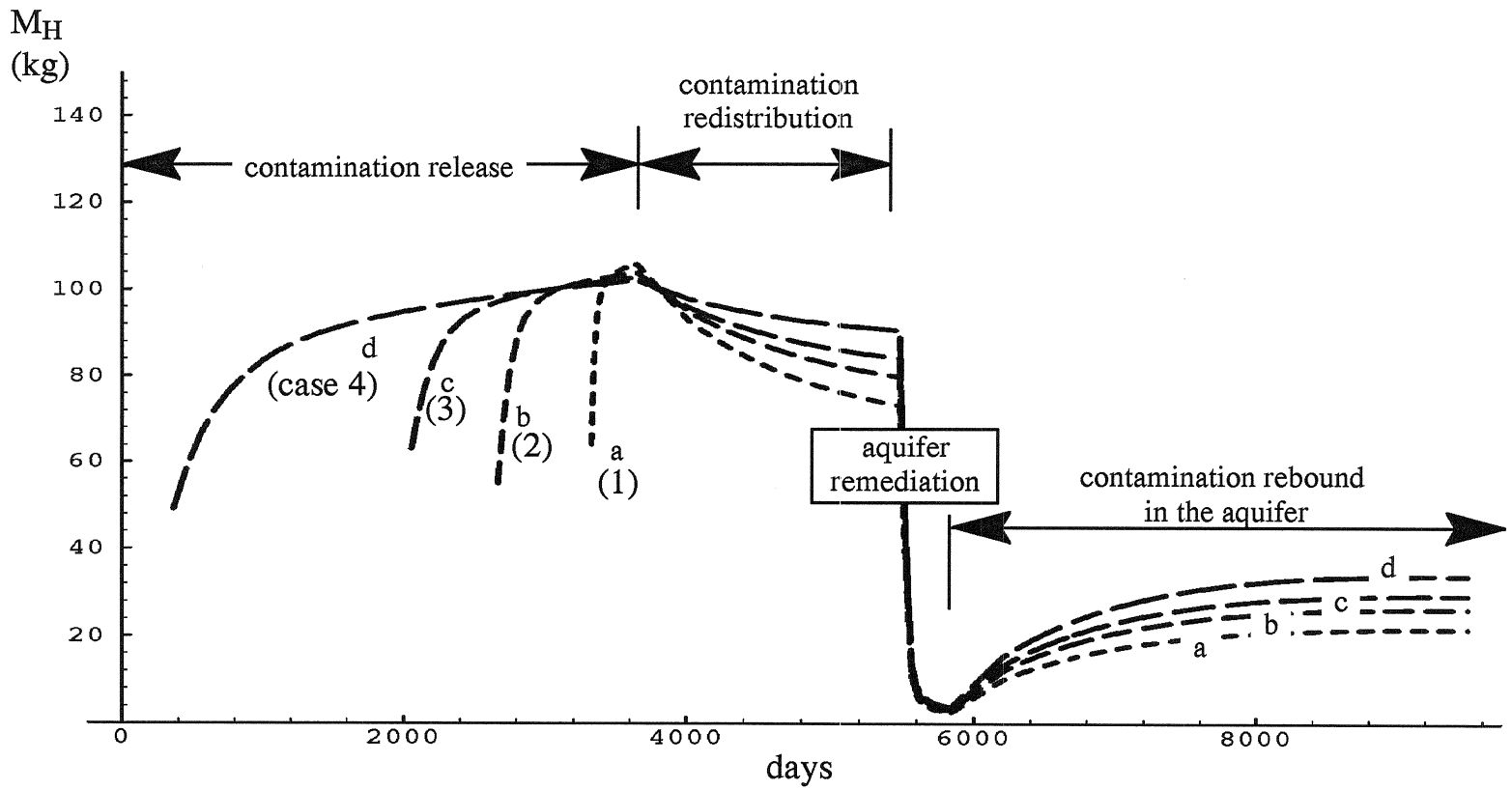

Figure 2.2.14 Comparison of the contaminant mass in the high–k aquifer showing the effects of contamination release duration. Curve a is for the 1 year's contamination; curve b is for the 3–years' contamination; curve c is for the 5–years' contamination, and curve d is for the 10–years' contamination. (k_h=50m/d, k_L=0.005m/d, R=2 and τ_s=40 days)

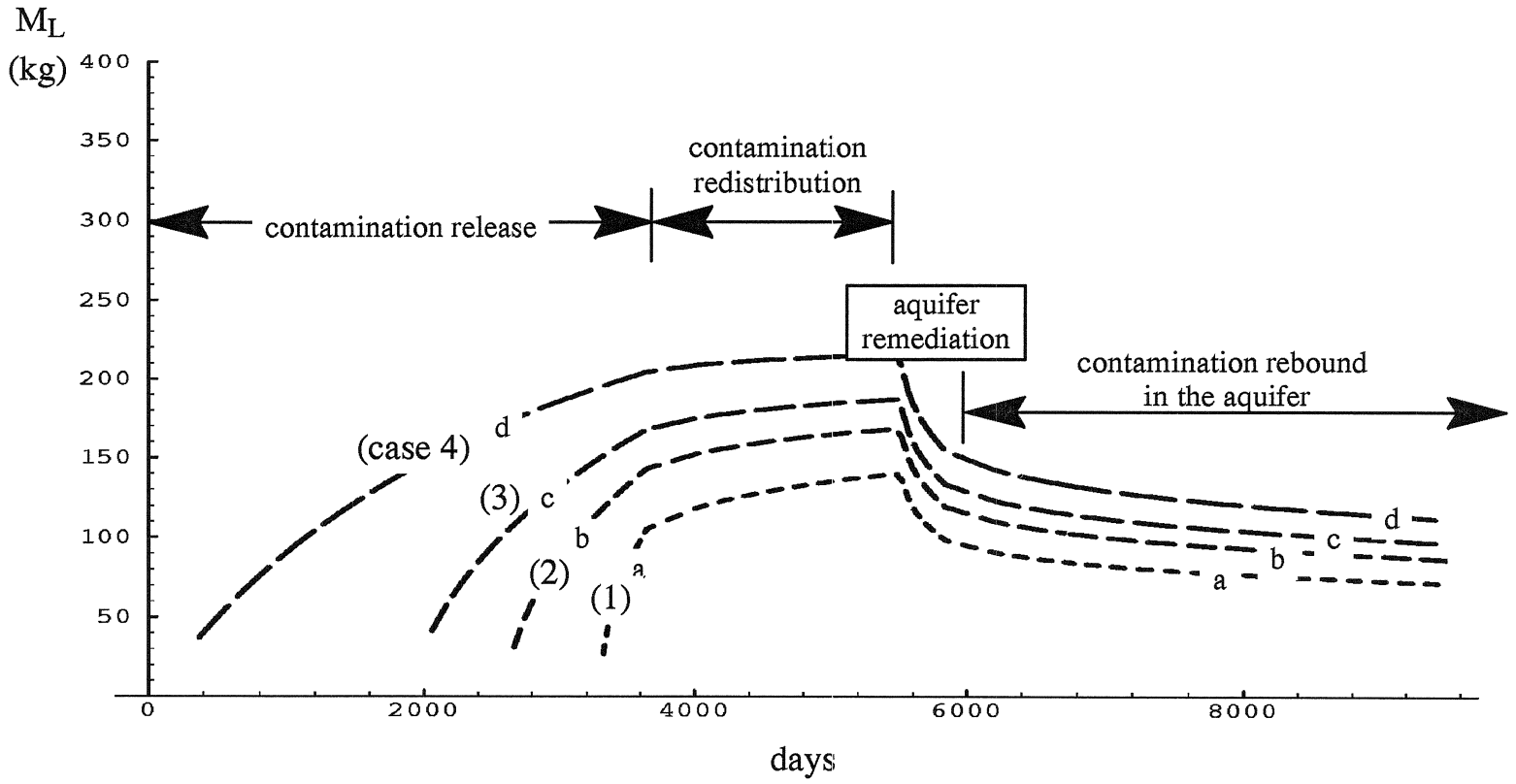

Figure 2.2.15 Comparison of the contaminant mass in lenses and aquitards showing the effects of contamination release duration. Curve a is for the 1 year's contamination; curve b is for the 3-years' contamination; curve c is for the 5-years' contamination, and curve d is for the 10-years' contamination. (k_h=50m/d, k_L=0.005m/d, R=2 and τ_s=40 days)

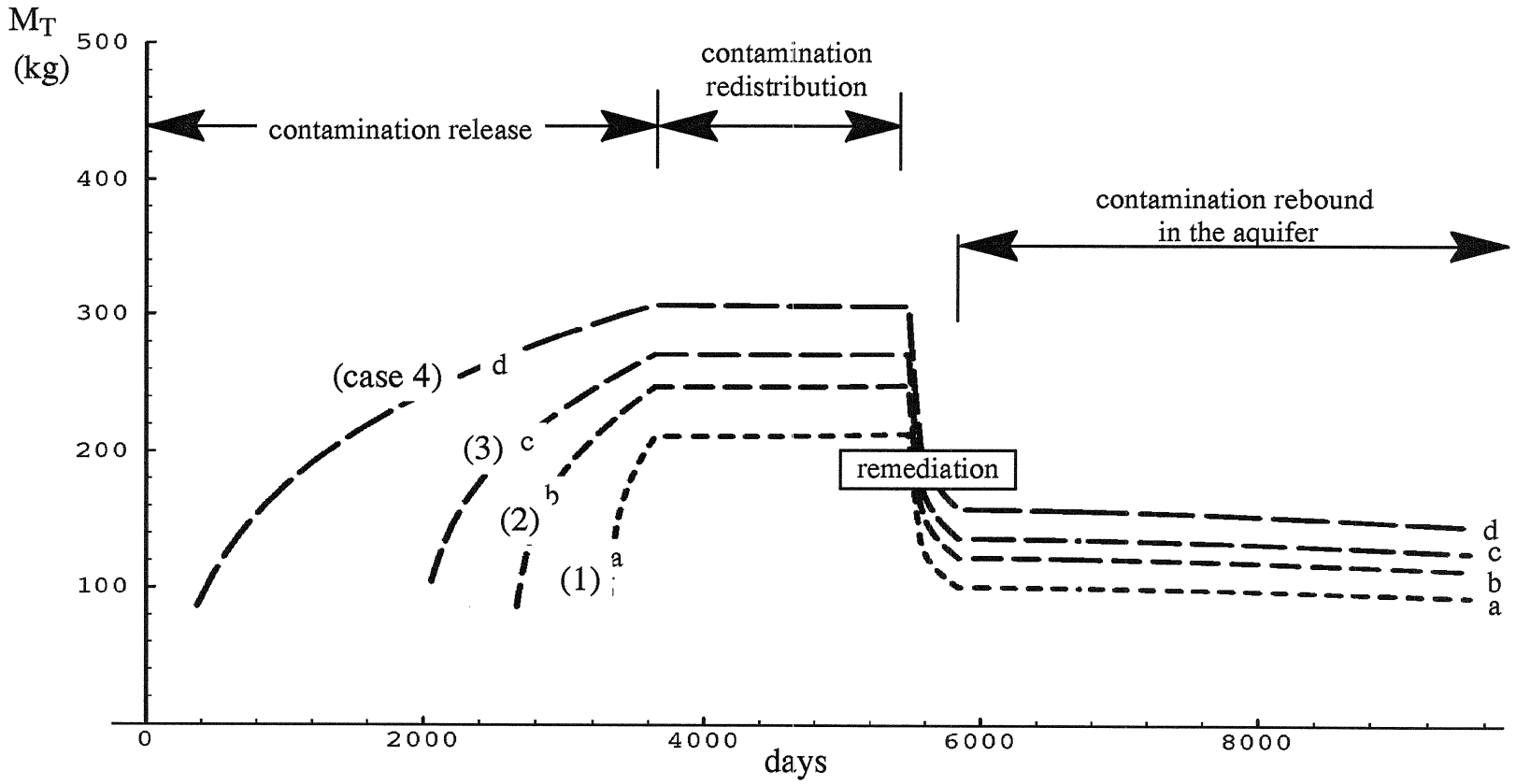

Figure 2.2.16 Comparison of the contaminant mass in the aquifer system showing the effects of contamination release duration. Curve a is for the 1 year's contamination; curve b is for the 3-years' contamination; curve c is for the 5-years' contamination, and curve d is for the 10-years' contamination. (k_h=50m/d, k_L=0.005m/d, R=2 and τ_s=40 days)

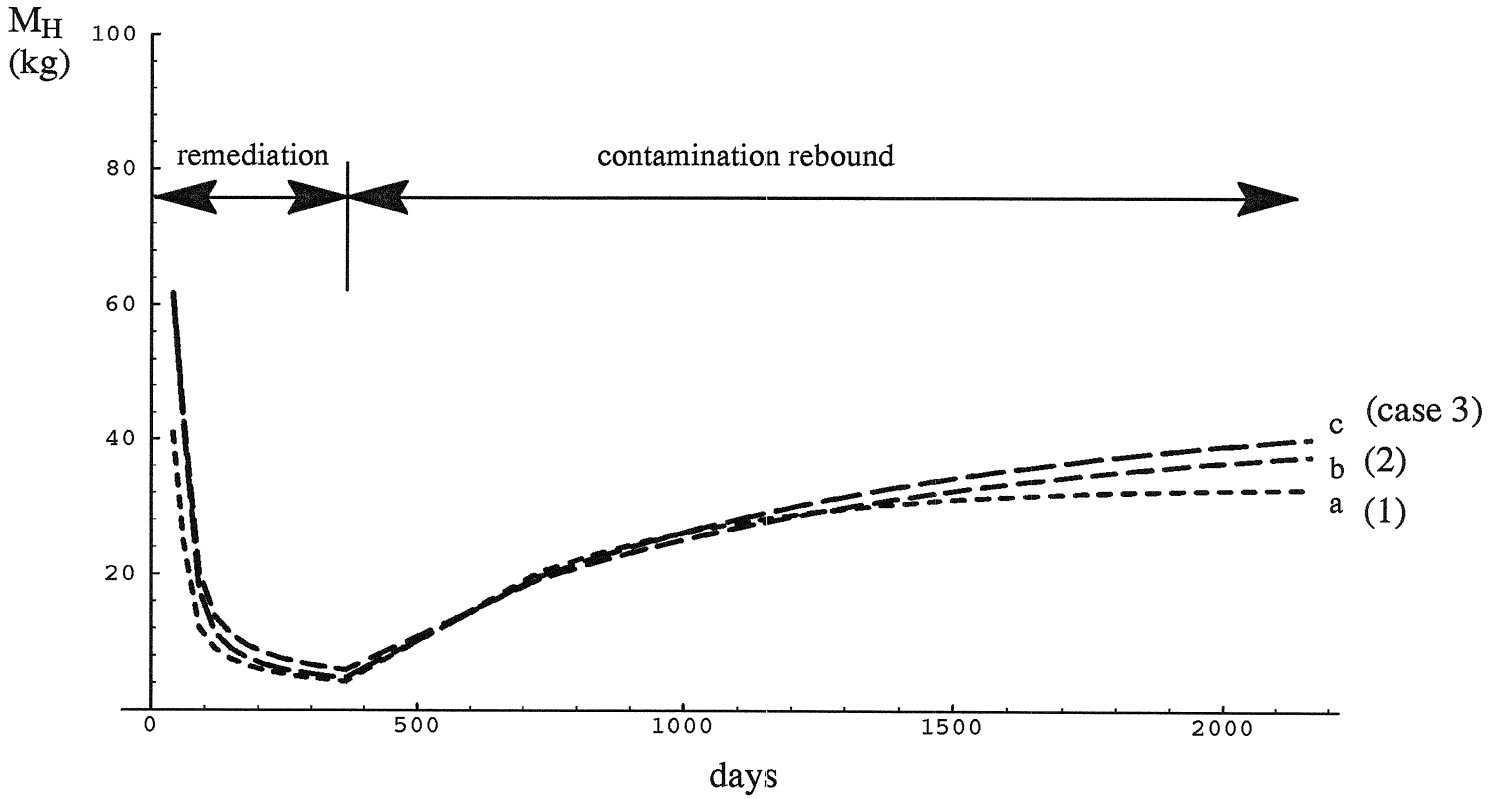

Figure 2.2.17 Comparison of the contaminant mass in the high–k aquifer showing the effects of the hydraulic fracturing. The aquifer system is fully contaminated before remediation. Curve a is for the cut–through fractures in lenses; curve b is for the not–cut–through fracture in lenses; curve c is for the case without hydraulic fractures in lenses. (k_h=50m/d, k_L=0.005m/d, R=2 and τ_s=40 days)

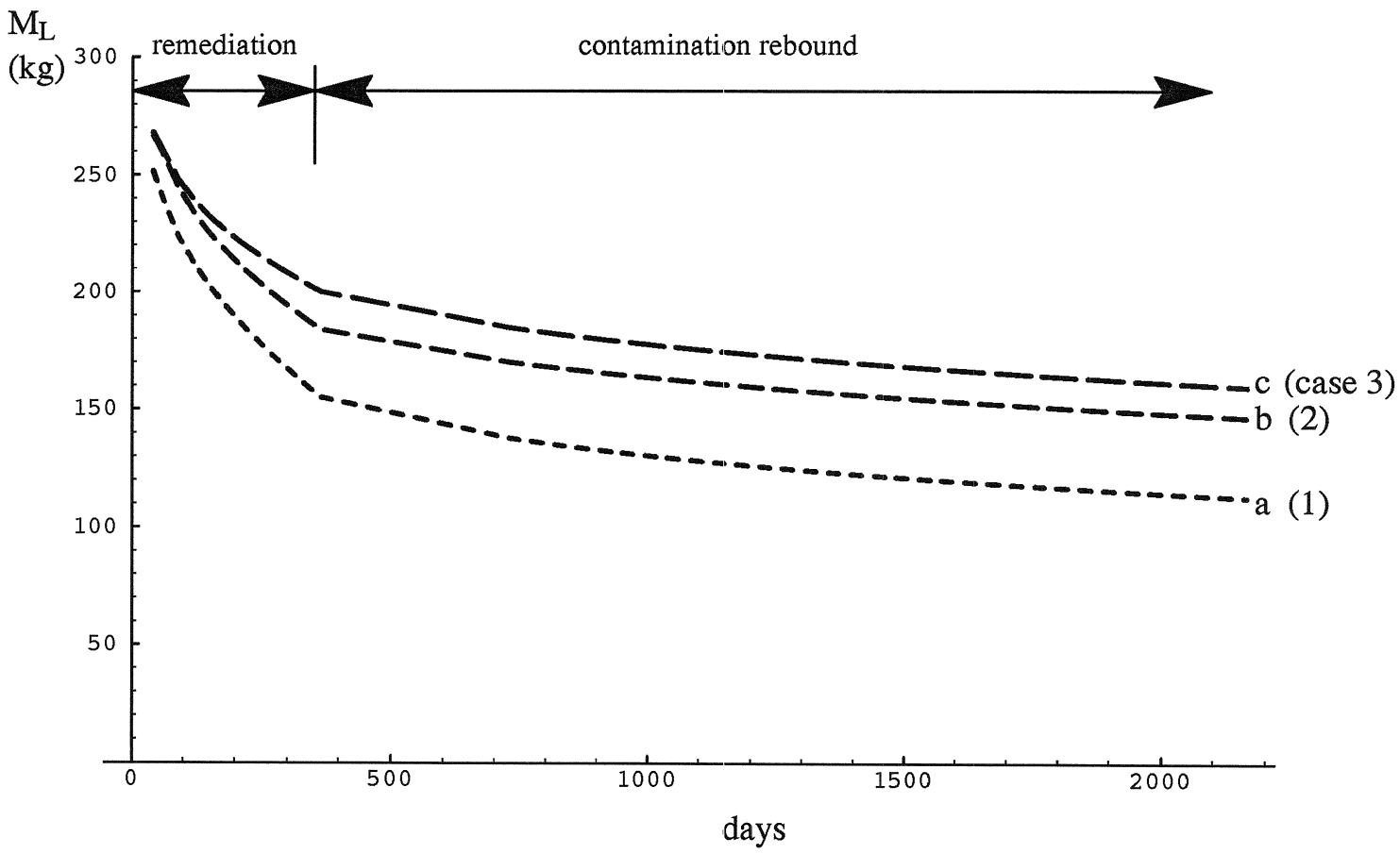

Figure 2.2.18 Comparison of the contaminant mass in lenses and aquitards showing the effects of the hydraulic fracturing. The aquifer system is fully contaminated before remediation. Curve a is for the cut-through fractures in lenses; curve b is for the not-cut-through fracture in lenses; curve c is for the case without hydraulic fractures in lenses. (k_h=50m/d, k_L=0.005m/d, R=2 and τ_s=40 days)

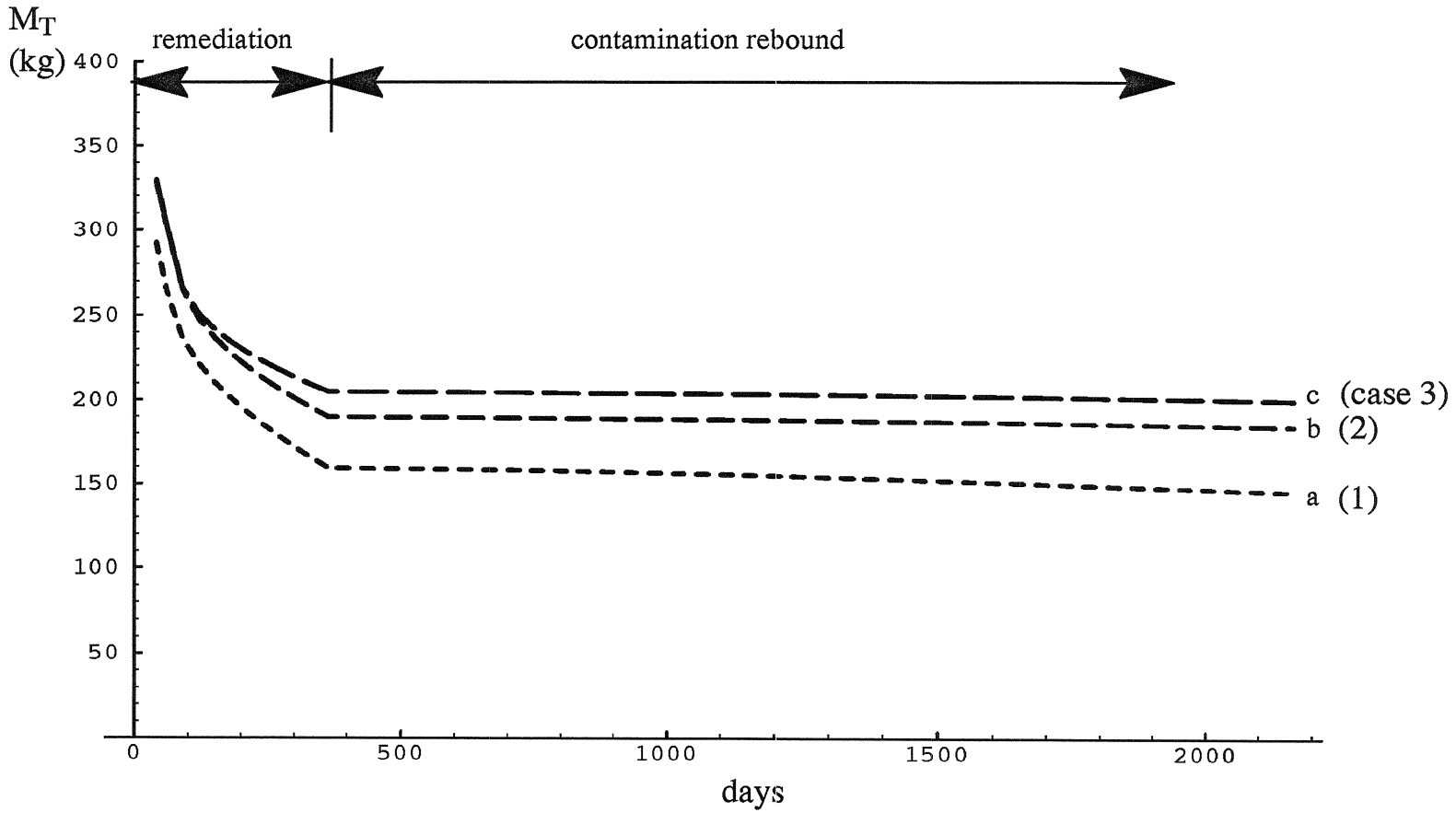

Figure 2.2.19 Comparison of the contaminant mass in the entire aquifer system showing the effects of the hydraulic fracturing. The aquifer system is fully contaminated before remediation. Curve a is for the cut-through fractures in lenses; curve b is for the not-cut-through fracture in lenses; curve c is for the case without hydraulic fractures in lenses. (k_h=50m/d, k_L=0.005m/d, R=2 and τ_s=40 days)

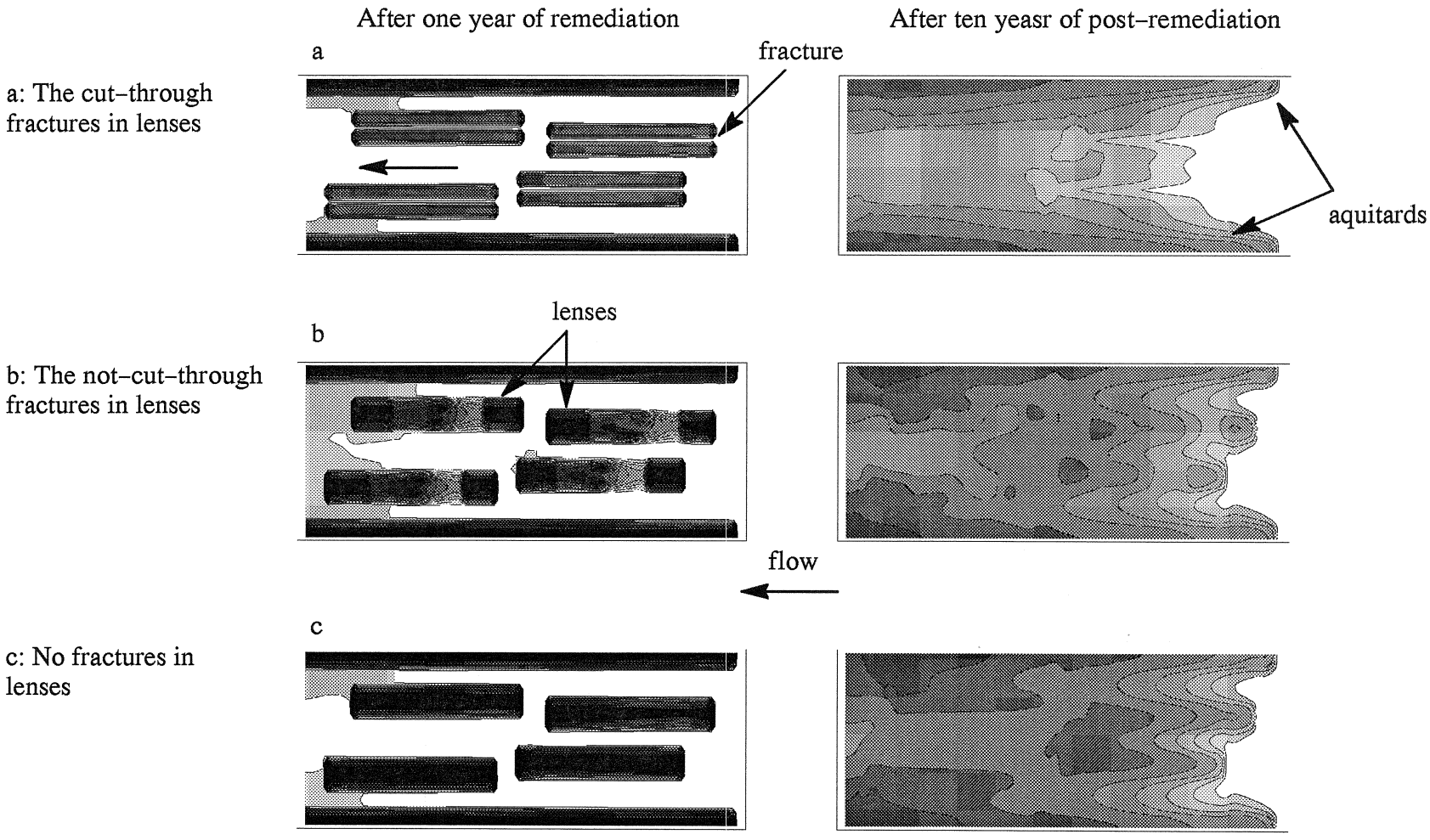

Figure 2.2.20 Comparison of the aqueous phase concentration showing the effects of fractures in low-k lenses. Contour lines are shaded from black (>0.9C_0) to white (<0.1C_0) (k_h=50m/d, k_L=0.005m/d, R=2 and τ_s=40 days).

3. FREQUENCY DOMAIN ANALYSIS FOR REACTIVE SOLUTE TRANSPORT

An aquifer and its relative hydrologic setting comprise a natural aquifer system. This system is often affected by many external impacts, such as recharge, pumping and injection. The response of this system to these impacts, described by groundwater level fluctuation, and a change of concentration with respect to time, depends upon the physical and chemical characteristics of the system itself and these various impacts. To evaluate the response of a system to a particular external impact, frequency domain analysis is often used to analyze the relationship between the input and output signals. The amplitude spectrum and phase spectrum provide insight into the system characteristics.

The frequency domain analysis of groundwater level fluctuation was developed by other investigators (*Gelhar*, 1974; *Gelhar and Wilson*, 1974). Several idealized homogeneous aquifer systems, including a linear reservoir, a linear Dupuit aquifer, and a Laplace aquifer, were used to analyze the system response to a time variation recharge and fluctuations in the adjacent stream stage. These models provide an analytical basis for interpretation of spectral data from the aquifer. Important applications of this analysis include the determination of aquifer parameters, the comparison of different flow models, and the design of observation networks. Frequency analysis is also used to compare different linear nonreactive solute transport models (*Duffy*, 1982; *Duffy and Gelhar*, 1985; *Duffy and Gelhar*, 1986). The procedures of parameter estimation and model identification, which involved the comparison of theoretical and experimental transfer functions and phase spectrums, were developed. All the above models assume that an aquifer is homogeneous with no chemical reaction involved in the solute transport.

The present research will extend the frequency domain analysis to the reactive solute transport model and a two–dimensional heterogeneous aquifer. Three kinds of reactive solute transport models are examined: (1) the lumped parameter model, (2) the one–dimension-

al advection–dispersion model; and (3) the two–dimensional physical and chemical heterogeneous solute transport model. The first order sorption model is also compared with three other diffusion–type sorption models using the frequency domain analysis. Sensitivity analysis is used to explore the relationship between the input period and time constants of an aquifer system. Frequency domain analysis for a two–dimensional heterogeneous aquifer system is being developed for the first time. This research concentrates on providing both a theory and technique for frequency domain analysis to reactive solute transport processes. Further work will extend to the applications of this theory and technique, including model identification and parameter estimation.

3.1 Spectral Analysis

Before we examine the frequency response of particular model, it will be useful to review the properties of spectral analysis. A process is said to be weakly stationary if its expected value is a constant and its variance depends only on the time interval. This kind of stationarity is also referred to as second–order stationarity. All stationary processes can be represented in the complex form as

$$X(t) = \int_{-\infty}^{\infty} e^{iwt} dZ_x(w) \tag{3-1}$$

where $dZ(w)$ are complex Fourier amplitudes of the process. This process is also called a process of non–correlated increments because it has the following properties:

$$\begin{aligned} E[dZ_x(w_1)\ dZ_x^*(w_2)] &= 0 \qquad && w_1 \neq w_2 \\ E[dZ_x(w_1)\ dZ_x^*(w_2)] &= \phi_{xx} dw \qquad && w_1 = w_2 \end{aligned} \tag{3-2}$$

where ϕ_{xx} is the power spectral distribution, the asterisk represents the complex conjugate, and E indicates expected value. The ϕ_{xx} can be found by taking the Fourier transform of the autocorelation function R_{xx}. Hence, R_{xx} and ϕ_{xx} have the following relationship:

$$\phi_{xx}(w) = \frac{1}{2\pi}\int_{-\infty}^{\infty} e^{-iw\tau}R_{xx}(\tau)d\tau \tag{3-3}$$

$$R_{xx}(\tau) = \int_{-\infty}^{\infty} e^{iw\tau}\phi_{xx}(w)dw \quad . \tag{3-4}$$

A bivariate random process, $X(t)$ and $Y(t)$, is stationary if the first and second moments are adequate to characterize this process. Thus, using the stochastic Fourier–Stieltjes integral, the series can be represented by

$$X(t) = \int_{-\infty}^{\infty} e^{iwt}dZ_x(w) \tag{3-5}$$

$$Y(t) = \int_{-\infty}^{\infty} e^{iwt}dZ_y(w) \quad . \tag{3-6}$$

The properties of this bivariate random process are

$$\begin{aligned} E[dZ_x(w_1)\ dZ_x^*(w_2)] &= 0 && w_1 \neq w_2 \\ &= \phi_{xx}dw && w_1 = w_2 \end{aligned} \tag{3-7}$$

$$\begin{aligned} E[dZ_y(w_1)\ dZ_y^*(w_2)] &= 0 && w_1 \neq w_2 \\ &= \phi_{yy}dw && w_1 = w_2 \end{aligned} \tag{3-8}$$

$$\begin{aligned} E[dZ_x(w_1)\ dZ_y^*(w_2)] &= 0 && w_1 \neq w_2 \\ &= \phi_{xy}dw && w_1 = w_2 \end{aligned} \tag{3-9}$$

where ϕ_{xx} and ϕ_{yy} are the power spectra of the series, $X(t)$ and $Y(t)$, respectively. ϕ_{xy} is the cross spectrum and it also can be represented by

$$\phi_{yx} = Co(w) + iQ(w) \tag{3-10}$$

where $Co(w)$ is called the co–spectrum and $Q(w)$ is the quadrature spectrum. The phase difference can be determined from $Co(w)$ and $Q(w)$

$$\theta_{yx} = tan^{-1}\frac{Q(w)}{Co(w)} \tag{3-11}$$

and is sometimes known as the phase spectrum of the process, $X(t)$ and $Y(t)$. The transfer function can be expressed by

$$|H(w)|^2 = \frac{\phi_{yy}(w)}{\phi_{xx}(w)} \tag{3-12}$$

which measures the amplitude magnification at different frequency components, and is sometimes known as the amplitude spectrum of the process, $X(t)$ and $Y(t)$. In this research, we will analyze the characteristic of the phase and amplitude spectrums in different models.

3.2 Lumped Parameter Model (LPM)

The LPM is one of the simplest models used to describe groundwater pollution problems. This model can be valid in cases where a system is well mixed, and it is especially useful when limited field data are available. The model can be written as

$$\begin{aligned} \theta\frac{\partial C}{\partial t} + \varrho_b \sum_{j=1}^{m} f_j \frac{\partial S_j}{\partial t} &= QC_q\text{-}PC \\ \frac{\partial S_j}{\partial t} &= \alpha_j(k_{dj}C\text{-}S_j) \end{aligned} \tag{3-13}$$

where θ is the porosity, ϱ_b is the dry bulk density, f is the fraction of the sorption site, m is the number of sorption sites, j represents the jth sorption site, C is aqueous concentration, Q is the recharge rate, P is the discharge rate, and C_q is the recharge concentration; S_j is the solid phase concentration, α_j is the rate coefficient, and k_{dj} is the distribution coefficient in jth sorption site. We assume that the groundwater flow is at steady state (Q=P) and the recharge concentration C_q is a time-dependent input variable. We now would like to construct a frequency domain solution to equation (3-13) when $C(t)$ and $C_q(t)$ are stationary stochastic processes. Taking the transformation of equation (3-5), the equation (3-13) can be written as:

$$dZ_C[\frac{P}{\theta}+\frac{\varrho_b}{\theta}\omega^2\sum_{j=1}^{m}F_j+i\omega(1+\frac{\varrho_b}{\theta}\sum_{j=1}^{m}\alpha_jF_j)]=\frac{Q}{\theta}dZ_{C_q}$$
$$dZ_{S_j}=\frac{\alpha_j k_{dj}}{\alpha_j+i\omega}dZ_C \tag{3-14}$$

where

$$F_j=f_j\frac{\alpha_j k_{dj}}{\alpha_j^2+\omega^2} \tag{3-15}$$

If we use the definitions of time constants developed in the previous chapter, equation (3-14) can be rewritten as

$$dZ_C[\frac{1}{\tau_a}+\sum_{j=1}^{m}\frac{R_j-1}{(1+(\frac{T}{2\pi\tau_j})^2)\tau_j}+i\frac{2\pi}{T}(1+\sum_{j=1}^{m}\frac{R_j-1}{1+(\frac{2\pi\tau_j}{T})^2})]=\frac{1}{\tau_a}dZ_{C_q}$$
$$dZ_{S_j}=\frac{k_{dj}}{1+i\frac{2\pi\tau_j}{T}}dZ_C \tag{3-16}$$

where

$$\tau_a=\frac{\theta}{P}\ ,\ \tau_j=\frac{1}{\alpha_j}\ ,\ T=\frac{2\pi}{\omega}\ ,\ R_j=1+f_j\frac{\varrho_b k_{dj}}{\theta}$$

τ_a is the non-reactive time constant for the advection process, τ_j is the time constant of sorption process in the jth sorption site, ω is the frequency of interest, T is the period of interest, and R_j is the retardation factor in the jth sorption site.

The transfer function and phase spectrum can be evaluated by equations (3-7) through (3-12). Assume that there are two sorption sites (m=2) in this model, figure 3.1 shows the relationship between the aqueous phase time constant and input period. The longer the input period, the greater the transfer function. The aquifer system is a typical low-pass filter. With the increase of the aqueous phase time constant, variations in continuous solute inputs will produce little variation in the aqueous phase concentration (figure 3.1a). This illustrates that the aquifer system with the larger nonreactive aqueous phase time constant is less sensitive to external input. The time constant at sorption site 1 is 10 days, which is less than or equal to the aqueous phase time constant; thus, sorption in site 1 can be regarded approximately as an equilibrium process, leading to the similar shape of the transfer function as that for the

aqueous phase concentration (figure 3.1a,b). The time constant at sorption site 2 is 60 days; thus, with the increase of the aqueous phase time constant from 10 days to 240 days, the sorption process in this site can be changed from a rate–limited process to the approximate equilibrium process (figure 3.1c). The negative phase spectrum for the aqueous phase concentration decreases with the input period from a maximum of $\pi/2$ radians, but from a maximum of π radian for the solid phase concentrations. Sorption site 2, with a larger sorption time constant, has the larger phase lag because of its slow response (figure 3.1b,c).

For a nonreactive aqueous phase time constant of 30 days and a site 1 time constant of 10 days, figure 3.2 shows the relationship between the time constant at site 2 and the input period. For larger site 2 time constants, the transfer function for the aqueous phase concentration, is larger for shorter input periods but smaller for longer input periods. The same result can be found for the sorption site 1 from the figures. Sorption site 2 cannot dampen the shorter period input because it has a slower response (figure 3.2b,c). With a larger time constant at site 2, the phase spectrum of the aqueous phase concentration output lags less for the longer input period. The sorbed phase transfer functions reveal that the aqueous phase and site 1 will respond to a quick change of input, but not much fluctuation will occur in the solid phase concentration at sorption site 2, with its larger time constant. Because of the approximate equilibrium sorption process at site 1, the shape of the transfer function and phase lag of sorption concentration are almost the same as that of an aqueous phase concentration.

Figure 3.3 shows the influence of storage capacity at the sorption sites on the amplitude spectrum and phase spectrums. With an increase of storage capacity at the sorption sites, the transfer function in the aqueous phase and the other two solid phase concentrations drops. This indicates that sorption can greatly dampen external input variations. The time constant in the mobile zone increases with the storage capacity at sorption sites, leading to a decrease in the effective mass transfer rate. Thus, the aquifer system is less sensitive to an external input. Also by increasing storage capacity, the aquifer has less phase lag for shorter input periods and a longer phase lag for longer input periods.

3.3 One-Dimensional Advection-Dispersion-Sorption(ADS) Model

For the same external input, the transfer function in each different location of the system can be different. Let us use a simple one-dimensional ADS model to examine the spatial distribution of the frequency response. For a single sorption site, the one-dimensional ADS model can be written as

$$\frac{\partial C}{\partial t} + \frac{\varrho_b}{\theta}\frac{\partial S}{\partial t} = D\frac{\partial^2 C}{\partial x^2} - V\frac{\partial C}{\partial x} \tag{3-17a}$$

$$\frac{\partial S}{\partial t} = \alpha(k_d C - S) \tag{3-17b}$$

where V is the pore velocity and D is the longitudinal dispersion coefficient. The transver dispersion has been neglected and uniform flow is assumed in the present study. The boundary conditions of this model are

$$C(0,t) = C_i(t) \qquad t > 0$$
$$C(\infty,t) = 0$$

where C_i is the input concentration at the outcrop(x=0).

The transformations of equation (3-5) results in the following ordinary differential equation:

$$iw(1 + \frac{\varrho_b}{\theta}\frac{\alpha k_d}{\alpha + iw})dZ_C = D\frac{\partial^2 dZ_C}{\partial x^2} - V\frac{\partial dZ_C}{\partial x} \tag{3-18a}$$

$$\frac{dZ_S}{dZ_C} = \frac{\alpha k_d}{\alpha + iw} \tag{3-18b}$$

with the boundary conditions specified as

$$dZ_C(0,w) = dZ_{C_i}(w)$$
$$dZ_C(\infty,w) = 0$$

Solving for dZ_C results in the frequency response function for aqueous phase concentration

$$\frac{dZ_C}{dZ_{C_i}} = exp[\frac{(V-\sqrt{4DF + V^2})x}{2D}] \tag{3-19}$$

where

$$F = iw(1 + \frac{\varrho_b}{\theta}\frac{\alpha k_d}{\alpha + iw})$$

The transfer function can be obtained from equations (3-7) through (3-9)

$$\frac{\phi_{CC}}{\phi_{C_iC_i}} = |exp[\frac{(V-\sqrt{4DF + V^2})x}{2D}]|^2 \tag{3-20}$$

If the longitudinal dispersion coefficient varies linearly with the pore velocity V, it can be expressed by

$$D = \alpha_L V$$

where α_L is the dispersivity length. The dimensionless form of this transfer function is

$$\frac{\phi_{CC}}{\phi_{C_iC_i}} = |H_C(x,w)|^2 = |exp[\frac{\xi}{2} - \frac{\xi}{2}\sqrt{1 + i8\pi\eta(\frac{1}{\lambda} + \frac{R-1}{2\pi i + \lambda})}\ ]|^2 \tag{3-21}$$

where

$$R = 1 + \frac{\varrho_b k_d}{\theta} \qquad \xi = \frac{x}{\alpha_L} \qquad \eta = \frac{\alpha_L}{V\tau}$$

$$\lambda = \frac{T}{\tau} \qquad T = \frac{2\pi}{w} \qquad \tau = \frac{1}{\alpha}$$

thus, the transfer function of a solid phase concentration is

$$\frac{\phi_{SS}}{\phi_{C_iC_i}} = \frac{\lambda^2 k_d^2}{4\pi^2 + \lambda^2}\ |H_C(x,w)|^2 \tag{3-22}$$

We will examine the amplitude filtering characteristics of the system as functions of the dimensionless parameters η, ξ, λ and R. Figure 3.4 illustrates the transfer function of an aqueous phase and a solid phase concentration for a range of η, ξ and R. Figure 3.4a shows that with the larger rate flow or a smaller dispersivity, the aqueous phase concentration is

more sensitive to the variation of input concentration, because the change of input can be transferred faster. Figure 3.4b demonstrates that as the distance away from the source location decreases, short-period input variations are filtered out, presumedly due to the cumulative effects of dispersion. Figure 3.4c shows that additional storage capacity at the sorption sites leads to additional amplitude attenuation. This indicates that the sorption sites dampen the effects of external inputs. The curve of the amplitude and phase spectrum for solid phase concentration is almost the same as that for an aqueous phase concentration for longer input periods, but just slightly different for shorter input periods. This shows that the solid phase concentration is as sensitive to a longer period inputs as the aqueous phase concentration.

3.4 Two-dimensional ADS model

Because of the complexity of a real aquifer system, the LPM and one-dimensional ADS models cannot represent the physical and chemical heterogeneity of an aquifer. A higher dimensional reactive solute transport model is more useful in providing insight into the behavior of contaminant transport in a heterogeneous aquifer. In this model, the frequency responses to a particular external impact is different at different locations; they depend on the combination of complicated system parameters. Frequency domain analysis gives us important information about the behavior of contamination/remediation at a given location in a physically and/or chemically heterogeneous aquifer system. Our goal is to develop a suitable numerical algorithm to calculate the transfer function in a two-dimensional model. Further work will extend to explore the relationship between the distribution of transfer function and a remediation scheme.

The two-dimensional ADS model can be written as

$$\frac{\partial C}{\partial t} + \frac{\varrho_b}{\theta}\frac{\partial S}{\partial t} = \frac{\partial}{\partial x}(D_{xx}\frac{\partial C}{\partial x} + D_{xz}\frac{\partial C}{\partial z}) + \frac{\partial}{\partial z}(D_{zz}\frac{\partial C}{\partial z} + D_{zx}\frac{\partial C}{\partial x}) - V_x\frac{\partial C}{\partial x} - V_z\frac{\partial C}{\partial z} = L(C)$$
$$\frac{\partial S}{\partial t} = \alpha(k_d C - S) \qquad (3\text{-}23)$$

with the following boundary conditions :

$$C|_{\Gamma 1} = C_i(t) \qquad t > 0$$

$$\frac{\partial C}{\partial n}|_{\Gamma 2} = 0$$

where n is the normal outward direction of a second type of boundary and C_i is the input concentration. More complicated combinations of boundary conditions will be considered in the future. Taking the transformation in (3–5), the equation can be rewritten as

$$L(dZ_C) = i\frac{2\pi}{T}(1 + \frac{T(R-1)}{T + i2\pi\tau})dZ_C \tag{3–24a}$$

$$\frac{dZ_S}{dZ_C} = \frac{\alpha k_d T}{\alpha T + 2\pi i} \quad , \tag{3–24b}$$

with the boundary conditions specified as

$$dZ_C(w)|_{\Gamma 1} = dZ_{C_i}(w) \qquad t > 0$$

$$\frac{\partial dZ_C}{\partial n}|_{\Gamma 2} = 0 \quad ,$$

simplifying the model by taking the following transformation

$$H_C(w, \boldsymbol{x}) = \frac{dZ_C(w, \boldsymbol{x})}{dZ_{C_i}(w)} \quad .$$

Equations (3–24) and its boundary conditions can then be written as

$$L(H_C) = i\frac{2\pi}{T}(1 + \frac{T(R-1)}{T + i2\pi\tau})H_C \tag{3–25a}$$

$$\frac{dZ_S}{dZ_{C_i}} = \frac{k_d T}{T + 2\pi\tau i}H_C \tag{3–25b}$$

$$H_C|_{\Gamma 1} = 1 \qquad t > 0$$

$$\frac{\partial H_C}{\partial n}|_{\Gamma 2} = 0 \quad .$$

Equation (3–25a) can be solved by a finite element or a finite difference scheme. T is an input period of interest and can be input first as a parameter. The transfer function then can be

calculated by

$$\frac{\phi_{CC}}{\phi_{C_iC_i}} = |H_C(x,w)|^2 \tag{3-26a}$$

$$\frac{\phi_{SS}}{\phi_{C_iC_i}} = \frac{\lambda^2 k_d^2}{4\pi^2 + \lambda^2} |H_C(x,w)|^2 \tag{3-26b}$$

Two examples show the distribution of the transfer function in an aquifer under the different input schemes. Figure 3.5 is the contour plot of a transfer function in a heterogeneous aquifer, whose external input is in the middle of the top boundary, just like the contamination period of the examples in Chapter 2. Because the reactive time constant is 6 years for lenses and aquitards (Chapter 2), the transfer function of an aquifer system is very small in the presence of an external input with only a 1–year or 3–year input period. With the increase of the input period of interest, more of the fluctuation is filtered out more components. It also shows that the high–k zones are more sensitive to these inputs than lenses and aquitards. Only for longer input periods, does the concentration in the lenses begin to fluctuate. Thus, if the input is associated with contamination in this aquifer system, it seems that the distribution of the transfer function can provide information about the behavior of contamination at different locations. Figure 3.6 illustrates that the different input locations and strength can lead to different distributions of the transfer function. It may be possible to set up a standard to evaluate the effectiveness of remediation in different spatial locations by using the distribution of the transfer function.

3.5 Comparison of Different Sorption Models

In the three models above, the sorption process is represented by a first–order sorption model. In fact, this model is a lumped parameter model because it does not closely represent the mechanisms of sorption process. However, if the rate–limited sorption is caused by a diffusion–controlled process occurring in aggregated soil, the sorption process can be modeled using Fick's law equation (2–4). The size and geometry of sorption sites should be known

in that model. Some investigators use moment analysis to determine the appropriate parameters to equal these models(*Parker* and *Valocchi*, 1986). Our research will use frequency domain analysis to evaluate the difference of these equivalent models.

If we regard the sorption site as the system, then the aqueous phase concentration is the external input of this system. The first-order model can be found in equation (3–17b), and the Fickian diffusion model can be found in equation (2–4). The transfer function of the solid phase concentration can be represented by

$$\frac{\phi_{SS}}{\phi_{CC}} = \frac{\alpha^2 k_d^2}{w^2 + \alpha^2} \qquad \textit{for first-order model} \qquad (3\text{–}27)$$

$$\frac{\phi_{SS_r}}{\phi_{CC}} = \left| \frac{k_d \cosh(r\mu)}{\cosh(b\mu)} \right|^2 \qquad \textit{for layer diffusion model} \qquad (3\text{–}28)$$

$$\frac{\phi_{SS_r}}{\phi_{CC}} = \left| \frac{k_d I_0(r\mu)}{I_0(b\mu)} \right|^2 \qquad \textit{for cylindrical diffusion model} \qquad (3\text{–}29)$$

$$\frac{\phi_{SS_r}}{\phi_{CC}} = \left| \frac{k_d i_0(r\mu)}{i_0(b\mu)} \right|^2 \qquad \textit{for spherical diffusion model} \qquad (3\text{–}30)$$

where $\mu = \sqrt{\frac{iw}{D_a}}$.

S_r is the solid phase concentration as a function of the intraparticle distance, r, D_a is the apparent diffusion coefficient, and b is the effective aggregate radius. The average solid phase concentration can be calculated by

$$S = \frac{k}{b^k} \int_0^b r^{k-1} S_r dr$$

where k=1, 2, and 3 represent layer, cylinderical, and the spherical diffusion model, respectively. Thus, the transfer function for average solid phase concentration in sorption site can be written as

$$\frac{\phi_{SS}}{\phi_{CC}} = \left| \frac{k_d \sinh(\sqrt{iw\psi})}{\sqrt{iw\psi}\cosh(\sqrt{iw\psi})} \right|^2 \qquad \textit{for layer diffusion model} \qquad (3\text{–}31)$$

$$\frac{\phi_{SS}}{\phi_{CC}} = \left| \frac{2k_d I_1(\sqrt{iw\psi})}{\sqrt{iw\psi}\, I_0(\sqrt{iw\psi})} \right|^2 \qquad \textit{for cylindrical diffusion model} \qquad (3\text{–}32)$$

$$\frac{\phi_{SS}}{\phi_{CC}} = \left| \frac{3k_d i_1(\sqrt{iw\psi})}{\sqrt{iw\psi}\, i_0(\sqrt{iw\psi})} \right|^2 \qquad \textit{for spherical diffusion model} \qquad (3\text{–}33)$$

where

$$\psi = \frac{b^2}{D_a}$$

The "equivalent" rate coefficients for the first-order model and the other three diffusion models have been derived by equating the second moments of the breakthrough curve (*Goltz and Roberts*, 1987).

$$\alpha = \frac{k(k+2)D_a}{b^2} \qquad k = 1,\ 2 \textit{ and } 3 \qquad (3\text{–}34)$$

where α is the rate coefficient of the first-order model, k=1, 2, and 3 represent the layer, cylindrical, and spherical diffusion model, respectively. The phase spectrums of these four model are also easy to be derived.

$$\theta_{SC} = Arg\left[\frac{k_d \sinh(\sqrt{iw\psi})}{\sqrt{iw\psi}\cosh(\sqrt{iw\psi})}\right] \qquad \textit{for layer diffusion model} \qquad (3\text{–}35)$$

$$\theta_{SC} = Arg\left[\frac{2k_d I_1(\sqrt{iw\psi})}{\sqrt{iw\psi}\, I_0(\sqrt{iw\psi})}\right] \qquad \textit{for cylindrical diffusion model} \qquad (3\text{–}36)$$

$$\theta_{SC} = Arg\left[\frac{3k_d i_1(\sqrt{iw\psi})}{\sqrt{iw\psi}\, i_0(\sqrt{iw\psi})}\right] \qquad \textit{for spherical diffusion model} \qquad (3\text{–}37)$$

where θ_{sc} is the phase spectrum of the processes, $S(t)$ and $C(t)$.

Figure 3.7 shows the amplitude spectrum and phase spectrum of these four sorption models under the "equivalent" relationship of equation (3–34). The three diffusion-type models can be well equivalent under the this relationship. However, the first-order model has a smaller transfer function for shorter input periods than other three diffusion-type mod-

els, but a much larger transfer function for longer input periods. It also has a much larger phase spectrum for the shorter periods, for all models converge for the longer periods. The first order model is generally more sensitive to the changes of an aqueous phase concentration. The frequency domain analysis here indicates that (1) the three diffusion–type sorption models are approximately equivalent under the "equivalent" relationship equation (3–34); or (2) the three diffusion–type models can have greater phase lag derivation from the first–order sorption model when aqueous phase concentrations change quickly, but they can be approximately equivalent if the aqueous phase concentration changes slowly.

3.6 Summary and Conclusions

In this chapter, frequency domain analysis is used to analyze the behavior of a reactive solute transport. The amplitude spectrums are derived for a lumped parameter model and a one–dimensional reactive solute transport model. The numerical solution for a transfer function in a two–dimensional heterogeneous aquifer system has been developed. The different sorption models are also compared by frequency domain analysis. The main conclusions in this chapter include

(1) The smaller time constant in the mobile zone leads to the aqueous phase concentration more sensitive to external impact. The effective transfer function in the mobile zone increases with the decrease of the time constant in mobile zone.

(2) The smaller time constant at the sorption sites makes the aqueous phase concentration less sensitive to external inputs with shorter input periods because the sorption can quickly dampen the external impact; but for an external input with a longer period, the relatively fast mass transfer process at the sorption site makes an aqueous phase concentration more sensitive.

(3) A sorption site can be used as a buffer to dampen external impacts. The more storage capacity in sorption sites, the more they can dampen external impacts, and this make the aqueous phase concentration less sensitive to a particular input.

(4) A one–dimensional model shows that larger flow rate and smaller dispersivity can make an aquifer more sensitive to input because the input can be transferred quickly by faster flow. Generally, the location closer to input will be more sensitive because it experiences less dispersion.

(5) The developed numerical scheme can effectively solve the transfer function in a physical and chemical heterogeneous two–dimensional aquifer system. The low–k zones are obviously less sensible to external input. A different input scheme will lead to different response from the aquifer system. The transfer function in different locations can be used to compare the propensity for contamination or remediation in an aquifer system.

(6) For a reasonable choice of rate coefficients, the three diffusion–type models are roughly equivalent as well. The first–order sorption model can represent approximately the other three diffusion models when the aqueous phase concentration slowly changes. But there is greater deviation in the phase lag if the aqueous phase concentration changes quickly.

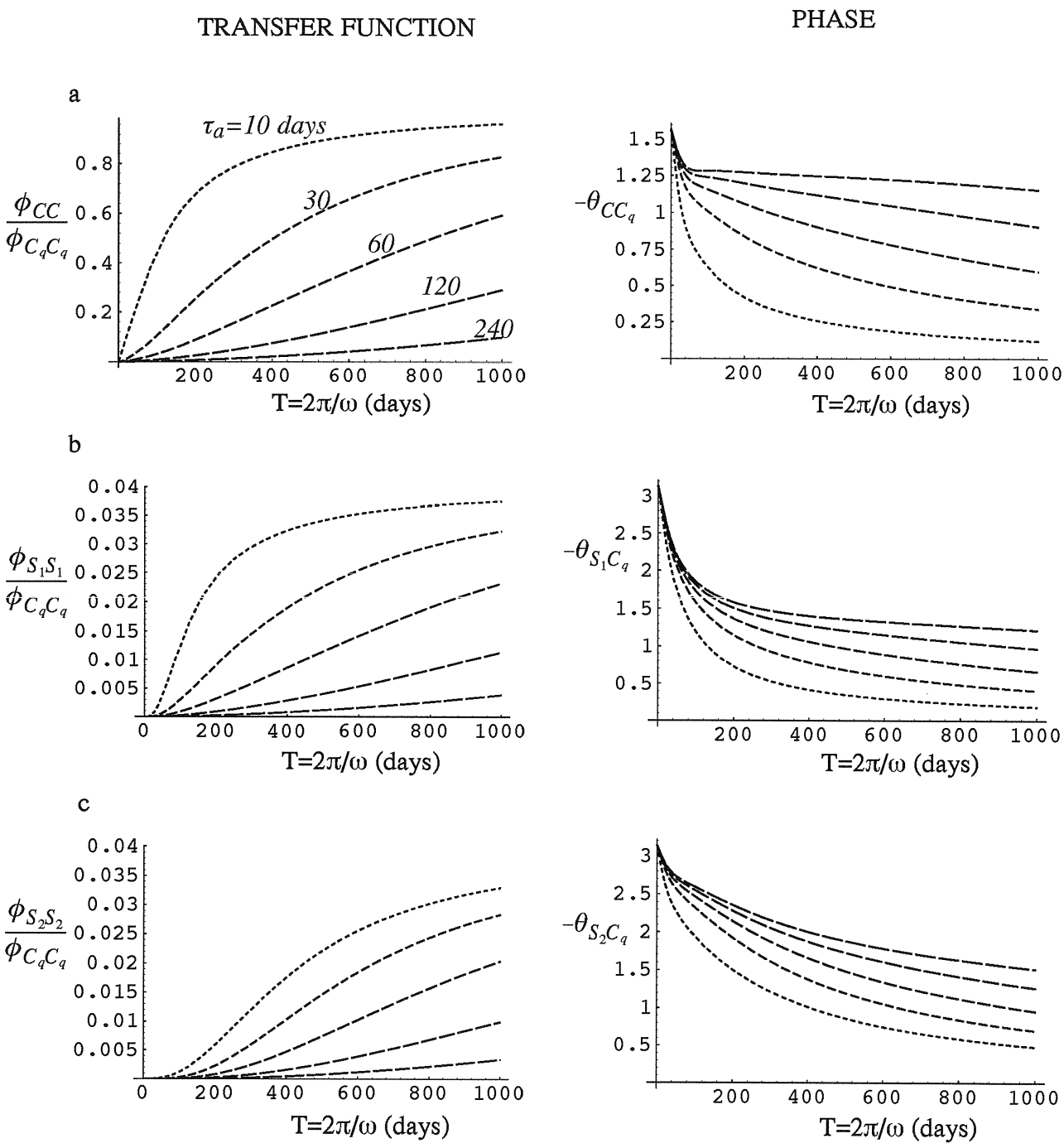

Figure 3.1 Comparison of frequency response characteristics showing effects of the aqueous phase time constant. (a), (b), and (c) represent the frequency characteristics of the aqueous phase concentration, sorped phase concentrations in sorption site 1 and in sorption site 2, respectively (τ_1=10 days, τ_2=60 days, f_1=0.5, f_2=0.5 and R=2).

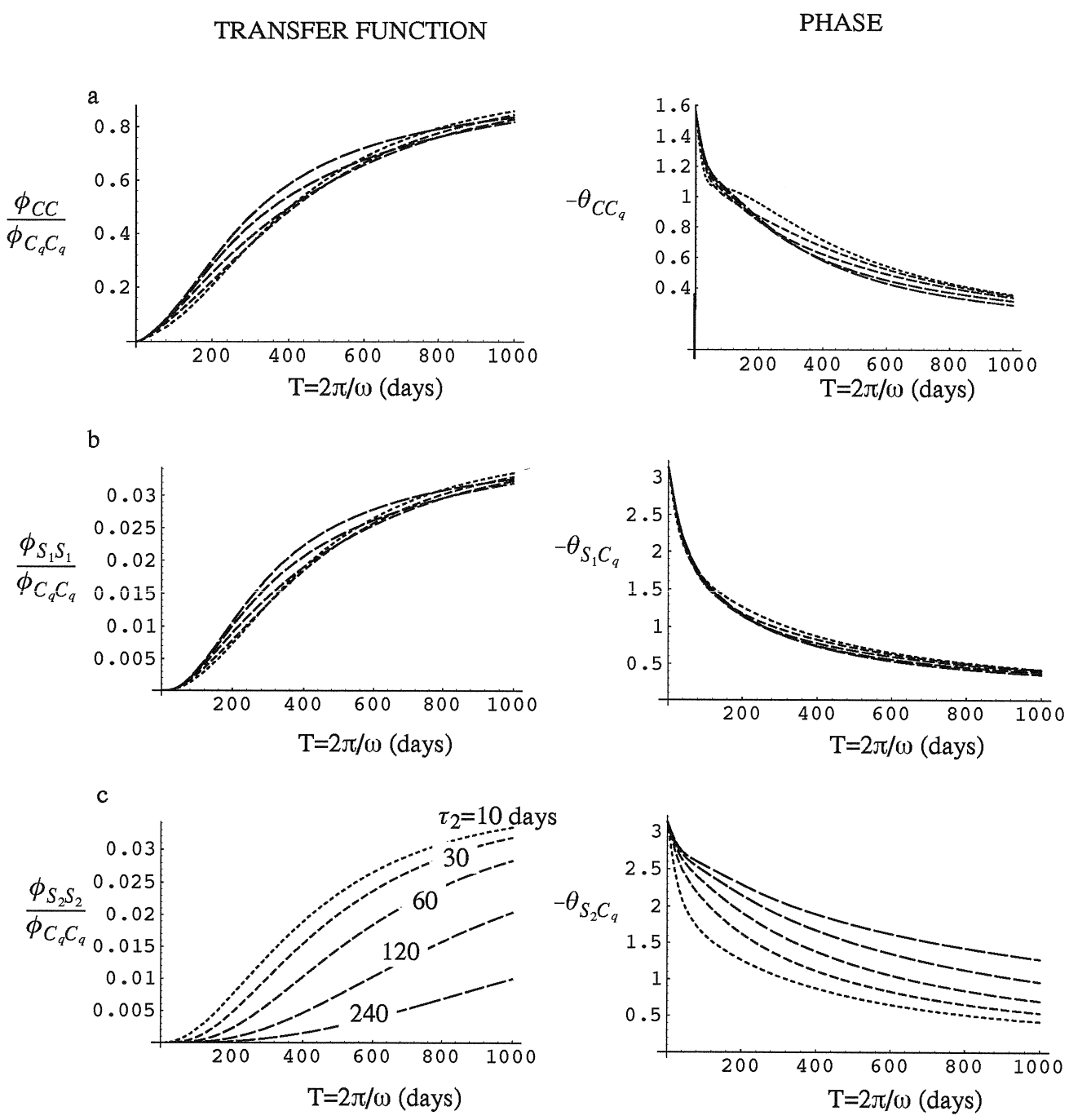

Figure 3.2 Comparison of frequency response characteristics showing effects of the solid phase time constant in sorption site 2. (a), (b), and (c) represent the frequency characteristics of the aqueous phase concentration, sorped phase concentrations in sorption site 1 and in sorption site 2, respectively. (τ_1=10 days, τ_a=30 days, f_1=0.5, f_2=0.5 and R=2)

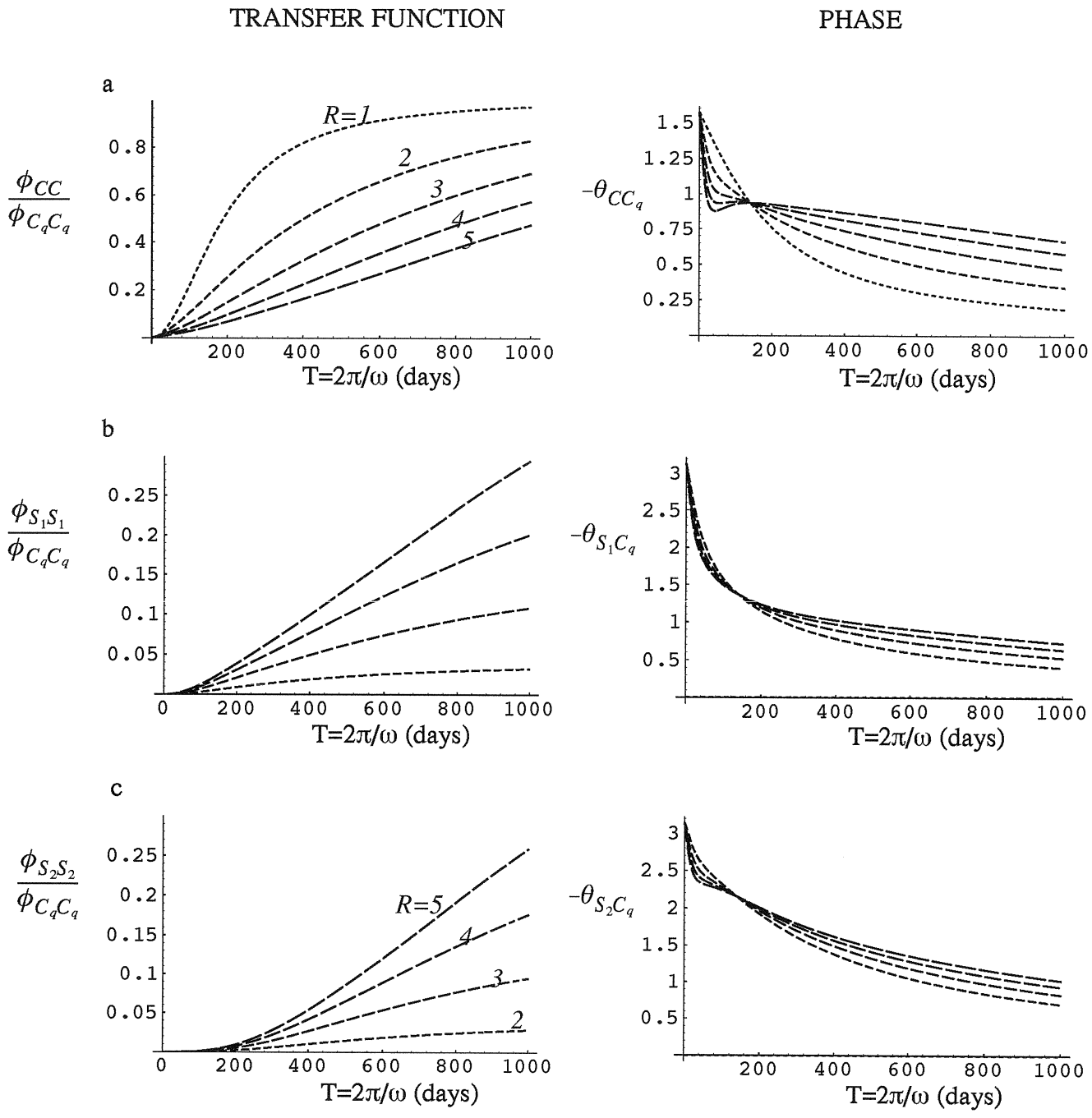

Figure 3.3 Comparison of frequency response characteristics showing effects of the storage capacity in sorption sites. (a), (b), and (c) represent the frequency characteristics of the aqueous phase concentration, solid phase concentrations in sorption site 1 and site 2, respectively. (τ_1=10 days, τ_2=60 days, f_1=0.5, f_2=0.5 and τ_a=30 days)

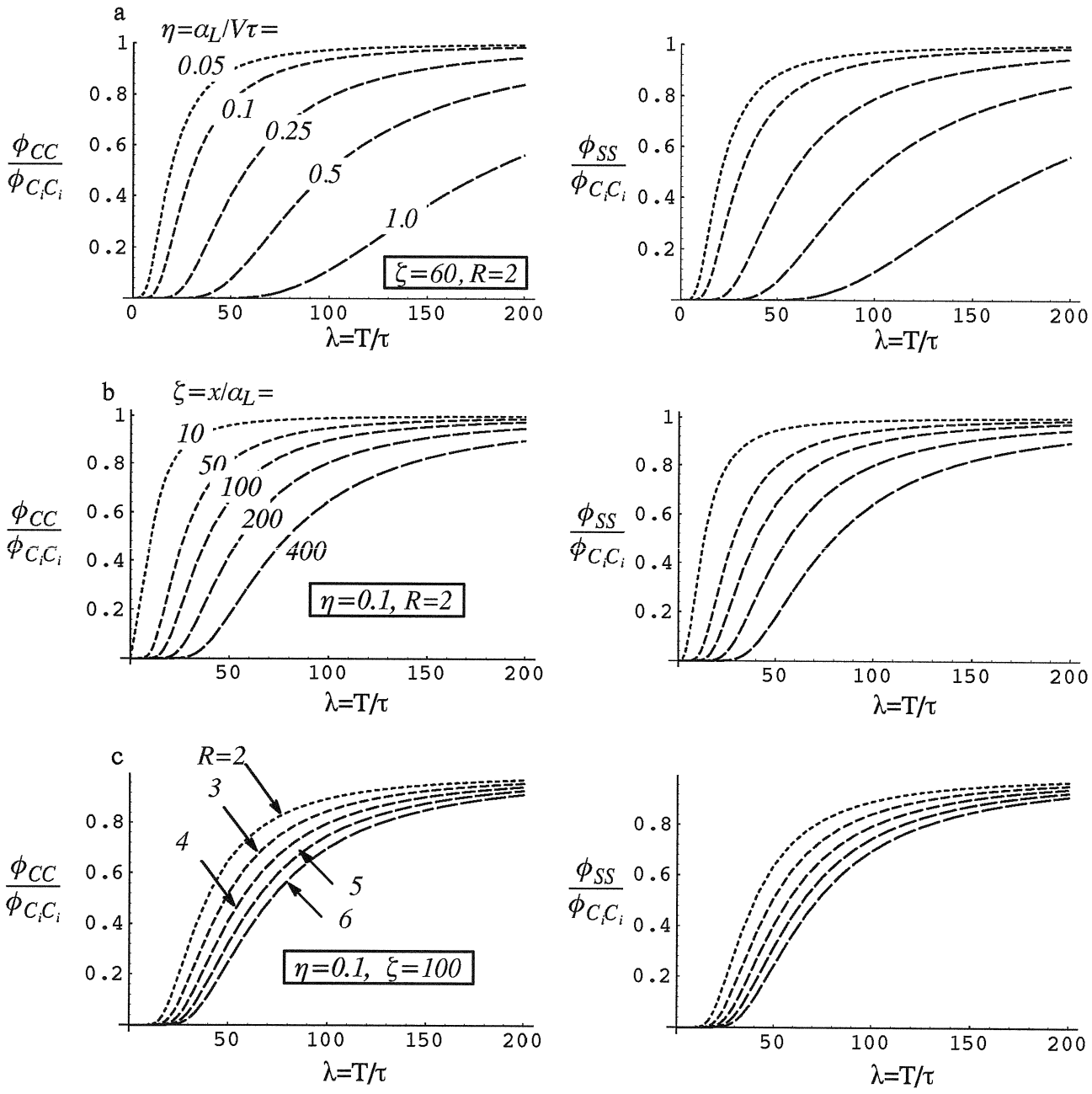

Figure 3.4 Transfer functions for the aqueous phase and solid phase concentration versus dimensionless period showing effects of (a) the dimensionless dispersivity, (b) the dimensionless distance, and (c) the dimensionless storage capacity at the sorption site (c).

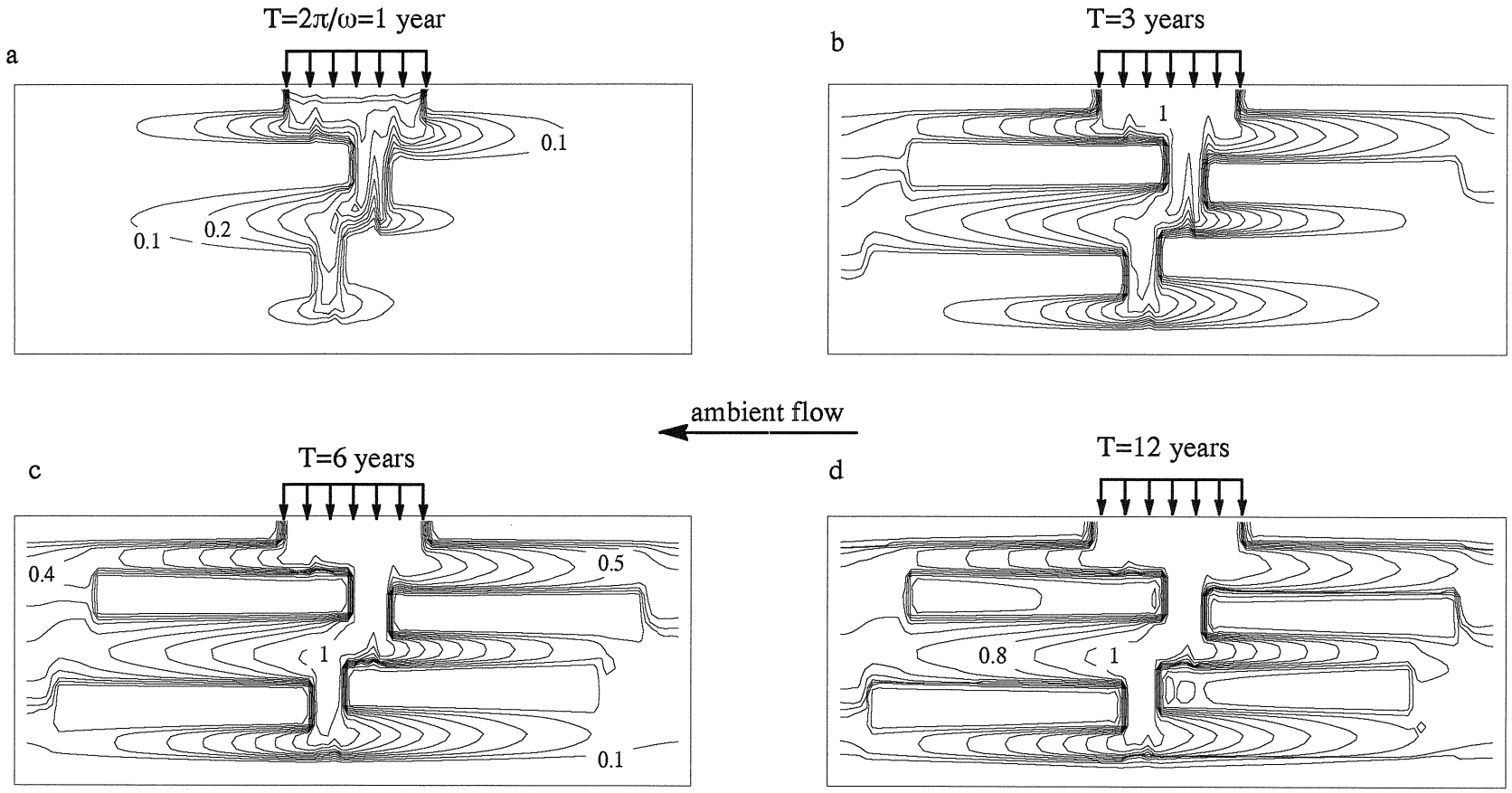

Figure 3.5 Comparison of the transfer function of the aqueous phase concentration in a heterogeneous aquifer system. (a)–(d) show the contour plots of the transfer functions with different input periods. The external input is uniform and locates in the middle of surface. The lenses and aquitards have 6 years of time constant. (k_h=50m/d, k_L=0.005m/d, τ_s=40 days, and R=2)

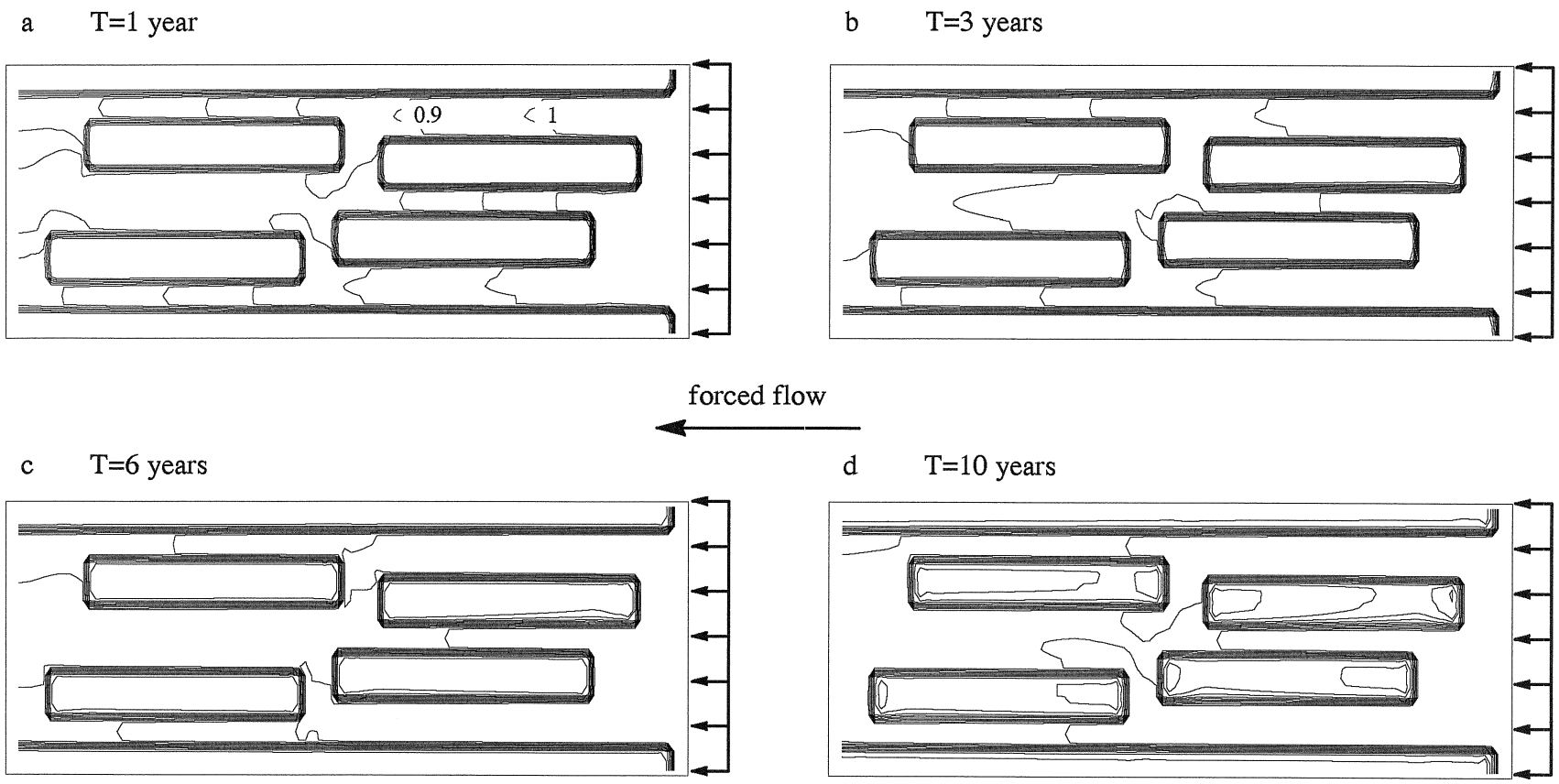

Figure 3.6 Comparison of the transfer function of the aqueous phase concentration in a heterogeneous aquifer system. (a)–(d) show the contour plots of the transfer functions with different input periods. The external input is uniform and locates in right boundary. The lenses and aquitards have 6-year time constant. (k_h=50m/d, k_L=0.005m/d, τ_s=40 days, and R=2)

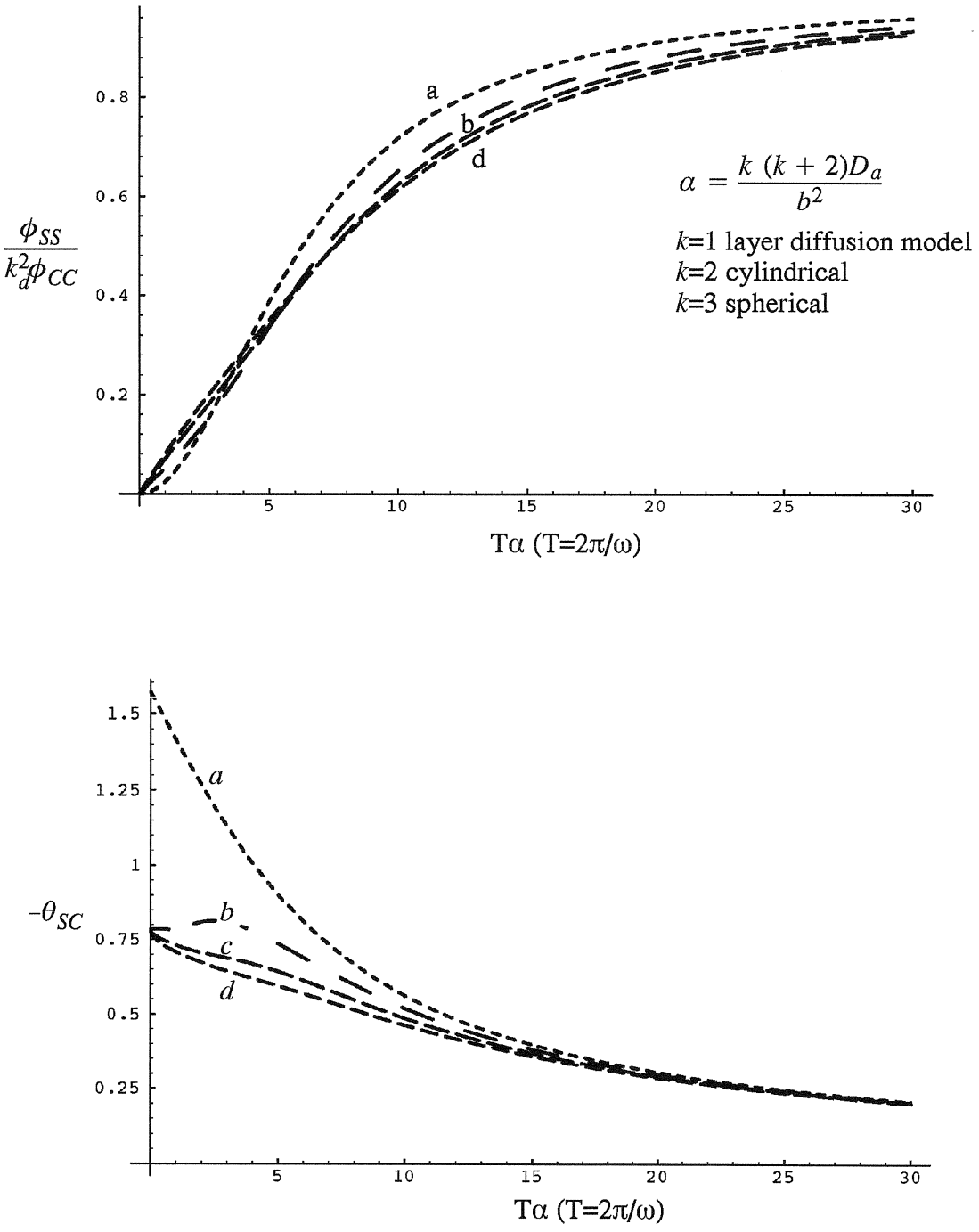

Figure 3.7 Theoretical amplitude and phase spectrum for the "equivalent" (a) first–order, (b) layer diffusion, (c) cylindrical diffusion, and (d) spherical diffusion sorption models.

4. INCOMPLETE MOMENT ANALYSIS FOR REACTIVE SOLUTE TRANSPORT

Moment analysis has been widely used to analyze the temporal data obtained from field and lab studies. Some investigators present a modified form of Aris's method of moment to derive the analytical solutions of temporal and spatial moments associated with the reactive solute transport model in a homogeneous aquifer under the steady and uniform flow (*Wakao and Kaguei*, 1982; *Valocchi*, 1985; *Goltz and Roberts*, 1987). Their research demonstrates that the zeroth and first temporal moments are independent of a mass transfer rate between mobile zones and sorption sites. Because analytical solutions are restricted to a homogeneous pore medium, moment-generating equations have been developed to handle a more complicated heterogeneous aquifer system (*Harvey and Gorelick*, 1995). Moment analysis can be used to estimate model parameters and analyze the statistical characteristics of a breakthrough curve.

In this chapter, we will develop the new concept of an incomplete moment and derive the corresponding incomplete moment-generating equations in a heterogeneous aquifer. This new concept may give us more information about the behavior of reactive solute transport than traditional complete moment analysis. A simple lumped parameter model is used to shape the general idea of this new concept. A numerical scheme for a two-dimensional model is also presented. The ideas are only preliminary and so are only introduced here. Further exploration of the utility of the incomplete moment method awaits future work.

4.1 Incomplete Moment

In the following equations, C represents the aqueous phase concentration in the mobile zone, and S represents the solid phase concentration in the sorption site. The incomplete moments for these two time dependent variables can be written as

$$N_n = \int_0^T C\ \tau^n\ d\tau \tag{4-1}$$

$$J_n = \int_0^T S\ \tau^n\ d\tau \tag{4-2}$$

where N_n and J_n represent the nth absolute incomplete moment of the aqueous phase concentration $C(x,t)$ and solid phase concentration $S(x,t)$, respectively. T is a particular time of interest. The difference of an incomplete moment with the traditional complete moment is that the upper limit of the integral is infinity for a traditional complete moment. Obviously, incomplete moments represent the statistical characteristic of a breakthrough curve at a truncated time period, and it can provide more information about the behavior of reactive solute transport.

4.2 Incomplete Moment-Generating Equations for LPM

The LPM representing multicell nonequilibrium sorption processes is given by equation (3–13). Applying the definitions of equations (4–1) and (4–2), and assuming the recharge and discharge rate are constant, the incomplete moment–generating equations can be written as

$$\theta\frac{\partial N_0}{\partial T} + \varrho_b\sum_{j=1}^{m} f_j\frac{\partial J_{0j}}{\partial T} = QC_qT - PN_0 + \theta C_{(t=0)} + \varrho_b\sum_{j=1}^{m} f_j S_{j(t=0)} \tag{4-3a}$$

$$\frac{\partial J_{0j}}{\partial t} = \alpha_j(k_{dj}N_0 - J_{0j}) + S_{j(t=0)} \tag{4-3b}$$

$$\theta\frac{\partial N_n}{\partial T} + \varrho_b\sum_{j=1}^{m} f_j\frac{\partial J_{nj}}{\partial T} = QC_q\frac{T^{n+1}}{n+1} - PN_n + \theta nN_{n-1} + n\varrho_b\sum_{j=1}^{m} f_j J_{(n-1)j} \quad n \geq 1 \tag{4-4a}$$

$$\frac{\partial J_{nj}}{\partial t} = \alpha_j(k_{dj}N_n - J_{nj}) + nJ_{(n-1)j} \qquad n \geq 1 \quad . \tag{4-4b}$$

Equation (4–3) represents a zeroth incomplete moment (n=0). The initial condition for N_n, J_n, N_0, and J_0 is zero according to the definitions of equations (4–1) and (4–2). The higher moments depend on the lower moments. By solving these equations, coupled with modified

boundary conditions, we can obtain the statistical characteristic of a breakthrough curve at any truncated time period. Assuming there are two sorption sites (m=2) and the aquifer is fully contaminated initially, a remediation scheme includes injecting clean water (C_q=0) and pumping out the dirty water. Figure 4.1 illustrates the influences of nonreactive aqueous phase time constants on zeroth, first and second incomplete moment, and residence time for the aqueous phase concentration. Figure 4.2 shows the effect of the sorption time constant. Although the breakthrough curves of concentration are almost the same for different sorption time constants, their zeroth, first, and second moments are much different. When the nonreactive time constant is much smaller than the sorption time constant, the curve of residence time has a clear plateau, distinguishing two main processes: advection and sorption. More work should be done to clarify the importance of the incomplete moment.

4.3 Incomplete Moment-Generating Equations for the 2-D ADS Model

Applying the definitions of an incomplete moment to the governing equation (3-23), we will obtain the incomplete moment-generating equations for a two-dimensional convection-dispersion-sorption model

$$\frac{\partial N_0}{\partial T} + \frac{\varrho_b}{\theta}\frac{\partial J_0}{\partial T} = L(N_0) + C_{(t=0)} + \frac{\varrho_b}{\theta}S_{(t=0)} \tag{4-5a}$$

$$\frac{\partial J_0}{\partial t} = \alpha(k_d N_0 - J_0) + S_{(t=0)} \tag{4-5b}$$

$$\frac{\partial N_n}{\partial T} + \frac{\varrho_b}{\theta}\frac{\partial J_n}{\partial T} = L(N_n) + nN_{n-1} + \frac{n\varrho_b}{\theta}J_{(n-1)} \qquad n \geq 1 \tag{4-6a}$$

$$\frac{\partial J_n}{\partial t} = \alpha(k_d N_n - J_n) + nJ_{(n-1)} \qquad n \geq 1 \tag{4-6b}$$

where $$L = \frac{\partial}{\partial x}\left(D_{xx}\frac{\partial}{\partial x} + D_{xz}\frac{\partial}{\partial z}\right) + \frac{\partial}{\partial z}\left(D_{zz}\frac{\partial}{\partial z} + D_{zx}\frac{\partial}{\partial x}\right) - V_x\frac{\partial}{\partial x} - V_z\frac{\partial}{\partial z}$$.

Although we deal only with the two-dimensional model, a more complicated three dimensional model is easily derived (in fact, we can just change the operator L for the 3-D model).

If the sorption process is modeled by Fick's law, which is shown in equation (2–4), equation (4–5b) can be replaced by

$$\frac{\partial J_{0r}}{\partial T} = \frac{D_a}{r^{k-1}} \frac{\partial}{\partial r}\left(r^{k-1} \frac{\partial J_{0r}}{\partial r}\right) + S_{r(t=0)} \tag{4–7a}$$

$$J_{0r}(0,r) = 0 \tag{4–7b}$$

$$J_{0r}(T,b) = k_d N_0 \qquad J_{0r}(T,0) < \infty \tag{4–7c}$$

$$J_0 = \frac{k}{b^k} \int_0^b r^{k-1} J_{0r} dr \tag{4–7d}$$

and equation (4–6b) can be represented by

$$\frac{\partial J_{nr}}{\partial T} = \frac{D_a}{r^{k-1}} \frac{\partial}{\partial r}\left(r^{k-1} \frac{\partial J_{nr}}{\partial r}\right) + nJ_{(n-1)r} \qquad n \geq 1 \tag{4–8a}$$

$$J_{nr}(0,r) = 0 \tag{4–8b}$$

$$J_{nr}(T,b) = k_d N_n \qquad J_{nr}(T,0) < \infty \tag{4–8c}$$

$$J_n = \frac{k}{b^k} \int_0^b r^{k-1} J_{nr} dr \tag{4–8d}$$

where J_{0r} and J_{nr} are the zeroth and nth, respectively, incomplete moments for solid phase concentration at the local scale; S_r is the solid phase concentration at the grain scale; k=1 is for the layer diffusion; k=2 is for the cylindrical diffusion; and k=3 is for the spherical diffusion.

The Laplace Transform Galerkin method can be used again to solve these equations. Because the higher moments depend on the lower moments, the Laplace form of lower moment should be obtained in advance. For example, to solve a second order incomplete moment, we should know the first order incomplete moment, and thus the zeroth order incomplete moment.

Laplace transformation of equations (4–5) and (4–6) leads to

for first-order sorption model

$$L(\overline{N_0}) = p(1 + k_d\frac{\varrho_b}{\theta}A_1)\overline{N_0} - \frac{\varrho_b}{\theta}A_0\overline{S_{(t=0)}} - \overline{C_{(t=0)}} \tag{4–9a}$$

$$\overline{J_0} = \frac{\overline{S_{(t=0)}}}{p} + A_0(k_d\overline{N_0} - \frac{\overline{S_{(t=0)}}}{p}) \tag{4–9b}$$

$$L(\overline{N_n}) = p(1 + k_d\frac{\varrho_b}{\theta}A_1)\overline{N_n} - \frac{\varrho_b}{\theta}nA_0\overline{J_{(n-1)}} - n\overline{N_{(n-1)}} \qquad n \geq 1 \tag{4–10a}$$

$$\overline{J_n} = \frac{n}{p}\overline{J_{(n-1)}} + A_0(k_d\overline{N_n} - \frac{n}{p}\overline{J_{(n-1)}}) \qquad n \geq 1 \tag{4–10b}$$

$$A_0 = \frac{\alpha}{\alpha + p}$$

where the bar symbol represents the Laplace transformation, and p is the parameter of the Laplace transformation. For the diffusion–type sorption model, equations (4–7) and (4–8), Laplace transformation can lead to

for diffusion controlled sorption model

$$L(\overline{N_0}) = p(1 + k_d\frac{\varrho_b}{\theta}A_1)\overline{N_0} - \frac{\varrho_b}{\theta}A_i k_d\overline{C_{(t=0)}} - \overline{C_{(t=0)}} \tag{4–11a}$$

$$\overline{J_0} = \frac{\overline{S_{(t=0)}}}{p} + A_i(k_d\overline{N_0} - \frac{k_d\overline{C_{(t=0)}}}{p}) \tag{4–11b}$$

$$L(\overline{N_n}) = p(1 + k_d\frac{\varrho_b}{\theta}A_i)\overline{N_n} - \frac{\varrho_b}{\theta}nA_i k_d\overline{N_{(n-1)}} - n\overline{N_{(n-1)}} \qquad n \geq 1 \tag{4–12a}$$

$$\overline{J_n} = \frac{n}{p}\overline{J_{(n-1)}} + A_i(k_d\overline{N_n} - \frac{n}{p}k_d\overline{N_{(n-1)}}) \qquad n \geq 1 \tag{4–12b}$$

$$A_1 = \frac{1}{\beta}\frac{\sinh(\beta)}{\cosh(\beta)} \qquad \textit{for layer diffusion model } (k = 1)$$

$$A_2 = \frac{2}{\beta}\frac{I_1(\beta)}{I_0(\beta)} \qquad \textit{for cylindrical diffusion model } (k = 2)$$

$$A_3 = \frac{3}{\beta}\frac{i_1(\beta)}{i_0(\beta)} \qquad \textit{for spherical diffusion model } (k = 3)$$

$$\beta = b\sqrt{\frac{p}{D_a}} \qquad D_a = \frac{D_p}{R_{im}}$$

After we obtain the solution of the incomplete moments in the Laplace domain, we can solve the time-domain incomplete moment in a particular time period, T, by applying a numerical inversion algorithm. Because the function forms of the incomplete moment are different with respect to the order, we cannot use only one of the existing inversion algorithms, which is just appropriate for some particular functions, to obtain all orders of the incomplete moment. Because of the limitation of time, we have not programmed this numerical scheme.

4.4 Summary and Conclusions

A new concept of an incomplete moment has been developed and reported in this chapter. The corresponding incomplete moment-generating equations are also derived. These generating equations can be applied in a heterogeneous aquifer system. A numerical scheme for solving two-dimensional incomplete moments is presented. The major conclusions include

(1) The incomplete moment obviously provides more information about a breakthrough curve than the traditional complete moment. It can analyze the statistical characteristic of a breakthrough curve at any truncated time period.

(2) The mass, passing every spatial point within a particular period of time, can be easily mapped by a zeroth incomplete moment and can be used to design a remediation scheme to control the amount of contaminant passing through a location of interest.

(3) The derived 2-D incomplete moment equations can be applied to a heterogeneous aquifer. Obtaining an incomplete moment by solving these equations can avoid a redundant integral for concentrations, which should be calculated in advance; thus, much more computational time and storage can be saved. The LTG method may be a better tool to solve these equations.

(4) An example problem for a lumped parameter model shows that when the aqueous phase time constant is much smaller than sorption time constant (for example, about 100 times), the curve of residence time in an incomplete moment analysis will have a very clear

plateau revealing an advection process and an sorption process. This clearly indicates that a slow mass transfer rate in the sorption site can lead to longer required cleanup time to restore the aquifer.

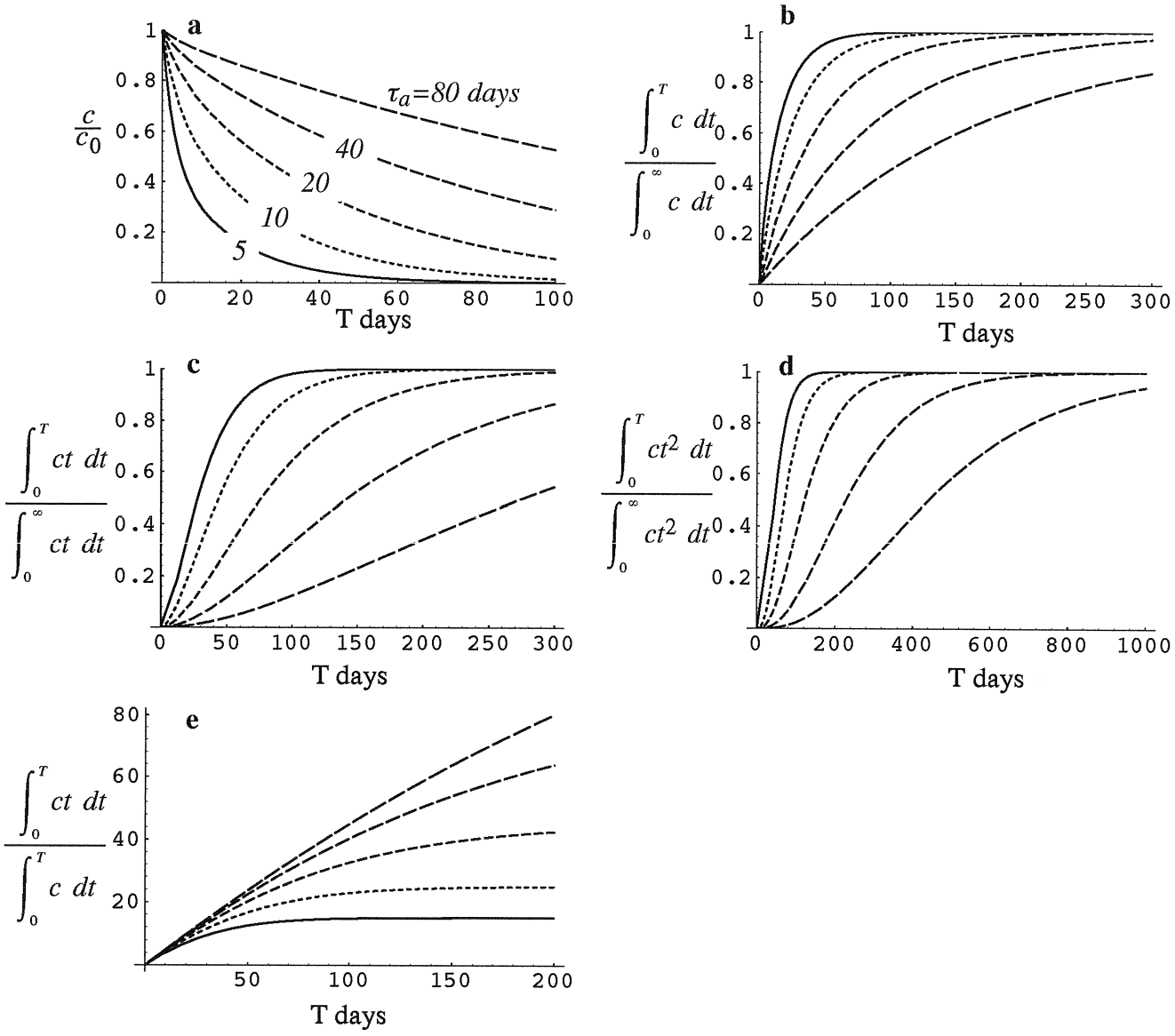

Figure 4.1 The effects of the aqueous phase time constant for (a) the aqueous phase concentration; (b) the zeroth order, (c) the first order, and (d) the second order incomplete moment; and (e) the incomplete residence time. (τ_1=10 days, τ_2=10 days, and R=2).

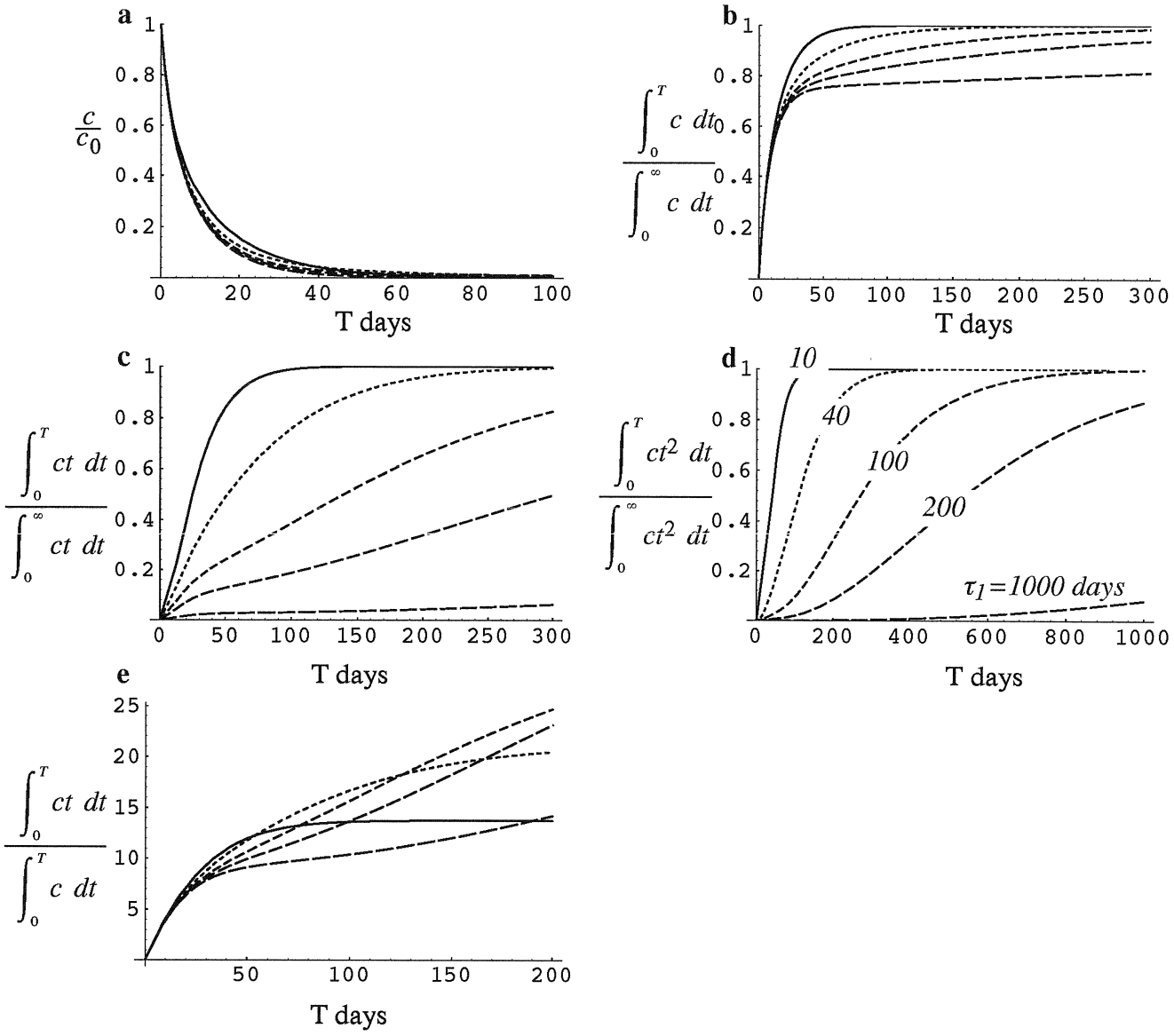

Figure 4.2 The effects of the sorption time constant in sorption site 1 for (a) the aqueous phase concentration; (b) the zeroth order, (c) the first order, and (d) the second order incomplete moment; and (e) the incomplete residence time. (τ_a=5 days, τ_2=5 days, and R=2).

5. CONCLUSIONS AND RECOMMENDATIONS

Time constants and storage capacity are used to characterize an aquifer system. They reflect the kinetic process and equilibrium properties of the system under external impacts. Time constant analysis can be employed to analyze the behavior of reactive solute transport in heterogeneous aquifer systems, and further evaluate the effectiveness of a remediation system. In this research, we do not consider the influence of NAPLs on remediation.

5.1 Conclusions

(1) A geological formation with a larger time constant and a significant amount of contaminant is difficult to remediate. A diffusion controlled process can be the major reason for this larger time constant. In a low–k zone, the diffusion may dominate advection, and the time constant depends on a pore diffusion coefficient and the characteristic length of this zone. At sorption sites, the larger time constant can be attributed to a larger internal retardation factor or a smaller apparent diffusion coefficient. Thus, the presence of heterogeneity and rate–limited sorption/desorption leads to a slow mass transfer in a remediation system and are major reasons contributing to the failure of a remediation system.

(2) Time constant analysis can be used to quantitatively estimate the results of a remediation system. The rule–of–thumb is that remediation needs at least three times the time constant to remove 95 percent of the contaminant out of a geological formation. By comparing the time constants with the duration of a remediation scheme, we can evaluate a remediation system.

(3) Sorption occurring in a diffusion controlled low–k zone will lead to both greater storage and a larger time constant. The larger storage capacity in sorption sites not only increases the amount of reserved contaminant, which is difficult to flush out by advection, but also increases the time constant in the mobile zone. Rate–limited sorption will reduce this effect at first: the contamination in the mobile zone can be removed quickly at the beginning of remediation because less contaminant in the sorption site can diffuse out; but sorption site

reserves more contaminant at the end of remediation, and then recontaminates the aquifer in the postremediation period.

(4) Biodegradation occurring in an aqueous phase contamination speeds up the remediation in the mobile zone, and thus, increases the concentration gradient between sorption sites and mobile zones. However, this scheme still cannot significantly improve the efficacy in removing contaminants from the sorption sites and low–k zones with a longer time constant because nutrients and electron acceptors are difficult to deliver to these diffusion controlled zones.

(5) Hydraulic fracturing is another technique used for improving the effectiveness of a PAT system. The cut–through fracture in a low–k zone can decrease the characteristic length in that zone and, thus, decrease the time constant. However, this scheme cannot be applied to remove the contaminant reserved in aggregated soil, and this technique, with not–cut–through fractures in a low–k zone, cannot greatly improve the effectiveness of remediation.

(6) Contamination history determines the distribution of the contaminants in the aquifer system, and can influence the results of a remediation system. Contamination present in the aquifer for only a shorter time relatively to the aquifer time constant can be remediated relatively easy. Contamination residing in the aquifer for many time constants can lead to a significant amount of contaminant storage which cannot be remediated quickly.

(7) Contaminant concentrations and resident mass in an aquifer system can be quickly calculated by solving advection–dispersion–sorption equations with a Laplace Transform Galerkin approach. This algorithm,which is restricted to linear mass transfer with a steady flow field, provides a highly accurate and robust time continuous solution. On the other hand, this approach avoids spatial discretization at grain scale for the diffusion–type sorption models, and thus saves computational storage and CPU time.

(8) Frequency domain analysis illustrates that the aqueous phase concentration is more sensitive to external impacts if the time constant in a mobile zone is smaller; sorption sites with a smaller time constant and larger storage capacity can dampen more input variations, and make aqueous phase concentration more sensitive. Faster groundwater flow can transfer more long period components of the external inputs.

(9) The developed 2–D frequency domain analysis model can be applied to a heterogeneous aquifer system. Two examples show that the response of an aquifer system to external input not only depends on the system itself, but also on input schemes, including input strength and input location. It is possible to use the distribution of the transfer function to determine the propensity for contamination or remediation in any spatial point of the aquifer system.

(10) A first–order sorption model is approximately equivalent to the other three diffusion–type sorption models under the relationship of equation (3–34) if the variation of the aqueous phase concentration is slow. The first–order sorption model is the least sensitive to input with a lower period, but the most sensitive to input with a higher period. The three diffusion–type sorption models can be well equivalent under the "equivalent" relationship of equation (3–34).

(11) Incomplete moment is a new concept for studying the characteristic of a breakthrough curve at any truncated time period. It can provide more information about reactive solute transport than a complete moment. An example shows that when the aqueous phase time constant is much smaller than the sorption time constant (about 100 times), the curve of the residence time for the aqueous phase concentration in incomplete moment analysis will have a very clear "plateau" to distinguish the advection process from the sorption process.

(12) The incomplete moment–generating equations for a lumped parameter model and a 2–D distributed parameter model have been derived. The 2–D equations can be applied to

a heterogeneous aquifer system. Obtaining the incomplete moment by solving these equations can avoid redundant integration operations.

5.2 Recommendations

Because time did not permit a careful study for all relative subjects, the following problems are recommended for the future work.

(1) The more complicated 3–D reactive solute transport model, considering the effect of the nonlinear sorption and NAPLs, should be developed to apply to the real aquifer system.

(2) The chemically enhanced PAT system and hydraulic fracturing technique should be further evaluated by mathematical modeling.

(3) The applications of frequency domain analysis to reactive solute transport, such as parameter estimation and process identification, should be explored in the future.

(4) The frequency domain analysis under complicated boundary conditions should be developed.

(5) The relationship between the distribution of transfer function and a remediation is an interesting topic. More attention should be paid in this aspect.

(6) More applications of incomplete moment analysis should be explored.

REFERENCES

Alvarez, P. J. J., P. J. Anid, and T. M. Vogel, 1991: Kinetics of aerobic biodegradation of benzene and toluene in sandy aquifer material. Biodegradation, Vol. 2, No. 1, 43–51.

Ball, W. P. and P. V. Robert, 1991: Long–term sorption of halogenated organic chemicals by aquifer material, 1: equilibrium. Environ. Sci. Technol., Vol. 25, 1237–1249.

Ball, W. P. and P. V. Robert, 1991: Long–term sorption of halogenated organic chemicals by aquifer material, 2: intraparticle diffusion. Environ. Sci. Technol., Vol. 25, 1237–1249.

Bouwer, E. J., and P. L. McCarty, 1985: Utilization rates of trace halogenated organic compounds in acetate–grown biofilms. Biotechnol. Bioeng., Vol. 27, 1564–1571.

Brusseau, M. L., R. E. Jessup, and P. S. C. Rao, 1989: Modeling the transport of solutes influenced by multiprocess nonequilibrium. Water Resour. Res., Vol. 25, No. 9, 1971–1988.

Brusseau, M. L., R. E. Jessup, and P. S. C. Rao, 1991: Nonequilibrium sorption of organic chemicals: elucidation of rate–limiting processes. Environ. Sci. Technol., Vol. 25, 134–142.

Brusseau, M.L., R.E. Jessup, and P.S.C. Rao, 1992: Modeling solute transport influenced by multiprocess nonequilibrium and transformation reactions. Water Resour. Res., Vol. 28, No. 1, 175–182.

Burr, D. T., E. A. Sudicky, and R. L. Naff, 1994: Nonreactive and reactive solute transport in three–dimensional heterogeneous porous media: mean displacement, plume spreading, and uncertainty. Water Resour. Res., Vol. 30, No. 3, 791–815.

Chen, C. S., and G. D. Woodside 1988, Analytical solution for aquifer decontamination by pumping. Water Resour. Res., Vol. 24, No. 8, 1329–1338.

Chen, C. S., 1985: Analytical and approximate solutions to radial dispersion from an injection well to a geological unit with simultaneous diffusion into adjacent strata. Water Resour. Res., Vol. 21, No. 8, 1069–1076.

Crittenden, J. C., N. J. Hutzler, D. G. Geyer, J. L. Oravitz, and G. Friedman, 1986: Transport of organic compounds with saturated groundwater flow: model development and parameter sensitivity. Water Resour. Res., Vol. 22, No. 3, 271–284.

Duffy, C. J., 1982: Stochastic modeling of spatial and temporal water quality variations in groundwater, Ph. D. thesis, New Mexico Tech, Socorro, NM.

Duffy, C. J. and L. W. Gelhar, 1985: A frequency domain approach to water quality modeling in groundwater: theory. Water Resour. Res., Vol. 21, No. 8, 1175–1184.

Duffy, C. J. and L. W. Gelhar, 1986: A frequency domain analysis of groundwater quality fluctuations: interpretation of field data. Water Resour. Res., Vol. 22, No. 7, 1115–1128.

Fry, V. A. and J. D. Istok, 1994: Effects of rate–limited desorption on the feasibility of in situ bioremediation. Water Resour. Res., Vol. 30, No. 8, 2413–2422.

Gelhar, L. W., 1974: Stochastic analysis of pheratic aquifers. Water Resour. Res., Vol. 10, No. 3, 539–545.

Gelhar, L. W., and J. L. Wilson, 1974: Ground–water quality modeling. Ground Water, Vol. 12, No. 6, 399–408.

Goltz, M. N. and P. V. Roberts, 1987: Using the method of moments to analyze three–dimensional diffusion–limited solute transport from temporal and spatial perspectives. Water Resour. Res., Vol. 23, No. 8, 1575–1585.

Goltz, M, N., and Mark E. Oxley, 1991: Analytical modeling of aquifer decontamination by pumping when transport is affected by rate–limited sorption. Water Resour. Res., Vol. 27, No. 4, 547–556.

Haggerty, R., and S. M. Gorelick, 1994: Design of Multiple contaminant remediation: sensitivity to rate–limited mass transfer. Water Resour. Res., Vol. 30, No. 2, 435–446.

Haley, J. L., B. Hanson, C. Enfield, and J. Glass, 1991: Evaluating the effectiveness of groundwater extraction systems. Ground water Monit. Rev., Vol. 11, No. 1, 119–124.

Harrison, B., E. A. Sudicky, and J. A. Cherry, 1992: Numerical analysis of solute migration through fractured clayey deposits into underlying aquifers. Water Resour. Res., Vol. 28, No. 2, 515–526.

Harvey, C. F. and S. M. Gorelick, 1995: Temporal moments of concentration: A new approach to modeling transport and mass–transfer in heterogeneous aquifers, submitted to Water Resour. Res.

Jury, W.A. and F. Roth, 1990: Transfer functions and solute movement through soils. Birkhauser, Boston.

Keely, J. F., 1984: Optimizing pumping strategies for contaminant studies and remedial actions. Ground Water Monit. Rev., Vol. 4, No. 3, 63–74.

Keely, J. F., 1989: Performance evaluations of pump–and–treat remediation. U.S. Enviro. Protect. Agency, EPA/540/4–89/005, Washington, D.C.

Lin, J. and J.L. Wilson, 1994: Time constant and its impact on the remediation of a contaminated aquifer. Abstract, EOS, Vol. 75, No. 44, 293.

Looney, B. B., D. S. Kaback, and J. C. Corey, 1992: Environmental restoring using horizontal wells: a field demonstration. Subsurface Restoration Conference – Third International Conference on Water Quality Research, 41–43.

Miller, C. T. And A. J. Rabideau, 1993: Development of split–operator, Petrov–Galerkin methods to simulate transport and diffusion problems. Water Resour. Res., Vol. 29, No. 7, 2227–2240.

Palmer, C. D. and Willian Fish, 1992: Chemical enchancements to pump–and–treat remediation. U.S. Enviro. Agency, EPA/540/S–92/001, Washington, D.C.

Parker, J. C. and A. J. Valocchi, 1986: Constraints on the validity of equilibrium and first–order kinetic transport models in structured soils. Water Resour. Res., Vol. 22, No. 3, 399–407.

Pedit, J. A., and C. T. Miller, 1994: Homogeneous sorption processes in subsurface system, 1. model simulations and applications. Environ. Sci. Technol., Vol. 28, 2094–2104.

Rabideau, Alan J., and Cass T. Miller, 1994: Two–dimensional modeling of aquifer remediation influenced by sorption nonequilibrium and hydraulic conductivity heterogeneity. Water Resour. Res., Vol. 30, No. 5, 1457–1470.

Sudicky, E. A., 1989: The Laplace transform Galerkin technique: A time–continuous finite element theory and application to mass transport in groundwater. Water Resour. Res., Vol. 25, No. 8, 1831–1846.

Sudicky, E. A. and R. G. McLaren, 1991: User's guide for FRACTRAN: An efficient simulator for two–dimensional, saturated groundwater flow and solute transport in porous or discretely–fractured porous formations. Waterloo Centrer for Groundwater Research, University of Waterloo, Ontario, Canada.

Sudicky, E. A. and R. G. McLaren, 1992: The Laplace transform Galerkin technique for large–scale simulation of mass transport in discretely fracture porous formations. Water Resource Research, Vol. 28, No. 2, 499–513.

Toride, N., F.J. Leij, and M.T. van Genuchten, 1993: A comprehensive set of analytical solutions for nonequilibrium solute transport with first–order decay and zero–order production. Water Resour. Res., Vol. 29, No. 7, 2167–2182.

Valocchi, A. J., 1985: Validity of the local equilibrium assumption for modeling sorbing solute transport through homogeneous soils. Water Resour. Res., Vol. 21, No. 6, 808–820.

Valocchi, A. J., 1986: Effect of radial flow on deviation from local equilibrium during sorbing solute transport through homogeneous soil. Water Resour. Res., Vol. 22, No. 12, 1693–1701.

Van Genuchten, M. Th. and W. J. Alves, 1982: Analytical solutions of the one–dimensional convective–dispersive solute transport equation. U.S. Dept. of Agriculture, Tech. Bull. No. 1661.

Van Genuchten, M. Th. and P. J. Wierenga, 1976: Mass transfer studies in sorbing porous media. 1. Analytical solution. Soil Sci. Soc. Am. J., Vol. 40, 473–480.

Van Genuchten, M. Th., and P. J. Wierenga, 1976: Mass transfer studies in sorbing porous media, I, Analytical solutions. Soil Sci. Soc. Am. J., Vol. 40, No. 4, 473–480.

Vigon, B. W., and A. J. Rubin, 1989: Practical considerations if the surfactant–aided mobilization of contaminants in aquifer. J. Water Pollut. Control Fed., Vol. 51, No. 7, 1233–1240.

Wilson, J. L., 1992: Removal of aqueous phase dissolved contamination: non–chemically enhanced pump and treat. Subsurface Restoration Conference – Third International Conference on Water Quality Research, Dallas, Texas, 54–56.

Wilson, J. L., 1995: Removal of aqueous phase dissolved contamination: Non–chemically enchanced pump and treat. Subsurface Restoration, C. H. Ward, J. Cherry, and M. R. Scalf, eds., Lewis Publishers, Bocaraton, Florida.